DANMARKS OG GRØNLANDS GEOLOGISKE UNDERSØGELSE RAPPORT 2014/81

Field report from the 2011 field season on the Skjoldungen Alkaline Provence, South East Greenland

Martin Broman Klausen & Thomas Find Kokfelt

GEOLOGICAL SURVEY OF DENMARK AND GREENLAND
DANISH MINISTRY OF CLIMATE, ENERGY AND BUILDING

GEUS

DANMARKS OG GRØNLANDS GEOLOGISKE UNDERSØGELSE RAPPORT 2014/81

Field report from the 2011 field season on the Skjoldungen Alkaline Province, South East Greenland

Martin Broman Klausen & Thomas Find Kokfelt

GEOLOGICAL SURVEY OF DENMARK AND GREENLAND
DANISH MINISTRY OF CLIMATE, ENERGY AND BUILDING

GEUS

Table of contents

Background

This report is based on field work carried out in 2011 in the Skjoldungen area, South-East Greenland within the framework of the SEGMENT project – a joint project between the National Geological Survey of Denmark and Greenland, GEUS, and Greenland Ministry of Industry and Mineral resources, MIM. The overall target of the project has been to assess the mineral potential of South-East Greenland by doing new field work and follow-up scientific research in the area. This GEUS report concentrates on the new findings made within the Skjoldungen Alkaline Province (SAP; Nielsen and Rosing, 1990), which is a worldwide rare occurrence of Archaean alkaline rocks (Blichert-Toft, 1995). The original geological mapping of the Skjoldungen area was done by GGU, mainly at a reconnaissance scale, in the late 1980's and early 1990's, resulting in the map compilation in scale 1:500 000 of Escher (1990).

The goal of the renewed field work in the Skjoldungen area was, through field work in selected key areas, to develop a more detailed understanding of the igneous rocks of the SAP and their petrogenesis, as well as evaluating the economic potential of the area. The specific key research objectives set out included: (1) to constrain the geographical extent of the SAP, (2) to identify any temporal evolution within the SAP from new zircon U/Pb age dates, (3) to characterize parental magma types for the SAP magmatism using geochemistry and isotope analytical work, and (4) to evaluate the geotectonic setting for the emplacement of the SAP.

Since the 2011 field season a follow-up season to the same area was conducted in 2012. The work described in this report only relates to the findings made during the 2011 field season; a separate GEUS report will describe the outcome of the 2012 season. Furthermore, a GEUS report related to the extensive new zircon U/Pb age dating work done on the rocks collected from both field seasons is planned, as well as on-going postgraduate research projects investigate the petrogenesis of the remarkable magmas that formed the SAP.

Geological setting

The Skjoldungen Alkaline Province (SAP), situated at *c.* 63º30'N in South-East Greenland, is part of the Archaean North Atlantic Craton (Figure 1). The SAP is one of the oldest alkaline provinces in the world and as such offers a rare opportunity to study alkaline magmatism in the early Earth system. The province constitutes a number of mainly mildly alkaline intrusions of mafic/ultramafic to intermediate and evolved compositions, but also includes a late stage of strongly alkaline character, the nephelinitic-carbonatitic Singertât Complex.

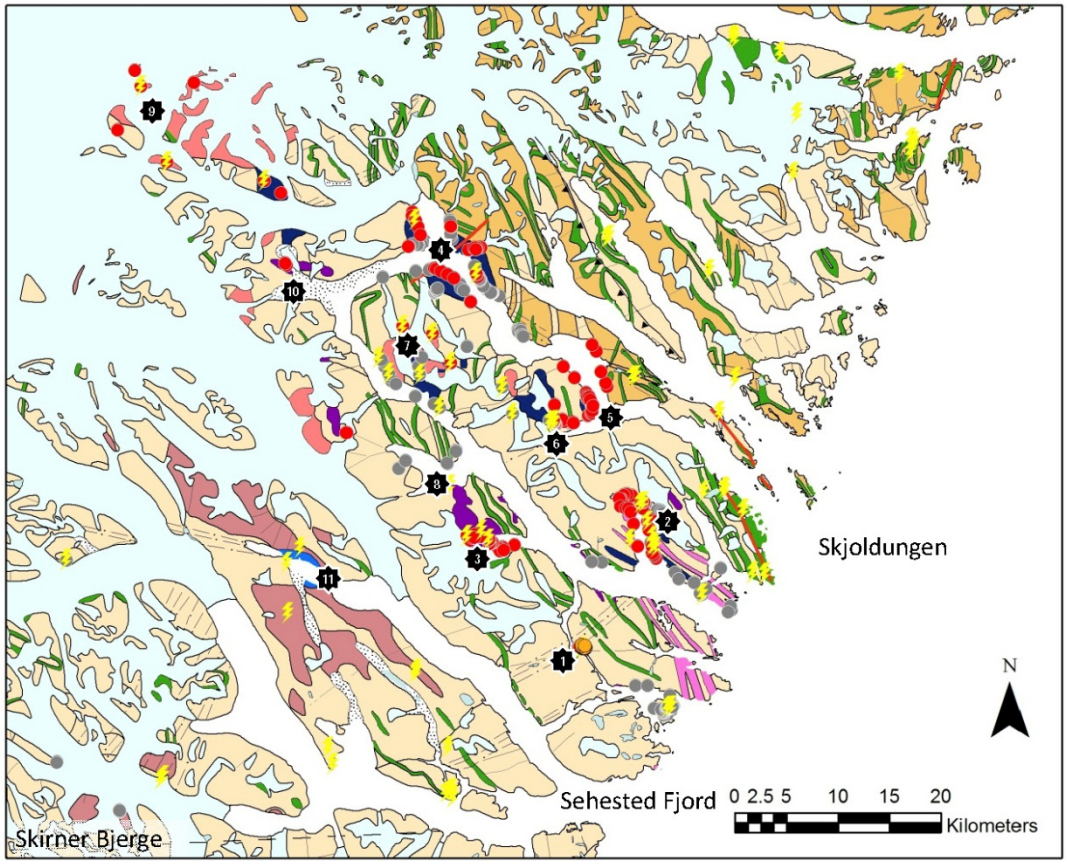

Legend

Archaean intrusive rocks (Skjoldungen Alkaline Province)

- Nephelinitic-carbonatitic complex (2664 +4/-2 Ma, Singertat)
- Gabbro, diorite, monzonite, locally deformed
- Granite and syenite
- Ultramafic rocks, locally deformed
- Syenite, locally deformed
- Granite, diorite, locally deformed (2698 ± 7 Ma in Skjoldungen area)

Archaean metamorphic rocks

- Mafic granulite, minor paragneiss, meta-peridotite, amphibolite
- Grey tonalitic to granodioritic gneiss (2781 ± 6 Ma in Skjoldungen area)
- Tonalitic to granodioritic gneiss, locally agmatitic

1. Vend Om
2. Halvdans Fjord
3. Stærkodder Vig
4. Ruinnæsset
5. Hermods Vig
6. Njords Gletscher
7. Sfinksen
8. Balders Fjord
9. Thrymheim
10. Dronning Maries Dal
11. Singertât

Figure 1. *Geological map of the Skjoldungen area (redrawn after Escher (1990)). Red circles indicate localities visited during the 2011 field season. Grey circles show the localities visited during the 2012 field season for reference. The Escher map is a compilation and simplification of the geology as compiled from field maps in 1:50.000 in the archive of GEUS.*

The SAP was emplaced syn- to post-tectonically during the 2750-2700 Ma Skjoldungen Orogeny (Kolb et al. 2013), into a basement of felsic agmatitic gneisses containing dismembered supracrustal rock units of Meso- to Neoarchaean age. Geographically most SAP intrusions occur within a *c.* 30 km wide by 80 km long NW-SE trending strip stretching from the Atlantic coast onto the inland ice cap, however, syenitic intrusions of early SAP ages are located further to the south down to Skirner Bjerge (Figure 1). During the Skjoldungen Orogeny peak metamorphic event, granulite facies conditions was reached at *c.* 2740-2750 Ma, followed by exhumation at modern comparable rates to shallow crustal levels at *c.* 2700 Ma (Berger et al. 2014). Several SAP intrusions show accordingly signs of being syn-tectonically deformed, both on outcrop scale and in thin section scale. Deformation in such intrusions is particularly pronounced towards lithological boundaries and regions of competence contrasts, and is expressed as foliated fabrics and bended crystals. Other intrusions show pristine magmatic textures, including igneous layering, cross bedding, drop stone structures and well defined intrusive contacts. The extent of deformation in each intrusion likely reflects the timing of emplacement in relation to the Skjoldungen Orogen, but also the depth of emplacement as well localized strain variations.

The first age determinations on SAP intrusions were based on zircon U/Pb TIMS dating (Nutman and Rosing, 1994) and Sm-Nd whole rock isochrons (Blichert-Toft et al. 1995), both indicating intrusion ages of around 2720 to 2700 Ma.

Field relationships

During the 2011 field season six study areas were investigated within the SAP by the authors over a period of *c.* 4 weeks, of which the first week was during partly poor weather conditions. In chronological sequence the authors moved their camps around using a rubber dinghy between the following localities (see also Figure 1):
(1) *Vend Om Fjord*, (2) *Halvdans Fjord*, (3) *Stærkodder Vig*, (4) *Balders Fjord*, (5) *Ruinnæsset*, and (6) *Hermods Vig*.

On average two to four days of efficient field work were used at each locality. Balders Fjord represents half a day's work, from our base ship 'Fox'. Each area incorporates (a) previously identified late-kinematic SAP-intrusion(s), on which our primary observations, structural measurements and sampling focused. However, similar work was also done on their gneissic host rocks and younger, cross-cutting intrusions and structures; and especially the contacts between older host rocks and younger intrusions. These field relationships for each area are described and interpreted in this report following the chronological order listed above.

Unless specified otherwise, all planar structural readings in this report are given using the right-hand rule, such that the plane dips to the right of the given strike/azimuth direction. Every rock sample is identified by a unique six-digit GEUS number.

Vend Om Intrusion

Glacier retreat now allows dinghy passage to a small mafic-ultramafic intrusion from the north, through the Vend Om Fjord. The Vend Om Intrusion (VOI) is exposed from the northern shore side of the fjord and up until an elevation of *c.* 220 m above sea level (Figure 2). The intrusion measures *c.* 250×400 m and is partially dissected by four gullies running orthogonally to the fjord, providing useful pathways for accessing and studying the entire intrusion. The VOI was investigated by the authors for 2.5 days from a camp site located just outside the intrusion. Three traverses were made, two along its SE- and NW-margins, and one through its central part. These profiles established a rough impression of the architecture of the intrusion as it is made up of an outer <100 m wide Marginal Zone and an inner Layered Sequence (Figure 3). It is uncertain whether the Marginal Zone completely envelopes the VOI, as vertical layers within the Layered Sequence was observed in direct contact with the gneissic host at one place along the intrusion's NE-margin and the remaining eastern part of this margin was never mapped. The intrusion is also cut by a number of younger felsic aplitic–pegmatitic sheets, mafic dykes of presumed Proterozoic age, and late faults (including pseudotachylites).

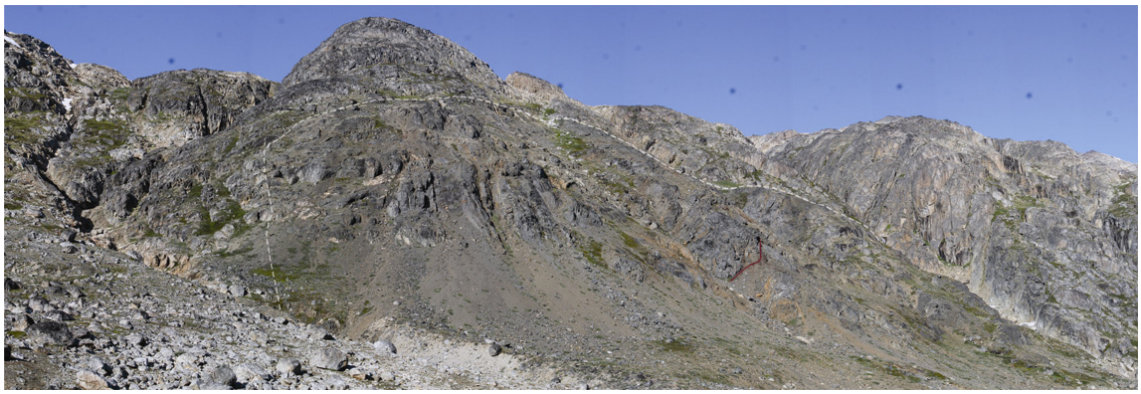

Figure 2. *The VOI as viewed east of camp. Dashed white line trace the exposed margin of the intrusion. Brown curving line in the internal part of the intrusion is a semi-continuous rusty magnetite-rich layer that was mapped out. Much of the northern (left) part of the intrusion exhibits some conspicuous sub-vertical structures that deserve further investigation. Uppermost margin of the intrusion lies at 220 m above the fjord (located to the lower right side of this picture).*

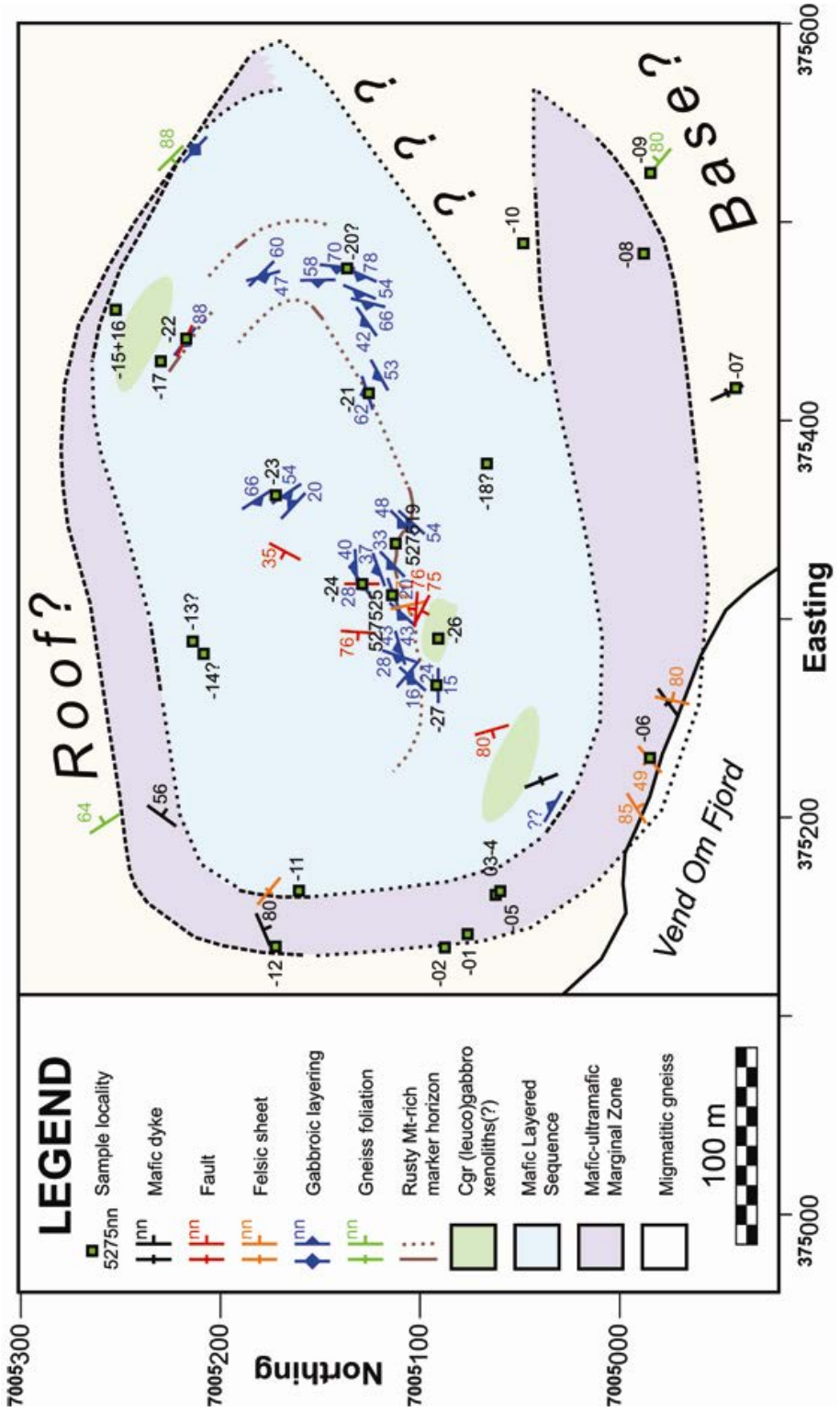

Figure 3. *Preliminary geological map of the VOI showing the major rock units, structures and sample localities. See text for rock types within each unit, structures and samples.*

The Marginal Zone

Hornblende- porphyroblastic pyroxenite

The rocks of the marginal zone are dominantly orthopyroxene pyroxenitic rocks, dominated by, and with distinctly large hornblende megacrysts that in some cases reach up to 8 cm in size (e.g. sample 527501 and 527503), and tend to form a semi-continuous layering within the rocks (Figure 4b). These layers are unlike typical magmatic layers seen in layered mafic intrusions elsewhere (e.g., Wager and Brown, 1953, Parsons, 1987), and we therefore consider it most likely that hornblende megacrysts represent porphyroblastic overgrowth formed during subsequent amphibolite facies metamorphism. This is supported by petrographical studies by Grobbelaar (2012). In between the hornblende-rich layers the coarse grained “matrix” rock contains interstitial plagioclase in addition to cumulus ortho- and clinopyroxene, and can therefore more appropriately be classified as a melagabbronorite (527504) (Figure 4c-e). These plagioclase-rich domains could perhaps be attributed to a late-stage mobilization of interstitial melts on a meter-scale, into plagioclase-rich and hornblende-oikocryst-poor pegmatitic pods.

Figure 4. (previous page) *The hornblende-porphyroblastic pyroxenite: (a) Arrows indicate two c. 10 cm-thick banded concentration of hornblende-oikocrysts within the intrusion's Marginal Zone, along the southern part of the intrusion (gneiss host in the background). (b) A close-up of a hornblende-rich band within another outcrop along the shores of the Vend Om Fjord. (c-e) Diffuse contacts between (mela)gabbronorites and hornblende-porphyroblastic pyroxenite within the Marginal Zone suggest that they represent patched variations within the same rock unit, which crystallized at roughly the same time.*

Mottled gabbronorites

Aphyric, medium grained and mottled gabbronorites (527512) locally outcrop within the Marginal Zone but may also represent a transitional subunit into the Layered Sequence (Figure 5). Their grain sizes and more sub-ophitic textures resemble those within the Layered Sequence more than the hornblende porphyroblastic pyroxenites and melagabbronorites of the Marginal Zone, and future investigations should constrain whether mottled gabbronorites also occur inside the Marginal Zone.

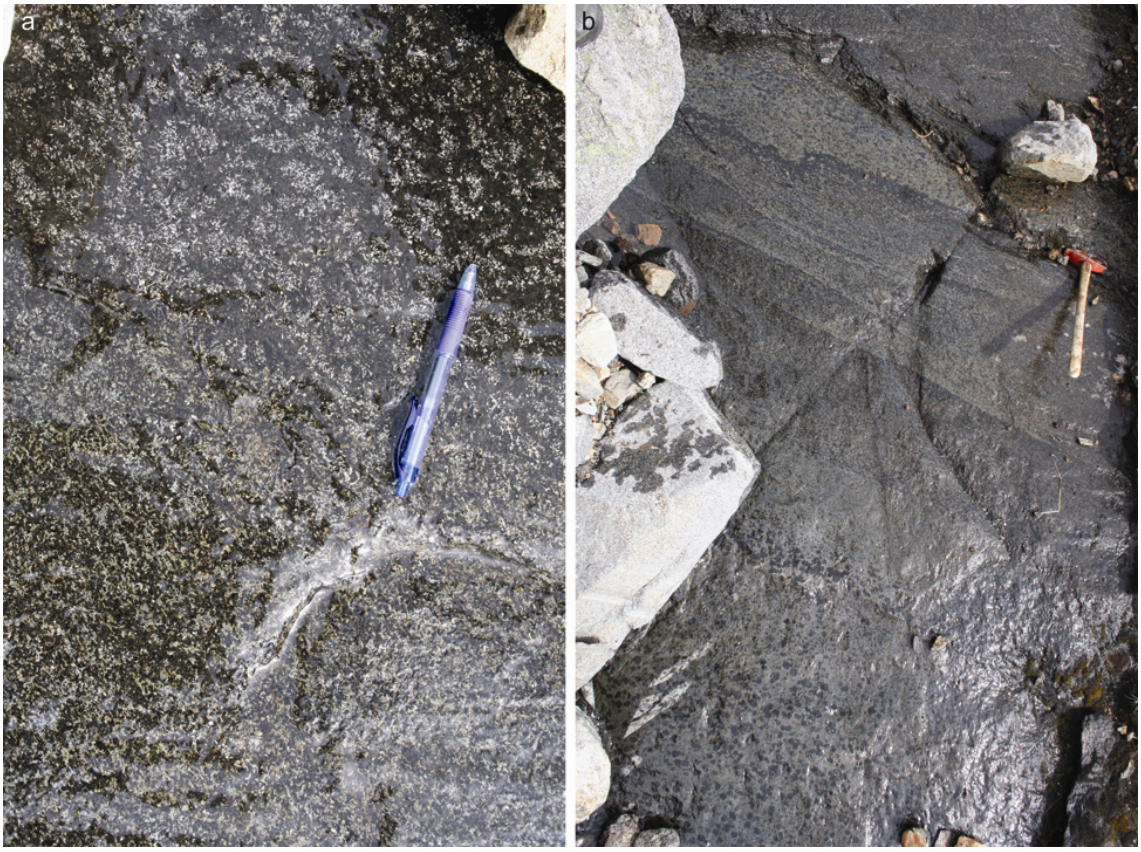

Figure 5. *(a) Mottled-textured medium grained gabbronorite in the transition zone between the Marginal Zone and the Layered Sequence. (b) Contact between the hornblende-bearing rocks of the Marginal Zone (lower part of photo) and the Layered Sequence including mottled gabbronorite (upper part) exposed in a stream.*

Potential parental melts

Two weakly foliated and SSE-NNW trending dykes (Figure 6) constrain a WSW-ENE directed least compressive stress regime, roughly parallel to the overall elongation of the SAP (Figure 1), and may therefore have intruded penecontemporaneous with the VOI. The more mafic of these two dykes was sampled (527507) as a possible representative of a parental melt. At one locality at the southern margin of the intrusion some fine grained and aphyric ultramafic bands, up to some tens of cm wide intrude the pyroxenite of the Marginal Zone (Figure 6). In this *c.* 3 m-long outcrop, several roughly margin-parallel and discontinuous bands may represent parental melts that intruded into and chilled within the Marginal Zone during the latter stages of this magma chamber's crystallization. The most ultramafic looking of these bands were sampled (527508) with the idea that this might represent the melt composition of the VOI.

Figure 6. *Fine grained ultramafic bands within the Marginal Zone are tentatively interpreted as late-stage wehrlitic intrusions into the base of this magma chamber. (a) >1 m wide zone of bands that are roughly parallel with the intrusion's S-margin. (b) Irregular fine grained veins of relatively felsic material cut and locally brecciate the ultramafic bands.*

The Layered Sequence

The measured orientations of magmatic layers inside the central to eastern parts of the VOI give an impression of a bowl-shaped geometry, generally dipping towards the west (Figure 3). Using the Skaergaard Intrusion as a model, it is thereby inferred that near-vertical layers on-lap and drape the northern and southern margins of the intrusion and the main Layered Sequence accumulated from a more primitive eastern base and up towards a more evolved western 'roof zone'. If so, the intrusion must also have been tilted towards the west. It is however, also possible that we observe an erosional section through a non-tilted layered intrusion, with steep marginal layering and shallower dipping layers into the centre of the

intrusion. In this case the intrusion shape would be akin a concentrically layered pipe where the most primitive cumulate rocks would be expected towards the margins and the more evolved compositions towards the centre of the intrusion.

The medium to coarse grained Layered Sequence includes various styles of layered gabbronoritic rocks, ranging from modally layered and graded pyroxene-plagioclase rocks to magnetite-rich layers (527518–527519 and 527521) and possibly chromite-rich layers (527520) placed within relatively uniform layers of melagabbronorite (527515–527527) and anorthosite (527533) (Figure 7). No clear stratigraphical variation was noted in the field that could be related to increasing differentiation up through a cumulate pile, such as progressively more leucocratic rocks towards the centre of the intrusion. There is also some uncertainty regarding whether possible chromite layers (conspicuously similar to bifurcating UG1 layers described by Nex, 2004) could have been deposited between two magnetite-rich layer at the eastern end of the intrusion, because this does not conform to the cumulate stratigraphy of the Rustenberg Layered Series in the Bushveld ComplexCawthorn et al. 2006).

Locally undulating and bifurcating layers, respectively, reflect possible late-stage deformations and on-lapping accumulation beds (Nex, 2004; Figure 7d). Drop-stone-like structures are not uncommon in certain parts of the Layered Sequence. One such example is shown in Figure 7f which shows a *c.* 1 m large xenolith (roof pendant?) of coarse grained leucogabbroic (527526) that suppresses the modal layering of the underlying rock. The more shallow dipping central part of the intrusion is characterized by several *c.* 1 cm thin plagioclase bands amongst a few uniform gabbronoritic and leucogabbronoritic layers (527523–527525 and 527527) (Figure 78a).

Figure 7. *(next page) Examples of magmatic layering within the gabbroic rocks of the Layered Sequence of VOI. (a) Modal rhythmical layering in gabbronorite with a near-vertical, graded bedding of layers to indicate an up-towards-left stratigraphy. (b) and (c) A rusty magnetite-rich layer, locally up to 2m in thickness, but generally < 1m, can be traced for more than 50 m along strike, constituting a marker horizon within the Layered Sequence. (d) Undulating, bifurcating and moderately to steeply inward dipping <5 cm-thick dark oxide-rich bands in relatively uniform leucogabbronorite layers, with some resemblance to the UG1 chromite layers within anorthosites of the Bushveld Complex (white arrow locates one bifurcation towards SW, away from the photographer). (e) An intermittent c. 1.5 m-thick and steeply inward dipping sequence of three uniform anorthosite layers punctuated by two uniform melagabbronoritic layers. Layers are displaced c. 1 m along an apparent dextral strike-slip fault with a pull-apart jug (cf., inserted sketch) located by a white arrow. (f) Drop stone structure in Layered Sequence; 1m sixed xenolith of leucogabbronorite has suppressed the underlying layering of the gabbroic rocks.*

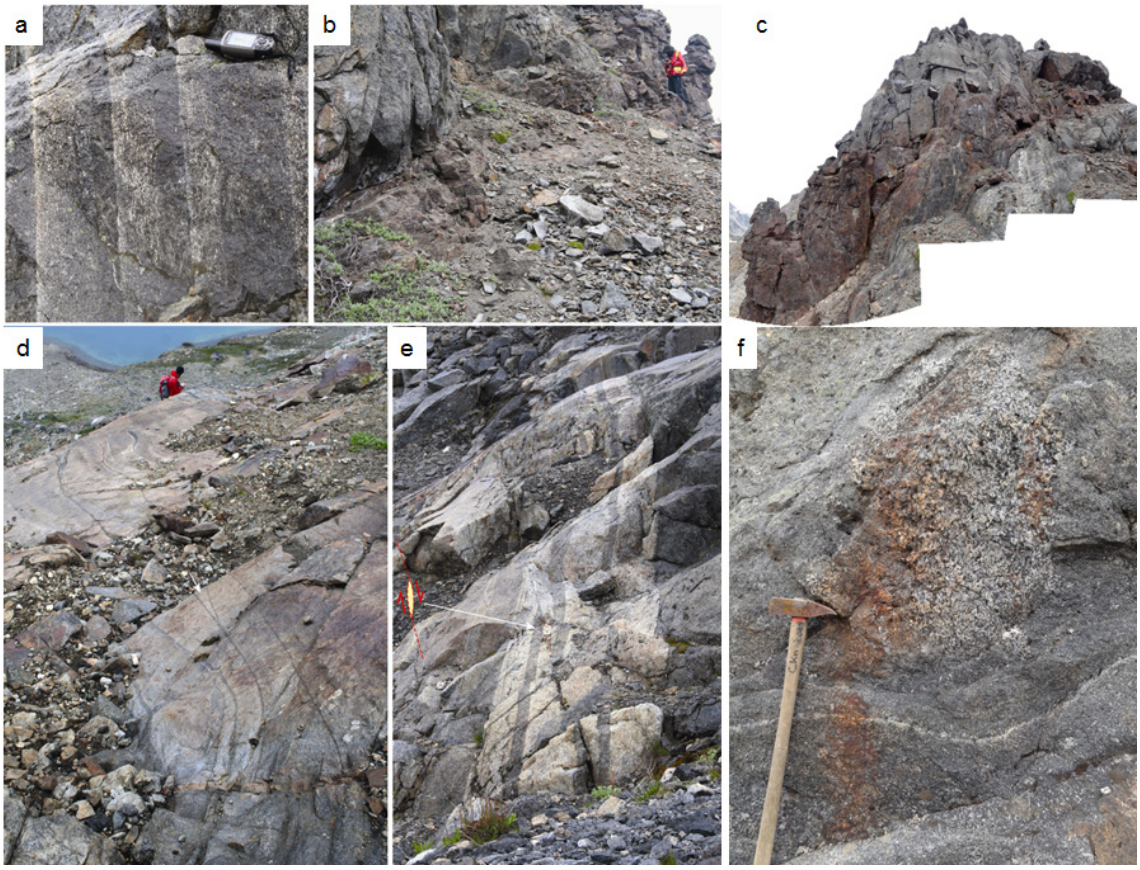

Late stage features

Brittle faults and pseudotachylites

Steep orange weathered brittle faults cut the central parts of the Layered Sequence and define a roughly N-S and E-W striking conjugate set (Figure 8 and Figure 9). Often these faults exhibit slicken-sided surfaces that indicate large strike-slip components. From just a small number of measured faults it may be inferred that such a conjugate strike-slip fault pattern is roughly consistent with the extension direction inferred by the assumed “feeder dykes” (Figure 6), described above. It is however not possible to rule out that these orange weathered brittle faults could be much younger than the VOI, and possibly be related to the emplacement of Proterozoic dolerite dykes, or even the Palaeogene opening of the Atlantic Ocean.

Some fault zones are intruded by a highly irregular network of dark aphanitic veins with rounded breccia clasts, which resembles pseudotachylite (Figure 9). One such, *c.* 1 m thick, sub-vertical and roughly NW-SE trending fault zone exhibits an apparent *c.* 4 m SW-block-down displacement of moderately NW-dipping igneous layers (Figure 9). In this case, it is believed (but not certain) that this represents a normal fault, because this is more consistent with the extensional regime inferred for both the conjugate strike-slip system and roughly parallel feeder dykes.

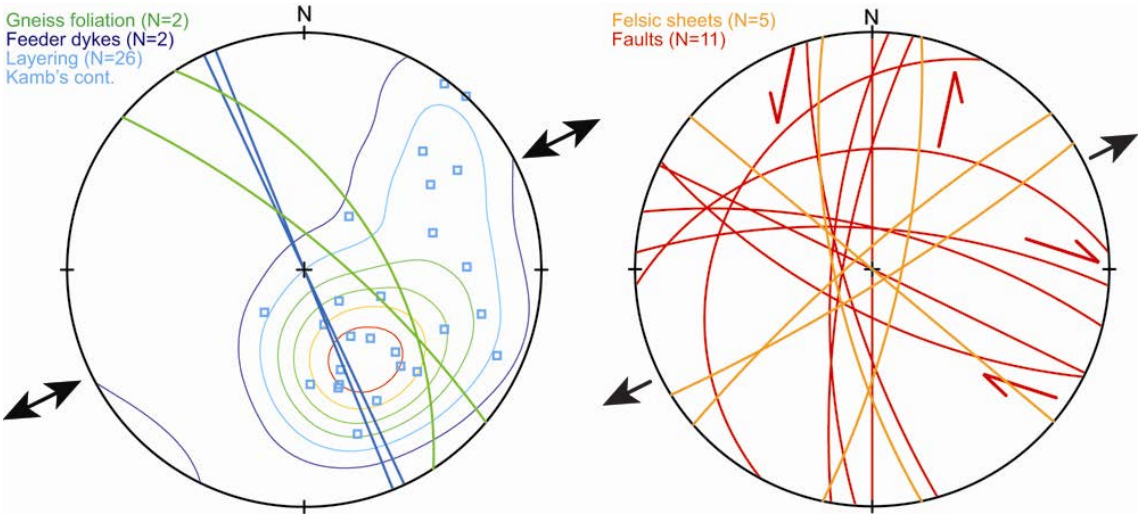

Figure 8. *Equal area lower hemisphere stereographical plot showing structural data from the Vend Om Area, mainly plotted as planes. Larger number of bedding plane measurements of magmatic layering are plotted as poles that have been contoured using Kamb's method on a fine grid and inverse area squared smoothing (contour start and intervals of 2).*

Figure 9. *(next page) Brittle deformation within the central parts of the Layered Sequence. (a) Cross section traced from (b), which shows a roughly NE-SW trending, steep and <1 m-wide pseudotachylite zone that offsets layers (250/37°) by an apparent SW-block-down displacement of c. 4 m. Secondary, minor thrust faults splay from the pseudotachylite. (c) Detail of a pseudotachylite vein within the deformation zone. (d) A nearby orange-weathered brittle fault (274/76°) also exhibits an apparent S-block-down displacement by c. 1 m (note that this outcrop is facing opposite to a-b). However, sub-horizontal slickensides indicate a much greater strike-slip component, which for this magmatic layer (266/48°) was dextral (as in Figure 8).*

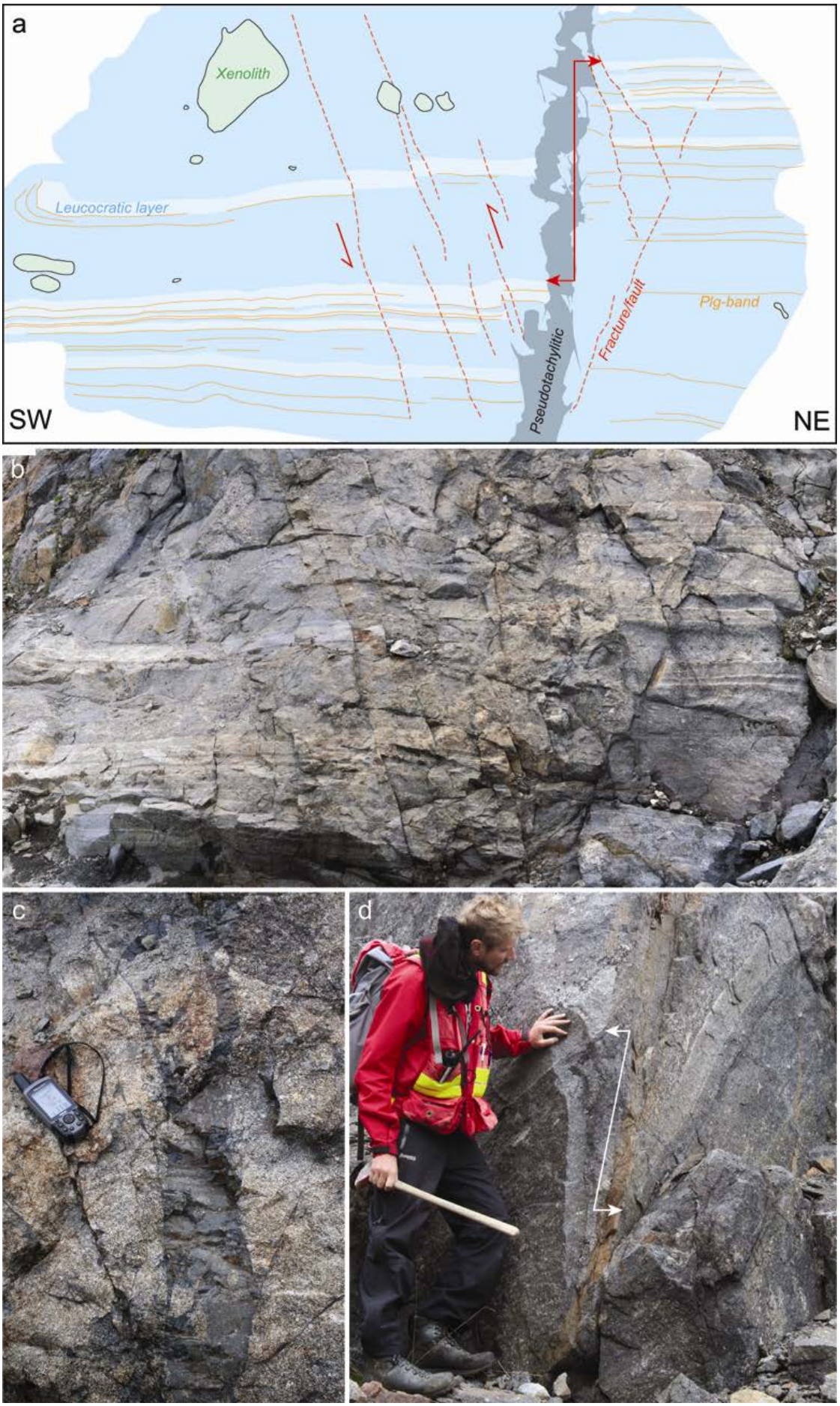
a
Xenolith
Leucocratic layer
Pig-band
Fracture/fault
Pseudotachylitic
SW
NE
b
c
d

Felsic sheets

Several felsic aplitic-pegmatitic sheets of variable and irregular orientations cut through the VOI. It is uncertain whether these intrusions are part of a regional set of late-kinematic intrusions or locally back-veined contact melts, as tentatively suggested for intermediate (granodioritic) rocks along the contacts of the VOI (Figure 10a). Along the northern, upper margin of the VOI, three moderately inclined felsic pegmatites are observed cutting the Marginal Zone, but apparently not extending into the Layered Sequence (Figure 10b). These pegmatites could be interpreted as having been injected into a crystallized Marginal Zone, when the interior of the VOI was still molten, and thereby supporting a local contact-melted origin. This may be investigated further by comparing samples from three felsic sheets (527505–527506 and 527510) with a hybrid contact unit (527502), a gneissic host rock (527509) and samples of the Marginal Zone units described above. If these felsic sheets indeed are the result of back-vening of mobilised basement wall rock, age determination by zircon U/Pb dating of the felsic sheets should give the emplacement age of the VOI (see below).

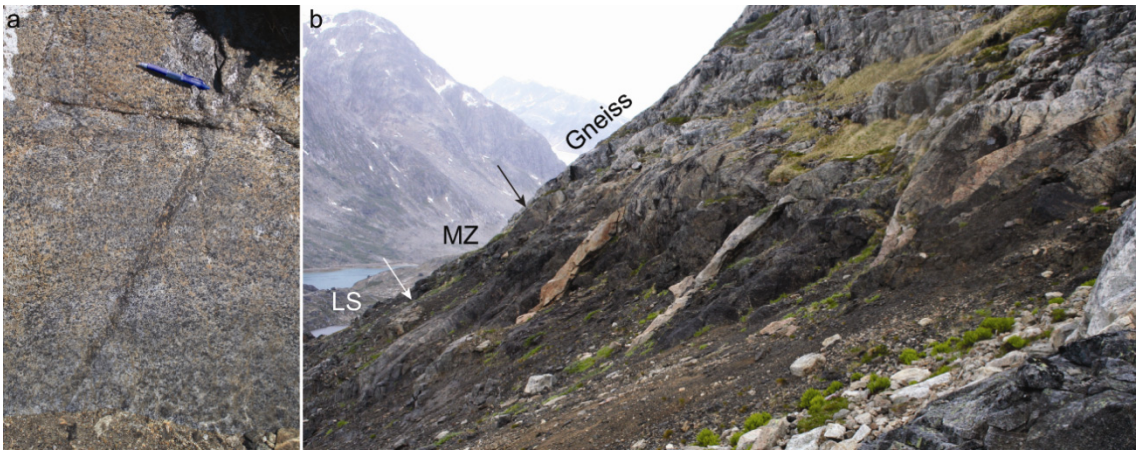

Figure 10. *Felsic units: (a) Granodioritic hybrid contact unit. (b) Northern margin of VOI viewed toward west, showing three distinct felsic aplite-pegmatite sheets that cut though the darker Marginal Zone (MZ) but do not seem to continue into the paler Layered Sequence (LS). Arrows locate contacts between units.*

Dolerite dykes

The VOI is cut by at least three *c.* 2 m-thick, sub-vertical and SW-NE trending dolerite dykes with distinct cooling joints and thin chilled contacts (Figure 11). None of these dykes were sampled, but three samples were collected from the southern contact (527602) and the centre (527603 and 527604 for geochronology and geochemistry, respectively) of a *c.* 30 m-thick and E-W trending dolerite dyke, south of VOI (Figure 11). The central part of another *c.* 50 m-thick and E-W trending dolerite dyke was also sampled (527605 and 527506 for geochronology and geochemistry, respectively) along the northern part of the Vend Om Fjord.

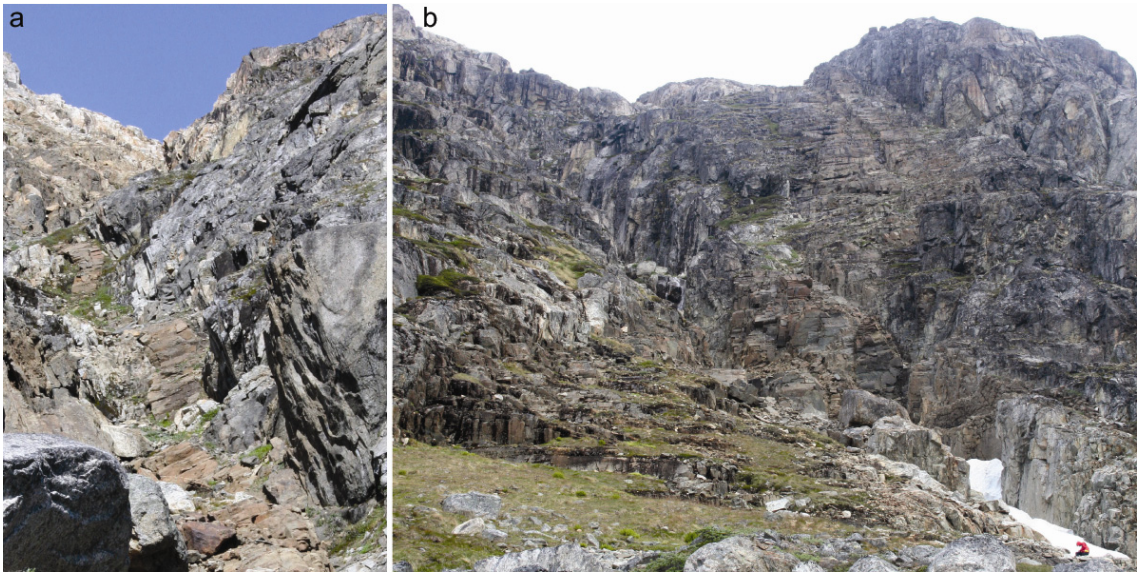

Figure 11. *Dolerite dykes: (a) SW-NE trending and c. 2 m-thick dyke just outside the northern margin of the VOI, looking northeast. (b) E-W trending and c. 30 m-thick dyke south of VOI, looking east.*

Petrotectonic implications and preliminary U/Pb age data

The intrusion depth for the VOI is presently not well constrained, but the field evidence for partial melting of the wall rock gneisses, indicate that the VOI intruded into hot crust, which either could reflect deep crustal levels, or that shallower crust was heated during prolonged period of magmatism prior to the emplacement of the VOI.

The surrounding migmatitic gneiss foliation follows a roughly NW–SE regional trend, with a steep dip towards NE that is consistent with a non-transpressional collision zone towards the NE (Kolb et al. 2013). The abundance of amphiboles within the VOI, which in places define a weak foliation that is slightly oblique to the magmatic bedding, suggest that it was emplaced during the waning stages of the orogeny that foliated the gneisses. In support of a late tectonic stage for the intrusion are preliminary age data on felsic sheets that occur locally in the contact zone, where they cut across the basement and into the Marginal Zone (Figure 10). Age dating by zircon U/Pb of two of such felsic sheets (back-veins) give a consistent age of 2690 ± 4 Ma (Kokfelt et al., unpublished data), suggesting that the VOI was emplaced relatively late, post-dating the main deformation phase. A late stage emplacement for the VOI seems to be generally consistent with the pristine magmatic textures characterising the intrusion.

The apparent lack of olivine yet abundance of pyroxenitic rocks along the Marginal Zone could reflect that the Vend Om magma chamber initially was filled by a MgO-rich and SiO_2-rich (boninitic) parental melt. However, three major element trends, consistently towards the accumulation of either (1) ~80% plagioclase (~An_{80}) and ~20% hercynite spinel (2) Fe-Ti oxide (ilm:mt = 1:3), or (3) pyroxene (cpx:opx = 3:2), all converge onto a possible parental magma with ~10 wt% MgO, ~42 wt% SiO_2, ~16 wt% Al_2O_3, ~10 wt% CaO, ~15 wt% Fe_2O_3 , ~2 wt% TiO_2, 2 wt% Na_2O and ~1 wt% K_2O (Grobbelaar, 2012). Thus, it may be

that olivine and clinopyroxene reacted with the remaining liquid and water to produce the poikolitic hornblende (Thomsen, 1998), leaving behind an apparent predominance of opthopyroxene in the marginal zone.

The most primitive potential feeder dyke lies on the ‘pyroxene accumulation’ trend with 15 wt% MgO and could therefore represent either a fine grained cumulate or a parent to the marginal zone. Compared to the slightly depleted, yet LILE-enriched and highly erratic incompatible element patterns for most cumulate rocks, with distinct negative anomalies for Th, U, Nb, P and Zr, this ‘feeder dyke’ has the most regular OIB-like incompatible trace element pattern, with only distinct negative Th and U anomalies.

Given that the marginal zone could have been an (ol)+px cumulate, derived from a more typical mantle-derived, yet possibly enriched OIB-like, basaltic primary magma, more evolved interstitial melts (e.g., identified by the converging ‘accumulation trends’, mentioned above, could subsequently have escaped, e.g. through filter-pressing processes) from this marginal mush and into still molten centre of the central magma. Eventually, the insulated and still molten core of the magma chamber continued to crystallize slowly enough to produce the Layered Sequence. It is possible, that this relatively small intrusion only was filled once and thereafter crystallized as a closed system, much like the Skaergaard Intrusion (Nielsen, 2004).
Possible feeder dykes trending NE-SE and a possible trough-like Layered Sequence that dips towards NE (Figure 8) loosely indicate that the VOI intruded during SW-NE extension and may subsequently have been tilted towards the NE. Thus, it is possible that deeper parts of the Layered Sequence are exposed in the SE whereas the upper roof of the intrusion is exposed towards the NW. Alternatively, igneous layers within a non-tilted intrusion concentrically on-lap its margins and dip progressively less towards its centre.

The above petrogenetic speculations are highly preliminary and based on samples collected in 2011 (Grobbelaar, 2012). Further systematic mapping and sampling of the magmatic layering across the VOI was carried out during the 2012, and subsequent field work and analytical results will be presented in the form of a M.Sc. thesis planned to be handed in at AAU by Bjørn Maarupgaard in spring 2015.

Halvdans Fjord

Several types of late-kinematic intrusions, ranging from pyroxenitic to granitic compositions, are exposed along the shores of Halvdans Fjord. Previous mapping (Escher 1990) generalized the geology in the area into granulite facies agmatitic tonalite-trondhjemite-granodiorite (TTG) gneisses, which host several NW-SE trending, foliation-parallel and SAP-related intrusive bands of either more mafic gabbro-diorite or felsic granite-diorite (pale purple and pink colours, respectively, in Figure 12a). Bad weather left the authors with little more than 2 days for a reconnaissance around the fjord and some systematic work at three localities. Our observations (Figure 12b) only verify the approximate location and distribution of (1) a more felsic (dioritic) intrusion in the innermost western part of the fjord, and (2) a more mafic (gabbroic) to ultramafic layered intrusion with large ultramafic xenoliths along the eastern shore of the outer (southern) to central parts of the fjord. The large gabbro-diorite intrusion in the north-eastern part of the fjord of Escher (1990) was not observed within the newly well exposed parts beneath a retreating glacier, but outcrop more southerly as a (leuco)gabbro in another side-valley and as a layered ultramafic-mafic base along the outer eastern shores of the fjord. Thus, the mafic-ultramafic intrusion does not extend as a NW–SE trending foliation-parallel band farther onshore, but appears for most parts to be restricted to the coastal parts by more inland agmatitic gneiss. The Escher map is an oversimplification and accentuation of the actual field relations as recorded in the reconnaissance mapping in 1:50.000 (Nielsen and. Rosing 1987, in archive of GEUS).

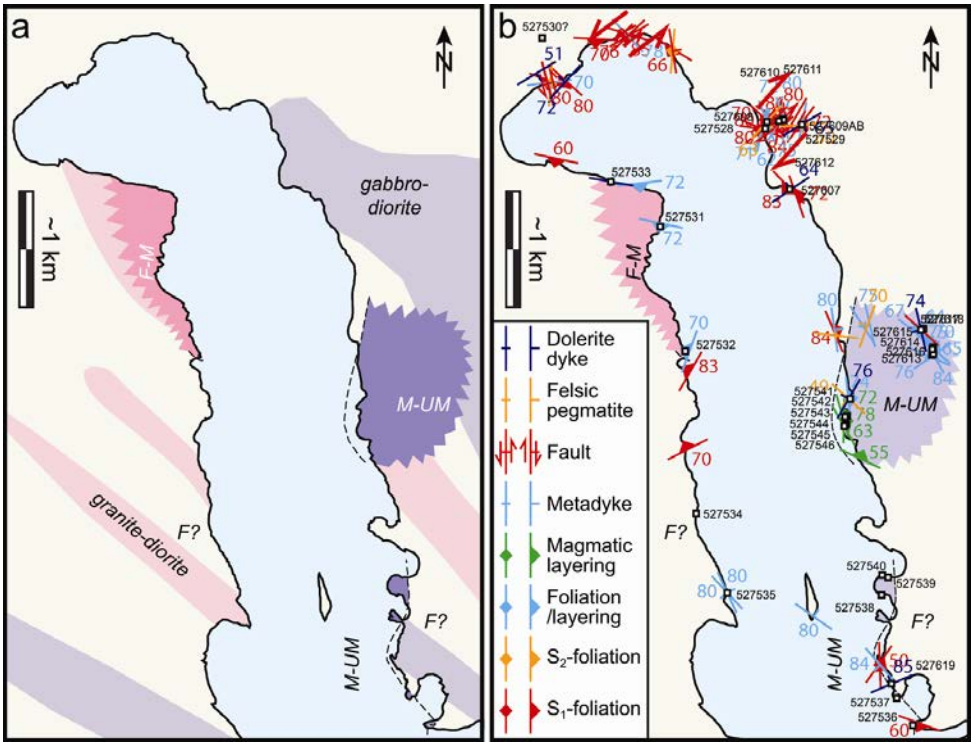

Figure 12. *Geological maps of the Halvdans Fjord area. (a) Original map of Escher (1990) with units of gabbro-diorite (pale purple) and granite-diorite (pale pink), and with the added new observations from 2011 of ultramafic (UM), mafic (M), and felsic (F) rock units. In some cases foliated felsic intrusives are difficult to distinguish from the granulite agmatitic gneiss (pale yellow). (b) Redrawn geological map shows new structural measurements and sample localities.*

Agmatitic gneiss basement

The high-grade granulite facies agmatitic gneisses are very leucocratic and only weakly foliated in a generally WNW–ESE orientation (Figure 13a,b). In some places, however, thin dark bands define a S_1-foliation, which in the innermost part of the fjord is overprinted by an oblique S_2-foliation (Figure 13c). Mafic inclusions are often highly deformed, small and scattered throughout the less foliated agmatitic gneiss, whereas in other parts distinct foliations wrap irregularly around sub-parallel bands of more angular and larger mafic inclusions (Figure 14).

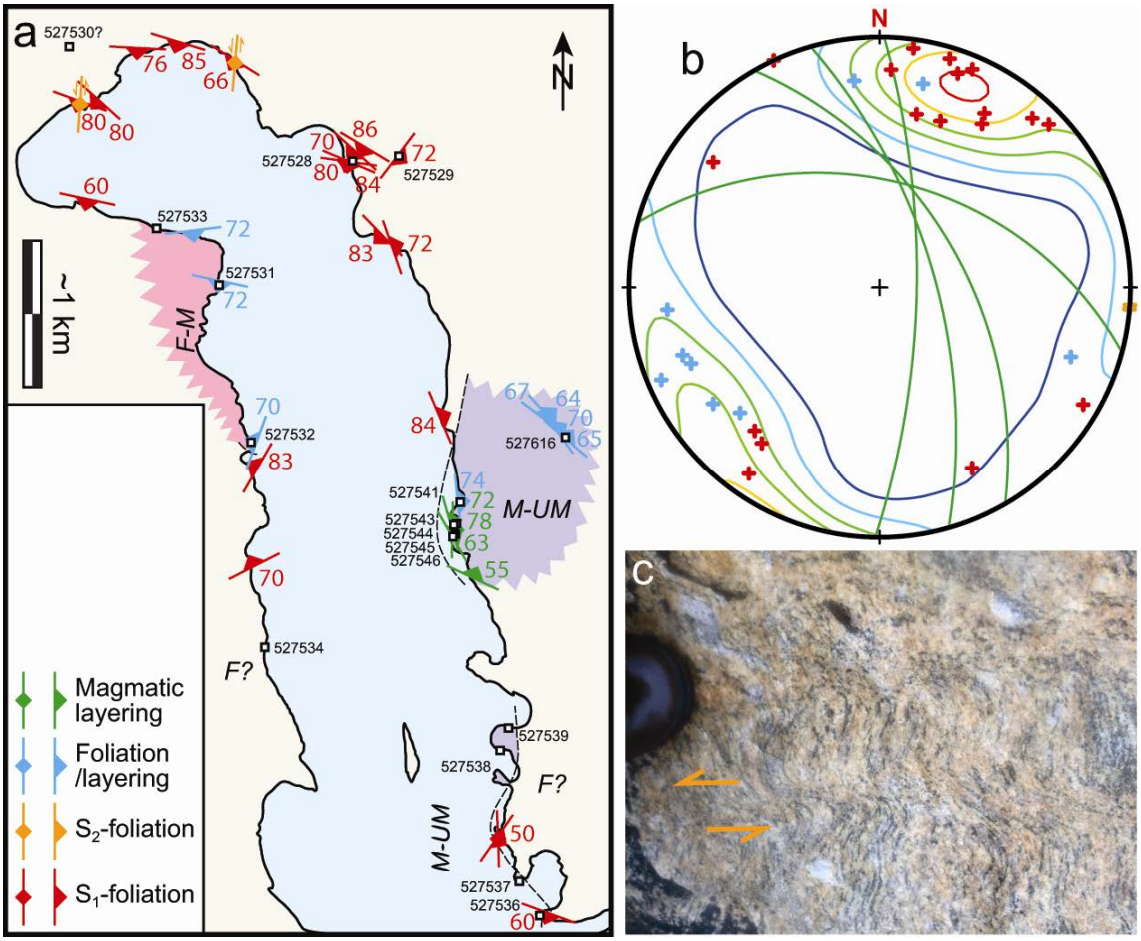

Figure 13. *Pervasive basement structures around Halvdans Fjord, including foliations and magmatic layering. (a) Map distribution of field measurements. M-UM = mafic-ultramafic gabbroic-pyroxenitic intrusion (pale green); F-M = felsic-mafic intermediate (grano)dioritic intrusion (pale orange); F? = uncertain felsic late-kinematic granitic intrusion (difficult to differentiate from agmatitic gneiss, pale yellow). (b) Stereographical presentation of all structures, as in Figure 8, and following the colour coding in (a). (c) Example of common S1-type foliation (roughly vertical in picture) in agmatitic gneiss, onto which a rarer S2-foliation is superimposed (roughly horizontal in picture, where orange arrows indicate sense of superimposed shear).*

The surrounding migmatitic gneiss foliation follows a mode WNW-ESE regional trend, with vertical to very steep dips towards SSE (Figure 13a-b). These strikes are roughly parallel to those around the Vend Om Intrusion (Figure 8), and can all be related to a collision zone towards the NE (Kolb et al. 2013). Slightly more easterly S_1-foliation strikes along the inner

parts of Halvdans Fjord are overprinted by vertical and N-S-striking S_2-foliations (S-C type fabric), with a sinistral strike-slip shear component.

Figure 14. *A heterogeneous agmatitic gneiss, including alternating mafic and felsic parts with steeply SSW-dipping irregular foliations. Older structures are offset by at least two fault sets, which are utilized by very pale felsic pegmatites. Outcrop is c. 8 m across.*

Late-kinematic SAP intrusions

It is sometimes difficult to discriminate between agmatitic TTG gneiss host rocks and younger intrusions that reputedly belong to the SAP. Poorly foliated agmatitic TTG gneisses with fewer amphibolite inclusions may be mistaken as late-kinematic SAP granite-diorites, and *vise versa*. Such uncertainties allow some amphibiolites within agmatitic gneisses to be SAP-related gabbro-diorite xenoliths within even younger SAP granite-diorite intrusions. As an example, it is debatable whether our reconnaissance mapping of a relatively large and partly migmatized amphibolite outcrop (Figure 15) is part of Escher's (1990) north-eastern gabbro-diorite intrusion, and thereby part of an even larger mafic-ultramafic intrusion that extends far south along most of the eastern side of Halvdans Fjord (cf., Figure 12a). Only the more evidently late-kinematic intrusions on Figure 12a are described below.

Figure 15. *Questionable basement rocks. (a) Highly deformed and migmatized mafic inclusions and dark bands that enhance foliation, is often diagnostic of amphibolite-bearing TTG gneiss but could also be features within a late-kinematic granite-diorite SAP intrusion. GPS receiver is c. 4 cm wide. (b) Station 11TFK008: Deformed and partially migmatized mafic rocks are also often diagnostic of TTG gneiss hosted amphibolites, but could be parts of a late-kinematic and granite-hosted gabbro-diorite intrusion, both of which are part of the SAP. This net-veined metagabbro outcrop is also cut by (1) a pale meta-dyke (MD; 527529) of an apparent intermediate composition, (2) a regular felsic pegmatite (FP; 527609), and (3) a dolerite dyke (DD, note horizontal upper chilled margin across the lower third of the picture).*

Mafic-ultramafic layered intrusions

At least two, several m-thick and steeply ENE dipping ultramafic layers were mapped and sampled (527539, 527543 & 527545) along the central eastern shores of Halvdans Fjord (Figure 16a,c). These pyroxene-rich layers are inter-bedded by more or less uniformly hornblende-poikolitic, schliered or layered leucogabbroic units (527541, 527544 & 527546). Assuming the stratigraphy to be up towards the ENE, it is tentatively suggested that these ultramafic units represent the lower part of an even thicker layered intrusion, perhaps extending >1 km ENE and up into some upper part that consist of less layered and more heterogeneously pegmatitoidal (leuco)gabbroes (cf., Figure 22). Further work needs to test this hypothesis, as well as continue a systematic sampling across the layered sequence.

The ultramafic units can probably be correlated roughly along strike and farther southwards along the fjord's shore (Figure 12a; 527537; Figure 18), where they tend to become more angularly brecciated, partly migmatized and pervasively intruded by felsic veins (Figure 19). The nearby eastern gneiss, bounding these ultramafic-mafic layers along this possible southern extent, is, however, difficult to reconcile with a proposed >1 km stratigraphical

thickness of more evolved gabbroic units along its northern extent of a single larger layered intrusion, and needs to be further investigated. Thus, it cannot be ruled out that a substantially larger layered ultramafic-mafic intrusion, than indicated by our mapping, covers most of the eastern side of Halvdans Fjord. The bedding of this layered intrusion is, furthermore, trending orthogonal to the foliation-parallel bands suggested by Escher (1990).

Figure 16. *(previous page) Meter-scale ultramafic-mafic layering. (a) Along-strike view of sharp, regular and steeply ENE-dipping contact between an ultramafic base and top of a schliered leucogabbroic layer. Brown notebook is 17×12 cm. (b) Close-up of contact in (a), showing large poikolitic hornblende (black) and sub-euhedral feldspar phenocrysts (white) in a coarse grained pyroxenitic matrix (predominantly brownish orthopyroxene), and the medium grained and slightly foliated texture of the underlying (right) leucogabbro. PDA-pen is ~0.1 m long. (c) Close-up and westward continuation of outcrop in (a), showing a second ultramafic layer at the base of the c. 6 m thick schliered leucogabbros (pale unit in right centre of picture), below which the layered gabbroic sequence in Figure 17 is located.*

Figure 17. *Steeply ENE dipping layering in the medium grained gabbroic base of the cross-section shown in Figure 16. (c). A coarse grained leucogabbroic xenolith deforms layering to the left in this picture, and both units are cut by a felsic pegmatite. Brown notebook is 17×12 cm.*

Figure 18. *Possible southward along-strike continuation of ultramafic-mafic layered sequence in Figure 17. (a) Relatively coherent sequence of steeply E-dipping layers of c. 4 m of gabbro (paler centre) bound by brown-weathered pyroxenites. Late felsic veins appear to preferentially have intruded along the relatively sharp layer contacts. (b) Felsic pegmatite veins brecciating a pyroxenite (and hosted grey meta-dyke) into angular blocks. Width of view c. 2 m.*

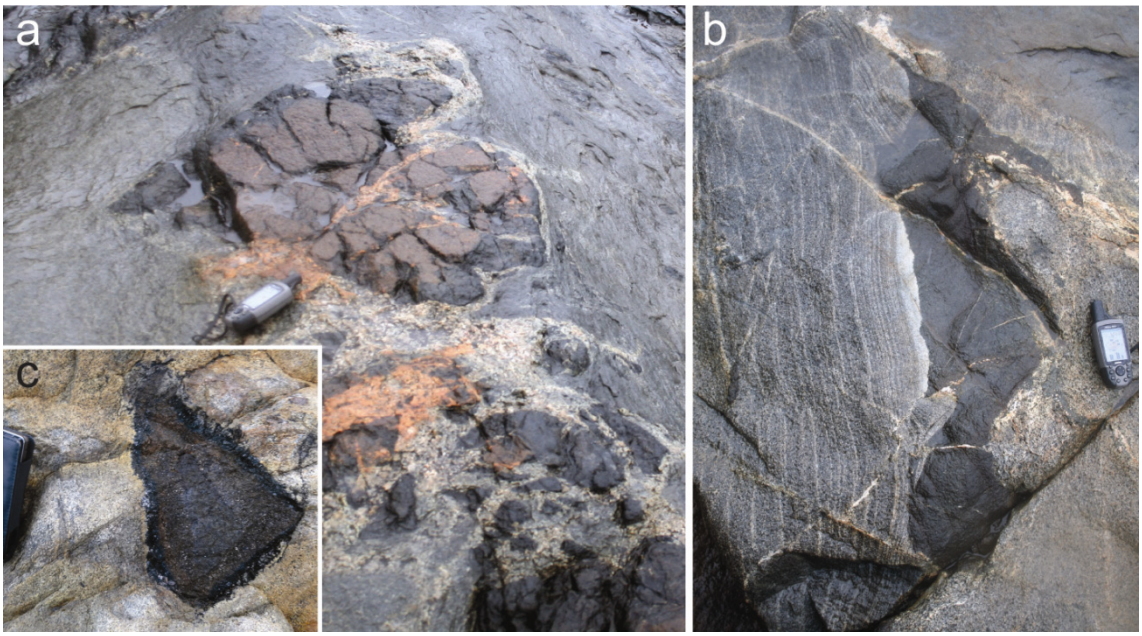

Figure 19. *Ultramafic xenoliths. (a) Pyroxenitic xenoliths in a pale grey gabbroic host separated by an envelope of felsic material, which also commonly vein the xenoliths in an anatectic fashion. Grey GPS receiver is ~15×5 cm. (b) Spectacularly zoned haloes around some ultramafic xenoliths possibly reflect some hydrous interaction during the crystallization of the surrounding gabbroic melt. GPS receiver is ~15×5 cm. (c) For comparison, an ultramafic xenolith within the more felsic diorite in Figure 20 is gradually metamorphosed into having a black phlogopite rim and a fibrous chrysotile zone surrounding a relict core. Visible edge of PDA is c. 14 cm long.*

Intermediate-felsic intrusions

As mentioned, Escher (1990) indicates the presence of several foliation-parallel and SE-NW trending granite-diorite bands across Halvdans Fjord, which we find are difficult to distinguish from weakly foliated agmatitic gneiss. More detailed field work may in the future should be able to distinguish between an older agmatitic TTG basement and reveal the presence of much more SAP-related felsic (granitic-dioritic) intrusions than we are able to, especially within areas labelled with an “F?” on all maps.

Figure 20. *Southern contact zone of a SAP-related, late-kinematic diorite intrusion, as exposed along the shores of Halvdans Fjord. (a, on previous page) Diorite (right) in contact (white arrow) with agmatitic gneiss (left). (b) Closer look at heterogeneous contact zone, consisting of irregular fine grained intrusive veins into the coarser grained diorite. Folded measuring rod c. 0.2 m long.*

One of Escher's (1990) less granitic and more dioritic intrusions, in the inner western part of Halvdans Fjord, is more easily recognised and confirmed in the field (Figure 20). Compared to the agmatitic gneiss, it stands out with its smoother and slightly more orange weathered surfaces, which expose a very weakly foliated and more homogeneously textured diorite that does not contain many inclusions. The angular ultramafic xenoliths in Figure 19c are exceptional and, together with an equally rare presence of meta-dykes and its weak foliation, consistent with this diorite being a relative young SAP-intrusion that may have engulfed some of the ultramafic layers described above. Only close to its southern contact along the shore of the fjord (Figure 20a), does the intrusion exhibit a more heterogeneous texture of irregularly intermingled coarse and finer grained parts (Figure 20b). It is uncertain whether these finer grained parts represent later magma pulses or felsic back-veining along the intrusion's contact.

Foliated dykes/sheets (so-called 'meta-dykes')

Most SAP intrusions, as well as their agmatitc TTG gneiss host, are intruded by finer grained, foliated, and even variably deformed meta-dykes, which are present right around Halvdans Fjord (Figure 21a; possibly less so within the diorite intrusion described above). The fact that such dykes are consistently cut by felsic pegmatites (e.g., Figure 22.), further testify towards these intrusions being related to the SAP. In fact, it is believed that these meta-dykes are associated with, and some within the host agmatitic gneiss may even represent feeders to the SAP intrusive complexes. Thus, the geometries and compositions of

these meta-dykes provide crucial information of both palaeo-stress fields and petrogenetic processes, respectively, during the formation of the SAP. Especially, since the whole rock geochemistry of possible cumulate samples from larger intrusions cannot directly provide liquid compositions.

Our compilation of 21 meta-dyke orientations shows a clear clustering of sub-vertical dykes within roughly NW-SE trending swarms (Figure 21b). Slightly different trending sub-swarms may be inferred, as well as it is also possible that some meta-dyke orientations have been tectonically rotated. Some pillow-like meta-dykes may represent intrusions into a still partly molten magma chamber or cumulates, but could also have experienced a higher degree of ductile deformation. Most other meta-dykes, however, are more regular and preserve relict brittle intrusive structures, such as offsets, horns and chilled margins (Figure 21c).

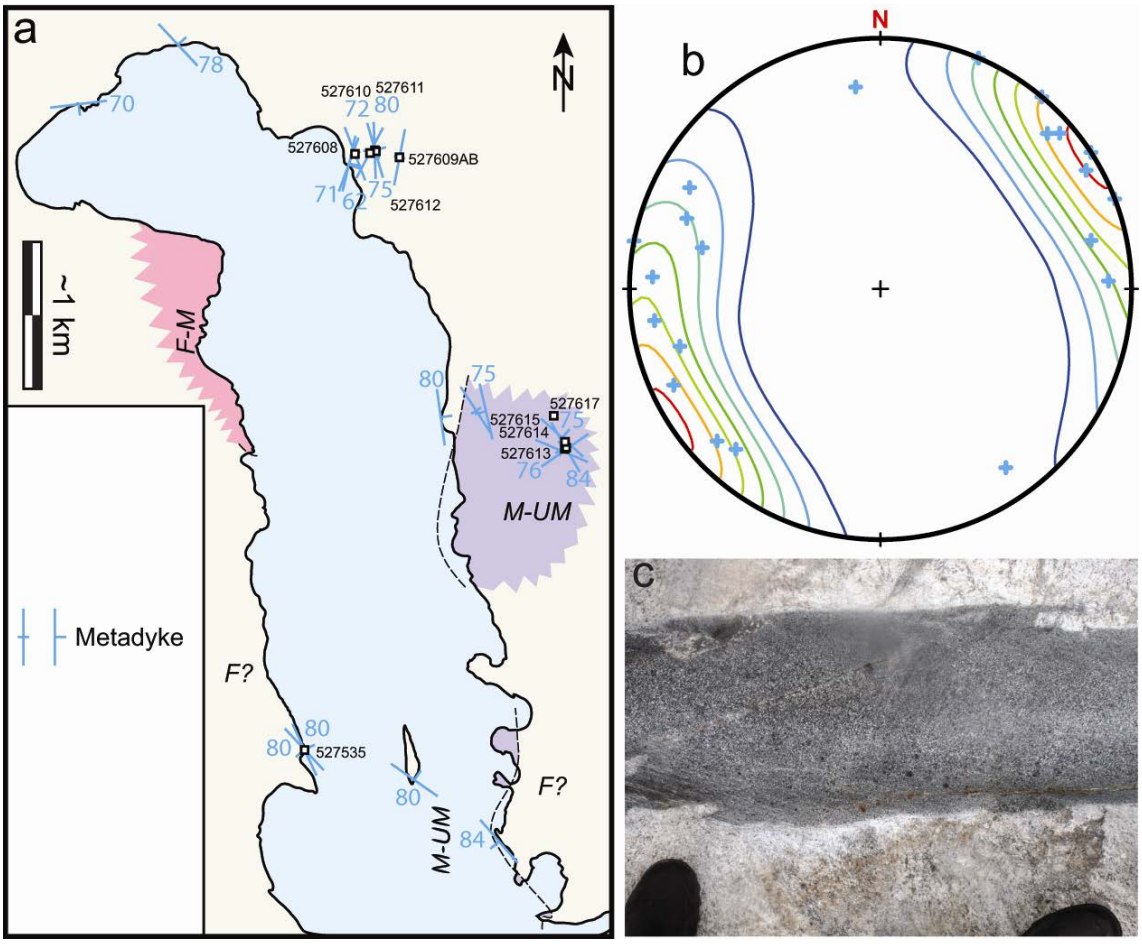

Figure 21. *Variably foliated and deformed meta-dykes around Halvdans Fjord. (a) Map distribution (location) of measurements and sampled dykes. (b) Stereographical presentation of measured dyke orientations, as in (Figure 8). Note predominant sub-vertical and NE- to N trends. (c) Field example of a c. 0.3 m thick and more regular meta-dyke in an agmatitic gneiss. Note broken bridges that may have been dextrally displaced along the dyke plane.*

Within the inland gabbroic part of the mafic-ultramafic intrusion along the eastern side of Halvdans Fjord (Figure 21a), meta-dyke cross-cutting relationships reflect a systematic intrusive sequence of progressively more evolved magma compositions (Figure 22). Thus, whole rock geochemical samples of melanocratic (527613), mesocratic (527608, 527610,

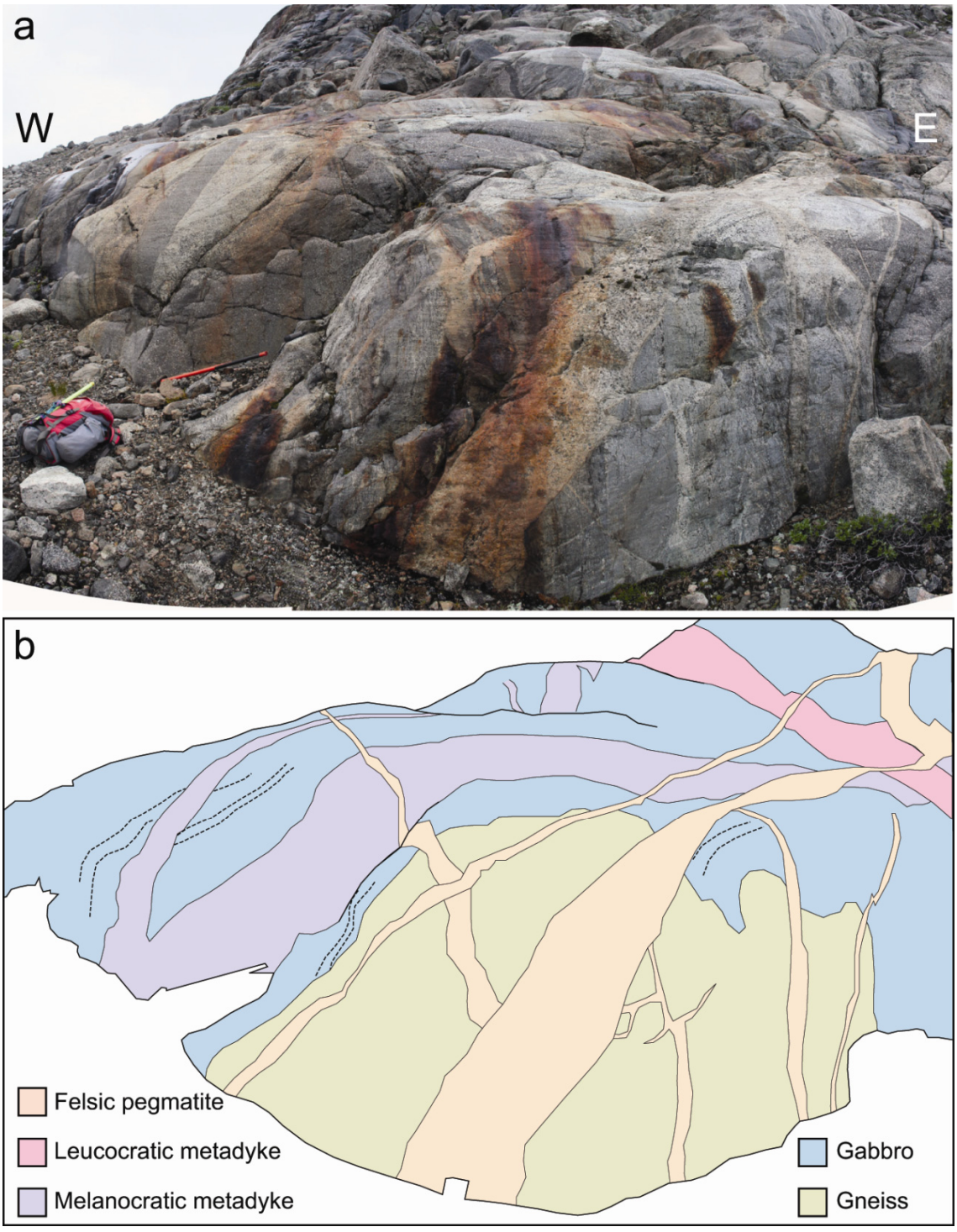

Figure 22. *(previous page) A locally layered (dashed lines) and heterogeneously pegmatitoidal (leuco)gabbro, hosting a gneissic xenolith (causes brown staining) is cut by several tabular intrusions: (1) an irregular and melanocratic intrusion (527613), typically cut by more mafic meta-dykes (not exposed in this outcrop; 527615), (2) a more regular and leucocratic meta-dyke (527614), and (3) two orthogonal sets of pegmatites. (b) Drawing of (a). Orange-black sledge hammer shaft is c. 1 m long.*

527611, 527615 & 527612) and leucocratic (527614 & 527616) meta-dykes will help constraining magmatic differentiation processes, during the formation of the SAP.

Most meta-dykes are <1 m thick, but one *c.* 7 meter thick meta-dyke like intrusion cut through the agmatitic gneiss in the outer western parts of the fjord (527535). In addition to being deformed, it also appears to be slightly migmatized, and/or possibly back-veined by partial melts from the host gneiss.

A petrogenetic study of 18 alkali (picro-)basalt to basaltic trachy-andesite meta-dyke and sheet samples, collected in 2011, is presented in an unpublished Honours Thesis (Graaf, 2012). Of these, six bulk rock analyses from Halvdans Fjord exhibit the widest compositional range between 17 to 4 wt% MgO and arguably have slightly higher Al_2O_3, K_2O, Ba and Eu than the other meta-dykes and sheets. Their incompatible element patterns – even of the most primitive 'Halvdan' sample – are not quite as enriched as the OIB-like 'feeder dyke' for the VOI, described above, and have distinct negative Th, U, Nb, P, Zr and Ti anomalies that characterize VOI's cumulative rocks, as well as most other SAP samples. Many of these anomalies are typical for subduction zone magmas, derived from a relatively pristine mantle wedge, apart from the unusual negative P, Zr (and Hf) that remain to be explained.

Younger features

Younger features refer to more angular (brittle) intrusions or structures, which have experienced both a lower metamorphic grade compared to their host rocks and very little ductile deformation. Around Halvdans Fjord, these features include felsic pegmatites, brittle faults and dolerite dykes, which are described in more detail below.

Felsic aplites-pegmatites

Most felsic pegmatites are relatively undeformed and angular, planar intrusions, which may locally be oriented in some systematic patterns (Figure 23). There is little clustering, however, exhibited by only five measured orientations from three localities along the inner, eastern part of Halvdans Fjord (Figure 23a-b). These felsic intrusions are rarely >1 m thick and more often pegmatitic than aplitic. Two aplitic-pegmatitic veins are sampled for U-Pb geochronology on extracted zircons (527540 & 527542).

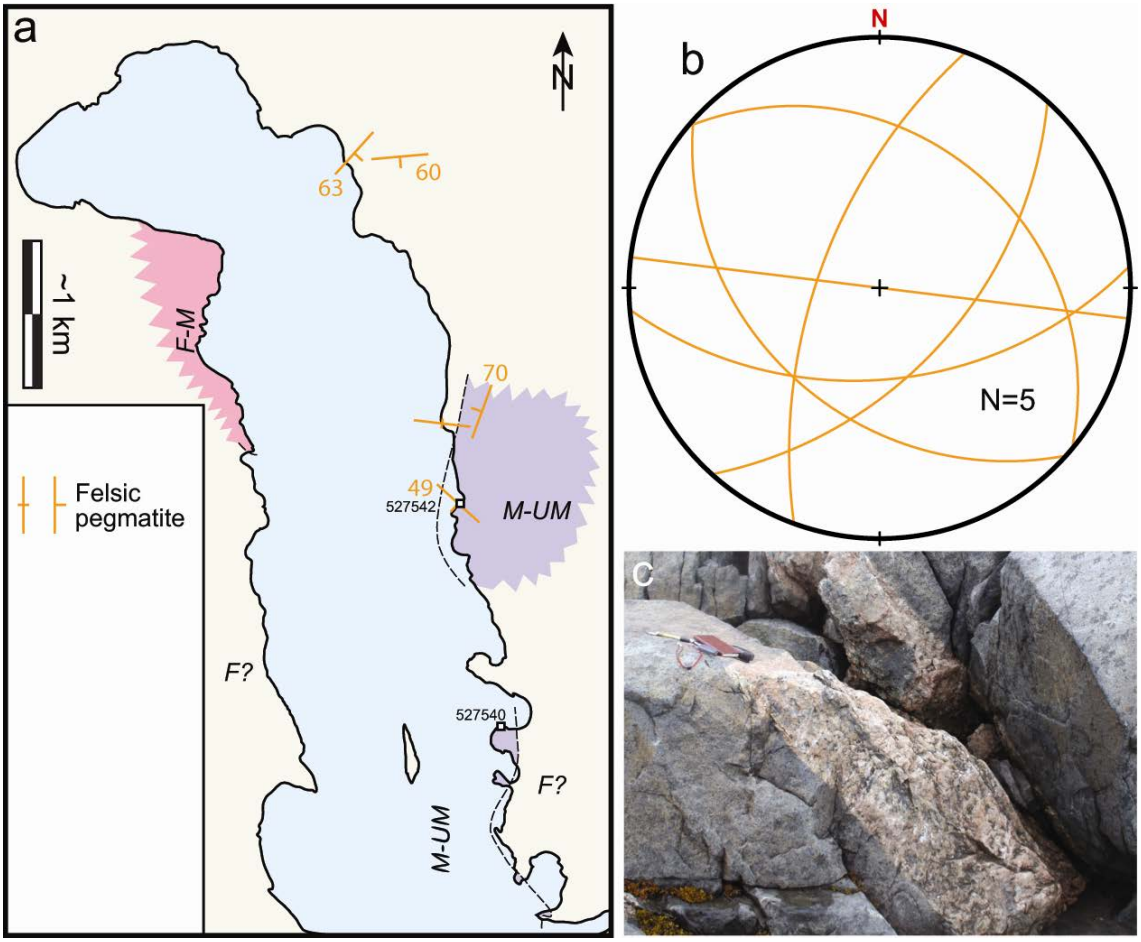

Figure 23. *Five mapped and sampled felsic pegmatites around Halvdans Fjord. (a) Map distribution. (b) Stereographical plot showing apparently unsystematic orientations of pegmatite planes, as in Figure 8. (c) Field example of a regular, c. 0.4 m thick and moderately SW-dipping pegmatite (sample 527542 in a), in a hornblende-poikolitic gabbro host. Note book, geological compass and pens for scale.*

Brittle faults

Some pegmatites appear to have intruded along older fault planes, but in most other cases brittle faults also cut felsic pegmatites (e.g., Figure 24c). Brittle fault zones are often hydrothermally altered into greenish epidote and/or red-coloured K-feldspar, and/or rusty weathered. Many faults with generally <1 m of apparent displacements were observed around Halvdans Fjord, but were mainly measured along the inner parts of the fjord (Figure 24a). There appears to be some clustering into SW-NE trending and steeply dipping to vertical faults within two localities. Most of these fault measurements were done on sub-horizontal outcrops and thereby mainly exhibit apparent strike-slip components (only in rare cases verified by sub-horizontal slickensides), with shear senses that are consistent *within*, but opposite *between*, each of the two localities (Figure 24a-b). Thus, it becomes more difficult to relate these few structural results to any single regional tectonic event, as, e.g., inferred from faults within the Vend Om Intrusion (Figure 8). No pseudotachylite faults, or apparent thrusts or normal faults, were observed around Halvdans Fjord.

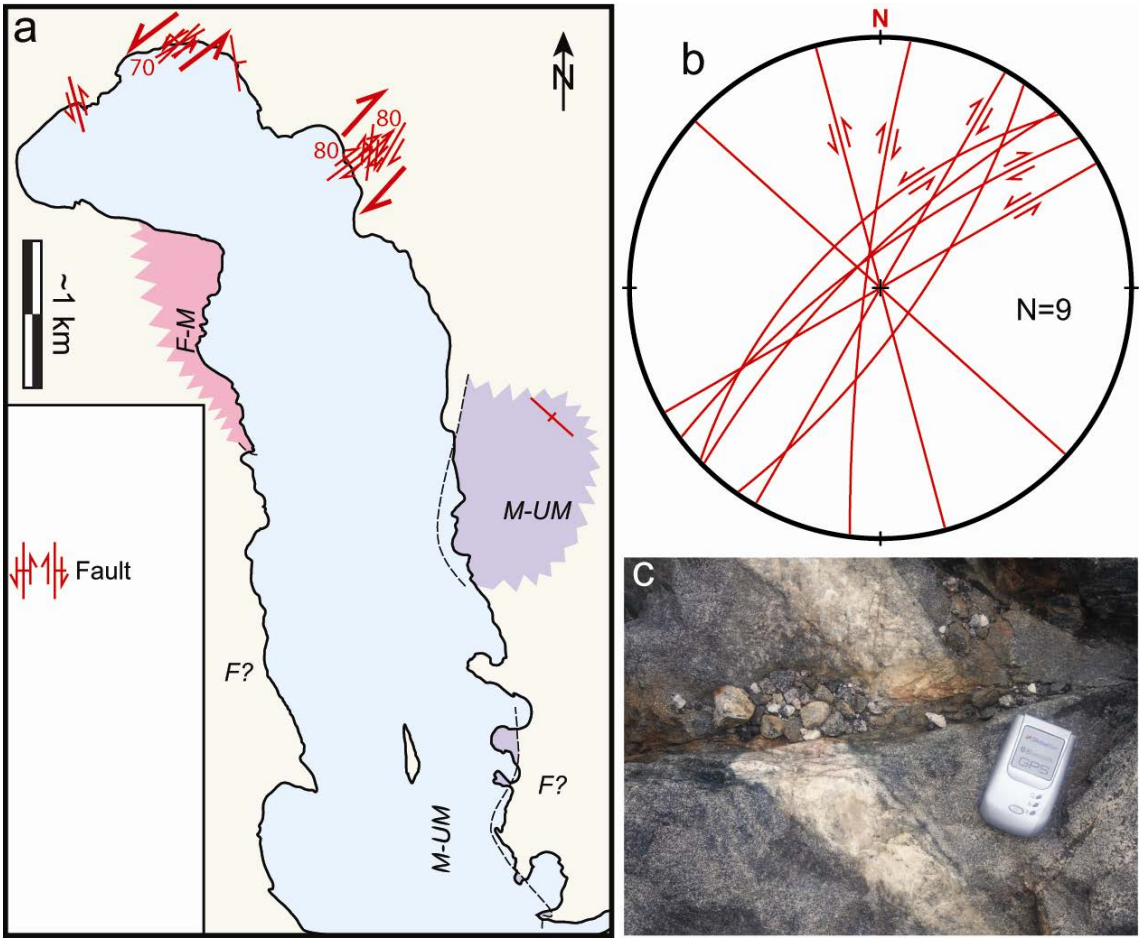

Figure 24. *Nine brittle faults around Halvdans Fjord. (a) Map distribution, where large displacement arrows indicate consistent shear indicators within a given area. (b) Stereographical plot showing fault planes with apparent horizontal displacement vectors, as in Figure 8. (c) Field example of a slightly rusty brittle fault that displaces a felsic pegmatite in an amphibolite host, by an apparently dextral strike-slip component of nearly 7 cm (~length of GPS transceiver).*

Dolerite dykes

Seven dolerite dykes were mapped (Figure 25a) and a few more were observed around Halvdans Fjord. It appears that the area is mainly transacted by a roughly SW-NE trending dyke swarm (527607 & 527619) and one ~24 m thick and NNW-SSE trending dyke (529618).

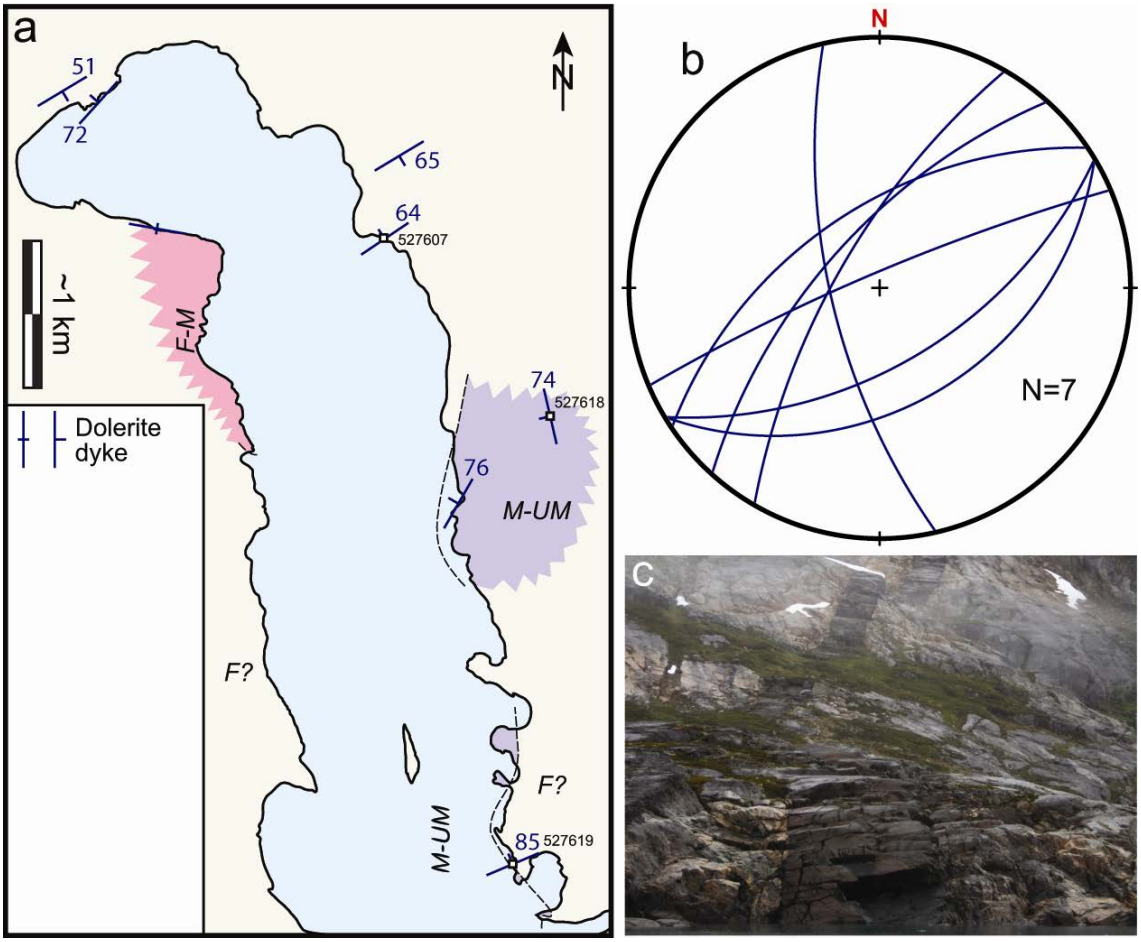

Figure 25. *Seven mapped and sampled doleritic dykes around Halvdans Fjord. (a) Map distribution. (b) Stereographical plot showing two major orientations (SW-NE and one NNW-SSE) of doleritic dykes, as in Figure 8. (c) Field example of a slightly irregular, c. 3 m thick and WSW-ENE trending dolerite dyke (sample 527619 in (a)) in an agmatitic gneiss. Looking ENE.*

Stærkodder Vig

The geological map of Escher (1990) indicates that granulite facies agmatitic TTG gneisses host a pair of NW-SE trending and foliation-parallel amphibolite bands across Stærkodder Vig, and larger intrusions farther west (Figure 26a). Some contact along the Stærkodder Vig and glacial valley appears to separate a more extensive body of amphibolite to the south from an abundance of ultramafic rocks to the north. An unidentified *c.* 1 km wide body is indicated within the southern amphibolite (? In Figure 26).

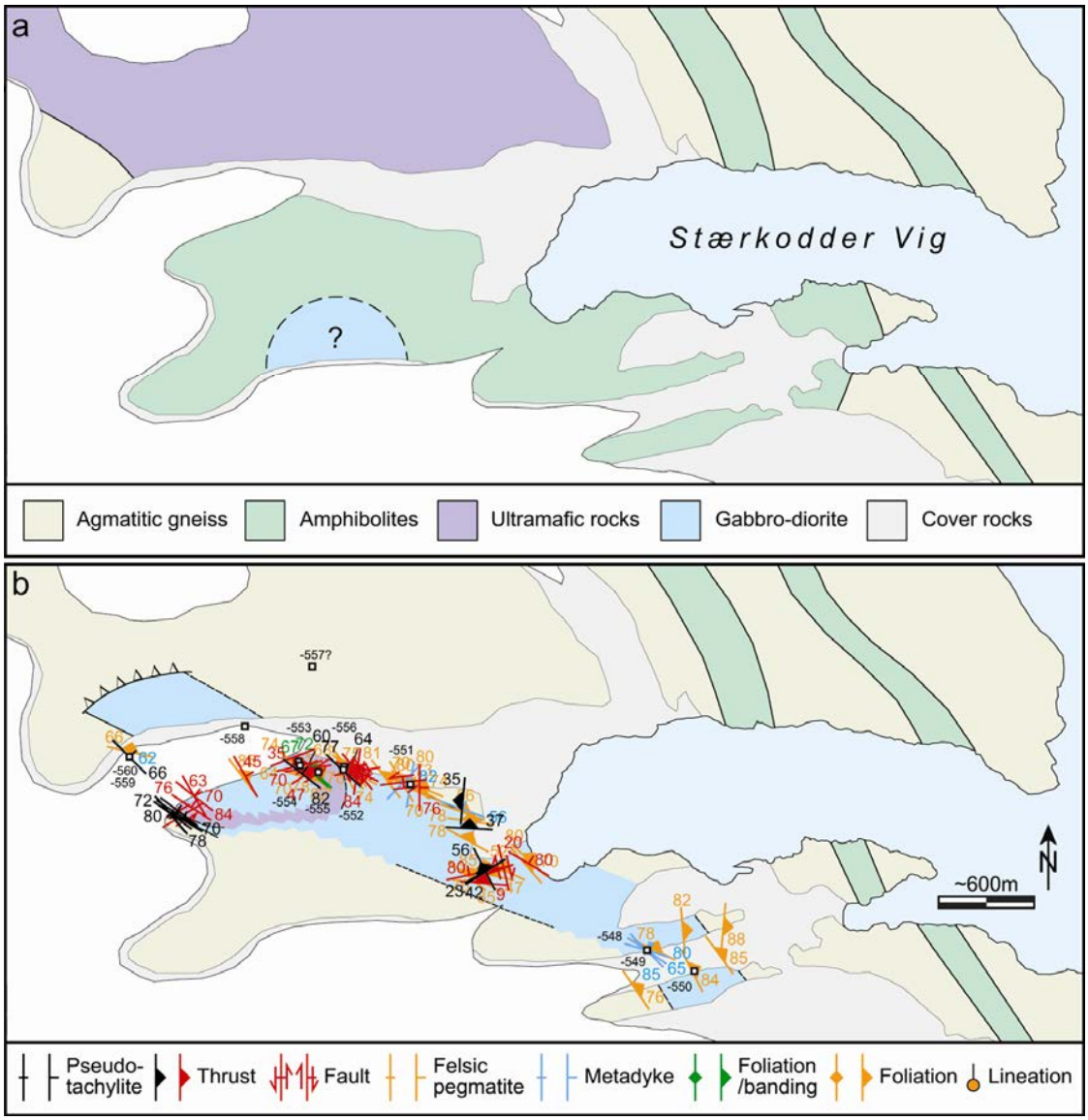

Figure 26. *Geological information on the area around Stærkodder Vig (pale blue). (a) Escher's (1990) map of basement gneiss, amphibolite and ultramafic rocks. Pale blue half circle may be miscoloured on Escher's (1990) map, unless indicating the unlikely presence of either a nephelinite intrusion or marble. (b) The authors could only verify an elongated, variably foliated and heterogeneous assemblage of variably preserved metadiorite to melagabbro (blue), onto which all of this report's structural measurements and sample localities (527-prefix omitted from each label) are superimposed. Escher's (1990) easterly amphibolite bands are kept on this and following maps, because these dark bands were observed from a distance.*

The geology depicted in Escher (1990) is both exaggerated and in part erroneous compared to the 1:50.000 field maps from which Escher made his compilation. The 1:500.000 compilation joins more exposures of mafic and ultramafic rocks in a major body without sufficient field control. The joining of the exposures is a consequence of the scale in which the geology is compiled. The unidentified body is mis-coloured and in fact gneiss. The ultramafics NW of Stærkodder Vig are seen in Fig. 29 as dark rounded exposures characterized by light-coloured to pinkish and irregular veins and pegmatites.

Our observations were made from 2.5 days of effective field work along three traverses along (1) the valley and ridge just west of the lesser bay in Figure 27, (2) the S-side of Stærkodder Vig valley, up to the glacier, and (3) along the westerly glacier tongue. Field work focused on what appears to be a band of variably deformed dioritic-melagabbroic intrusions, surrounded by agmatitic gneiss and cut by relatively few meta-dykes. Most of these SAP-related igneous intrusions are pervasively sheared and foliated. In comparison, the area is also much more heavily deformed by brittle faults and thrusts, including an abundance of pseudotachylite breccia veins.

Foliated felsic to mafic basement rocks

The blue band in Figure 27 outlines a more complex but roughly foliation-parallel alignment of dioritic to melagabbroic intrusions.

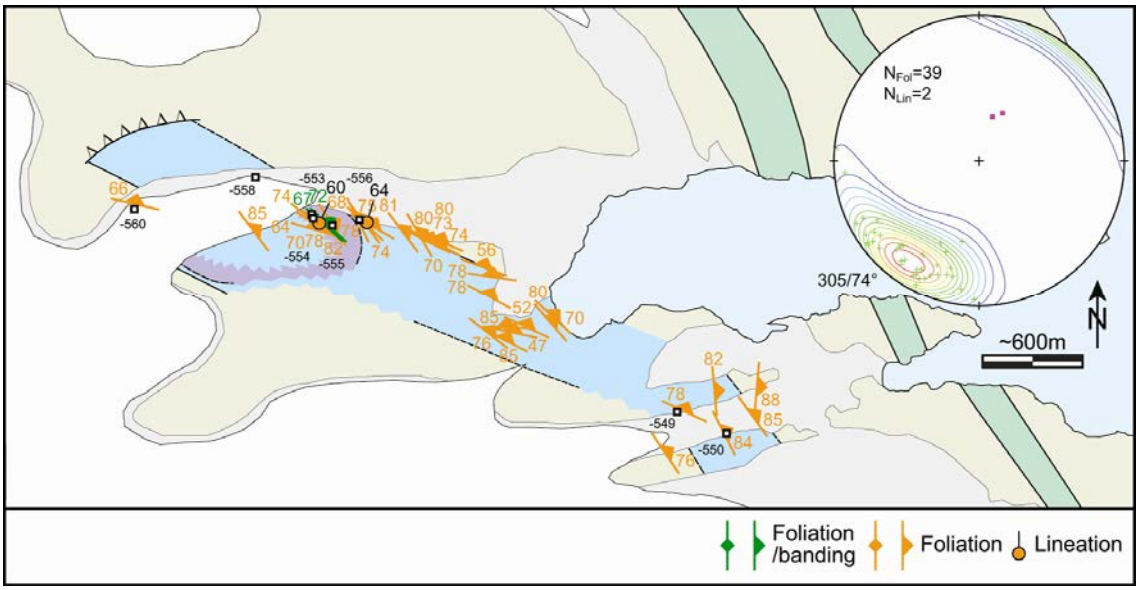

Figure 27. *Sample localities of mafic and felsic basement rocks, as well as measured ductile structures, west of Stærkodder Vig. The mode orientation (i.e., peak of the contoured foliation poles) is 305/74° (RHR) and two lineations (red dots on stereographical plot) plunge on average 62°→021. Map details as in Figure 26 and stereographical plot as in Figure 8.*

Figure 28. *WNW-view from near sample site 527549 (Figure 27) across a minor glacial gully and towards ridge that exposes a contact between paler felsic rocks (left) and darker mafic rocks (right). The ridge is also cut by several gently N-dipping thrusts (indicated by arrows), as well as roughly foliation-parallel felsic pegmatite veins in the foreground.*

The roughly foliation-parallel S-contact was traced up behind the ridge along the S-side of the Stærkodder Vig glacier (Figure 28), and presumably extends to the inner N-side of the Stærkodder Vig glacier (Figure 29), where the band also appears to 'terminate' along what is tentatively interpreted as a partly thrust-generated 'roof' contact.

Figure 29. *Northwards view across glacial valley towards the northern termination of mafic band (pale grey metagabbro) in Figure 27(b). A faulted(?) SW-contact of the mafic intrusion is exposed above the scree cone to the left of the waterfall, whereas the thrusted(?) roof of the intrusion appears to follow a prominent ledge that separates grey gabbroic outcrops below from apparent gneissic outcrops above. Height of waterfall is c. 50 m.*

The contact was accessed on a well exposed glacial outcrop along the inner S-side of the Stærkodder Vig glacier (Figure 31), where several roughly foliation parallel pseudotachylite faults appear to have produced a repetition of contacts between paler gneiss and darker gabbroic rocks (Figure 32). Most outcrops are homogeneous grey diorites to gabbro, but more melanocratic and hornblende porphyroblastic varieties are concentrated at both ends of the traverse along the S-side of the Stærkodder Vig glacier (Figure 30). This distribution is interpreted to be part of a more (ultra)mafic marginal zone that surrounds a nested intrusion, much like the Vend Om Intrusion (Figure 3).

Figure 30. *Main traverse across the northern contact of the mafic band across an inner melanocratic gabbro intrusion (note that its contact appears to bend off to the upper right), bound by a more foliated and dioritic transitional zone into basement gneisses (paler rocks in upper left side of glacial outcrops). There may be at least two up to 10 m thick ultramafic layers in the foreground, separated by a schliered gabbro layer. Intrusions are cut by some meta-dykes, felsic pegmatite veins and greenish epidote faults/veins. View looking ESE.*

Figure 31. *Overview of fault-repeated southern contact between the predominantly mafic band (upper left) and the agmatitic gneiss host (lower right). Field of view (towards E) across centre of photograph is c. 40 m.*

The proposed (ultra)mafic contact-zone around a possible nested intrusion is also characterized by relatively well preserved but heterogeneous primary igneous features, such as magmatic layering on both larger (Figure 30) and smaller (Figure 33a) scale, and a large variety of angular igneous breccias (Figure 33b-c). An uneven size distribution and an apparent absence of hornblende oikocrysts (Figure 34) indicate that these crystals are metamorphic porphyroblasts, which grew in more mafic rocks under amphibolite facies conditions (cf., previous section on the Vend Om Intrusion).

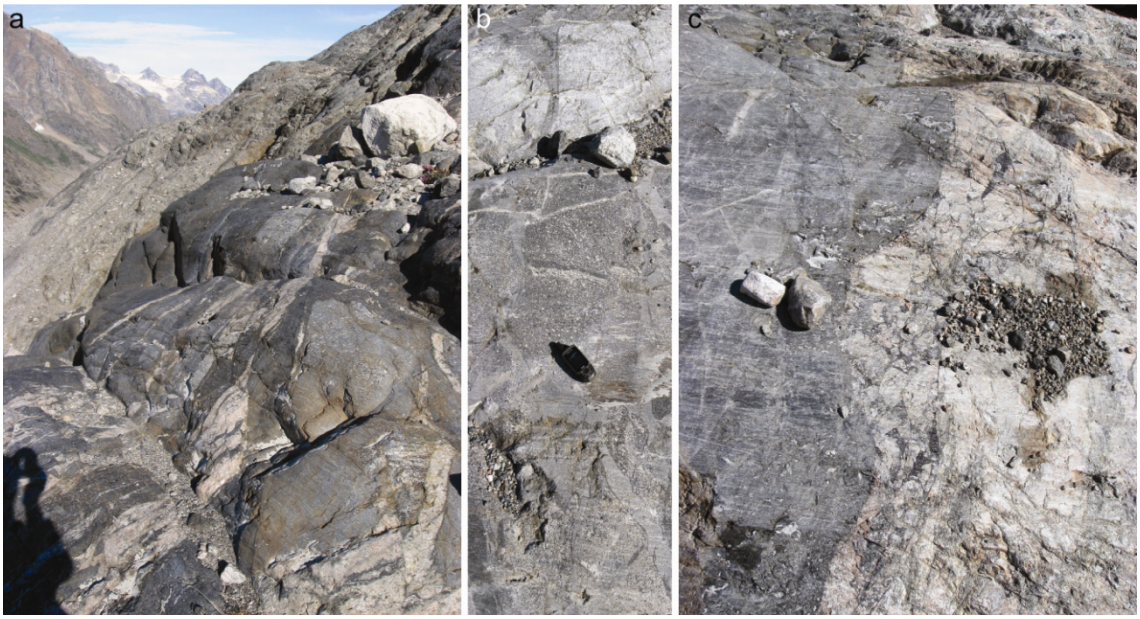

Figure 32. *Details within the faulted southern contact between (ultra)mafic and gneissic rocks shown in Figure 31. (a) Faulted contact between ultramafic and mafic rock units, intruded by pre-tectonic felsic pegmatite veins (shadow of photographer provides some scale). (b) A network of fine grained grey veins intrude a coarse grained gabbroic host. (c) Pseudotachylite breccia vein along contact between a mafic and gneissic unit (c. 2 m across centre of picture).*

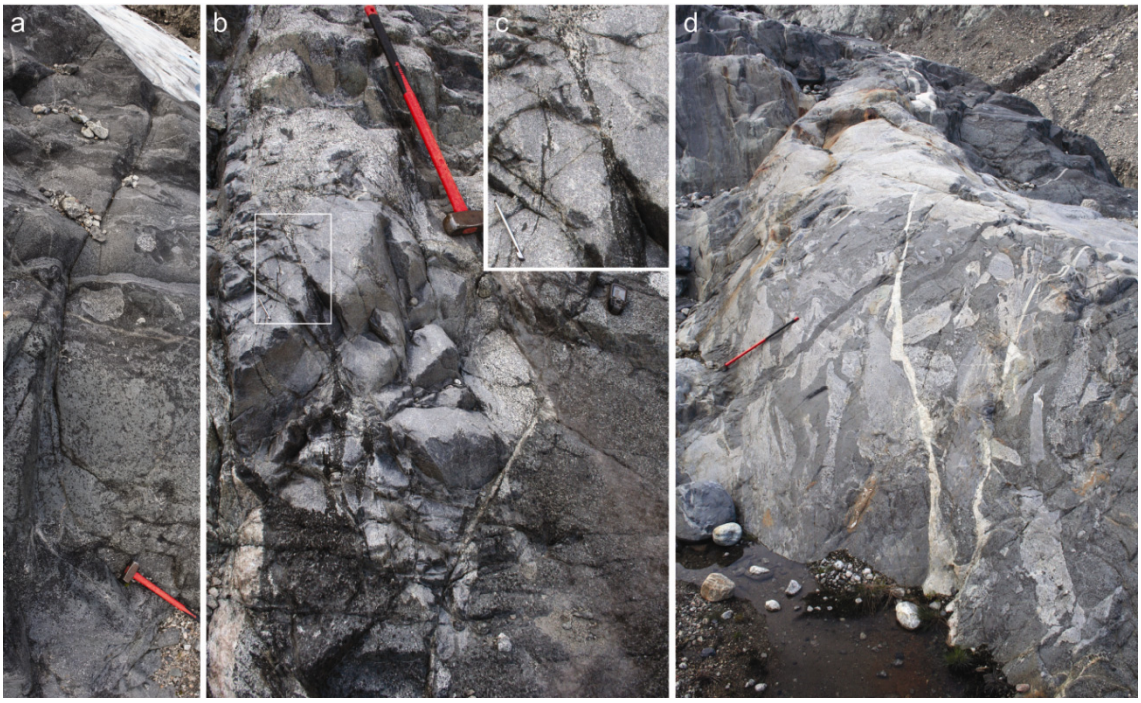

Figure 33. *Heterogenous and xenolithic gabbro along possible intrusive contacts. (a) Possible layered medium grained sequence with rounded coarse grained leucogabbroic xenoliths, much like within the Vend Om Intrusion. (b) Angular and fine grained basaltic xenolith intruded by coarse grained and either highly leucocratic or highly melanocratic veins. (c) Close-up of how the more leucocratic and melanocratic veins interact. (d) Angular leucocratic xenoliths in a gabbroic host cut by first a meta-dyke (parallel to 0.9 m-long hammer shaft) and then an orthogonal felsic vein.*

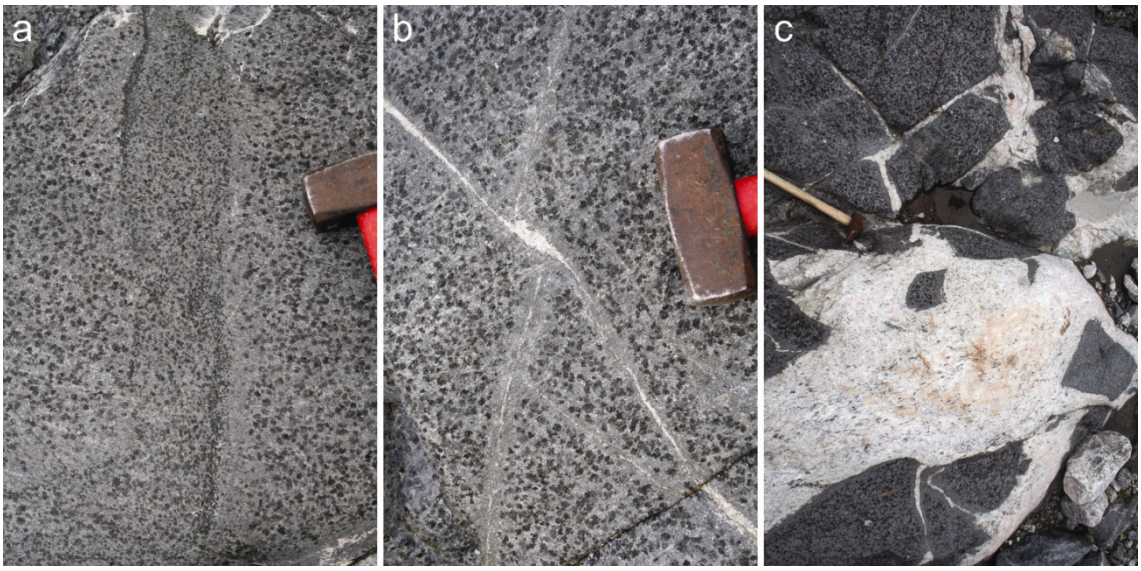

Figure 34. *Hornblende poikolitic melagabbro. (a) Band of smaller oikocrysts. (b) Apparent absence of oikocrysts in narrow zones around thin felsic veins. (c) Similar absence of oikocrysts in narrow zones around brecciating thick felsic pegmatite veins. Large hammer head is 6 cm wide, small hammer head is 4 cm wide.*

Mafic and felsic sheets and dykes

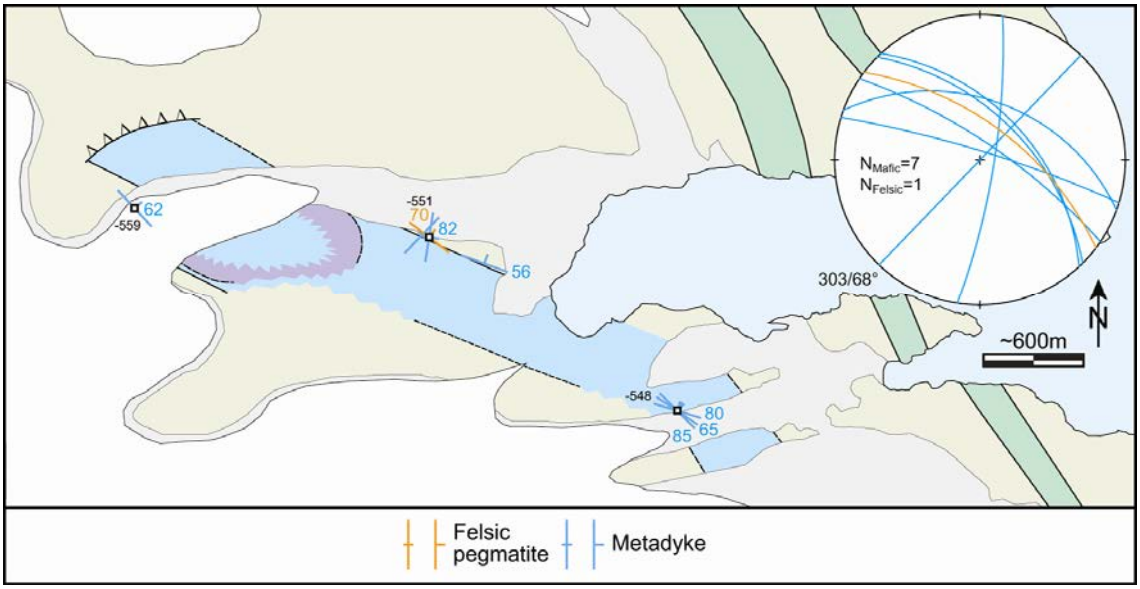

Figure 35. *Sample localities of meta-dykes and a felsic pegmatite vein, as well as measured orientations west of Stærkodder Vig. Limited number of planes indicate that meta-dykes (and felsic veins?) either are orientated sub-parallel or sub-orthogonally to the foliation. Map details as in Figure 26(b) and stereographical plot as in Figure 8.*

Compared to Halvdans Fjord, relatively few meta-dykes outcrop in or around SAP-related intrusions west of Stærkodder Vig. Of the 7 meta-dykes that were mapped and measured (Figure 35), 5 are roughly foliation-parallel – as many meta-dykes in Halvdans Fjord also are – whereas the other two intruded orthogonal to the foliation. As judged from their colour, there is a variation in apparent compositions ranging from intermediate (Figure 36a) to mafic (Figure 36b). Most meta-dykes appear to cross-cut felsic veins and thereby represent the last phase of igneous activity during ductile deformation, but may still appear relatively deformed (Figure 36b). One sampled felsic vein (527551) is also foliation-parallel.

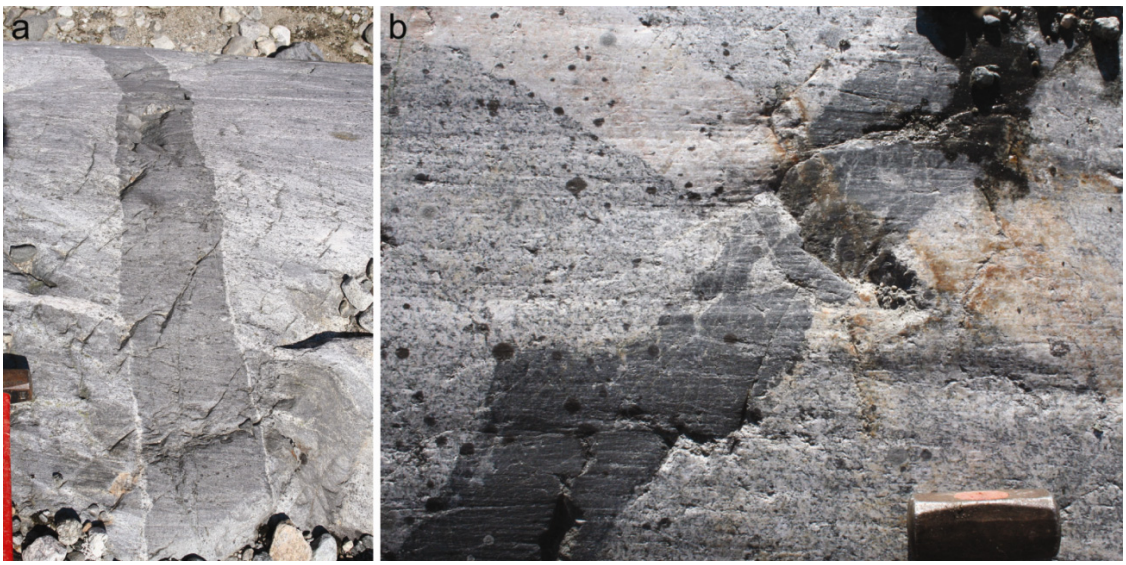

Figure 36. *Meta-dyke examples of (a) intermediated composition, and thin felsic margins that may represent anatectic contact melts, and (b) mafic composition, and a possible anatectic net-veined interior. Both meta-dykes cut felsic veins. Hammer head is ~6 cm wide.*

Brittle deformation

Several roughly NNE-dipping and sub-parallel thrusts outcrops just west of Stærkodder Vig (Figure 28). In detail these thrust have evidently dragged hanging wall foliations into fault planes (Figure 38) that may contain thin pseudotachylite veins (not shown). Judging from the drag folds, presence of pseudotachylite, the accumulative top-to-SSW displacement along these thrusts must have been substantial. Such large thrusts thereby also offer an explanation to the apparent upward termination of gabbroic outcrops along the N-side of the Stærkodder Vig glacier (Figure 29).

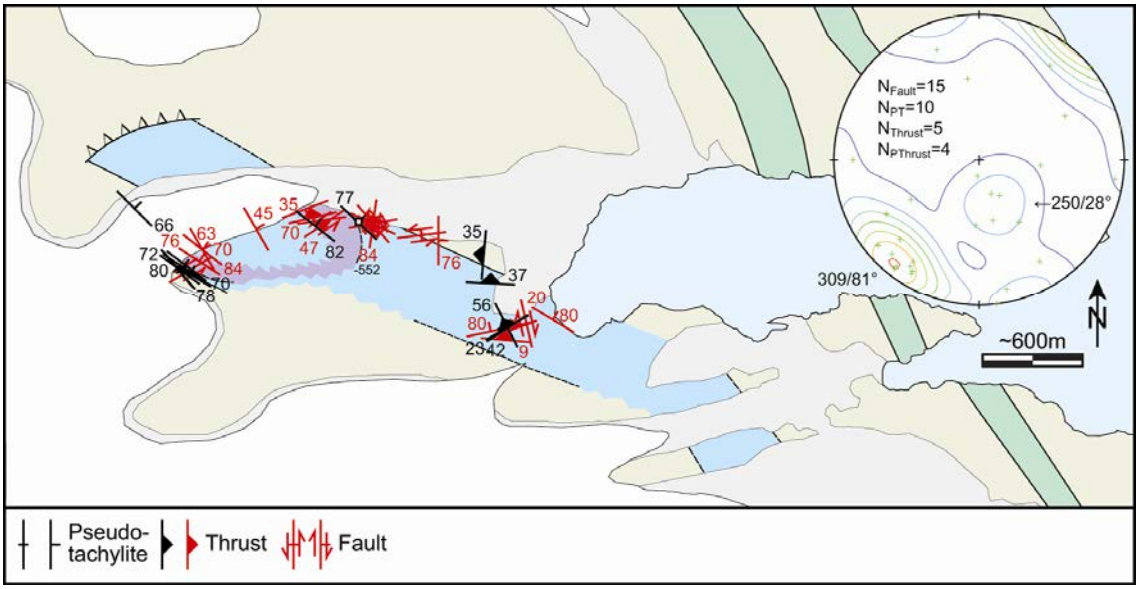

Figure 37. *Sample localities of measured pseudotachylites, as well as brittle thrusts and faults west of Stærkodder Vig. Map details as in Figure 26. (b) and stereographical plot as in Figure 8.*

Figure 38. *Drag-folded foliation bend into a gently N-dipping and top-to-SSW displaced thrust fault plane (sinistral in outcrop, looking NW). Hammer shaft is 0.6 m long.*

Figure 39. *(Previous Page) Fault breccia within (a) an 8 cm wide and highly chloritized or epidotized vein inside a melagabbroic host, with a variety of sub-rounded and foreign clasts, and (b) a typical pseudotachylite vein with both angular and rounded clasts from the (grano)dioritic host rock. Note substantial, yet unquantified, displacement indicated by different rock types on either side of the pseudotachylite as well as the displaced felsic vein. Pen for scale.*

It is possible that steeper NNE-dipping secondary faults link neighbouring thrusts. The dense swarm of steeply NE-dipping pseudotachylite faults along the S-margin of the mafic band (inner S-side of the Stærkodder Vig glacier, Figure 37) cannot be directly related to the thrust as accommodating transverse strike-slip faults, but could represent R_1 faults within a foliation-parallel dextral shear zone (Figure 41b).

It generally appears that pseudotachylites cut felsic veins (Figure 39) and are themselves often cut by more or less epidotized and K-feldspatized brittle faults. The epidotization is greater within plagioclase-rich mafic intrusions (cf., Figure 40d), whereas reddish secondary K-feldspar predominate as a hydrothermal alteration imprint within more felsic host rocks. It is difficult to differentiate between brittle faults that may or may not be associated with the pseudotachylites, but the general impression is that most brittle faults were formed in response to a later and different tectonic event. Thus, while the pseudotachylites were more likely formed in response to a top-to-SSE directed compressional stress field, a small conjugate set (many from the outcrop in Figure 40a and Figure 41a) of 4 sinistral (Figure 40b) and 4 dextral (Figure 40c) strike-slip faults are more consistent with a NNE-SSW directed compressional stress field (Figure 41c).

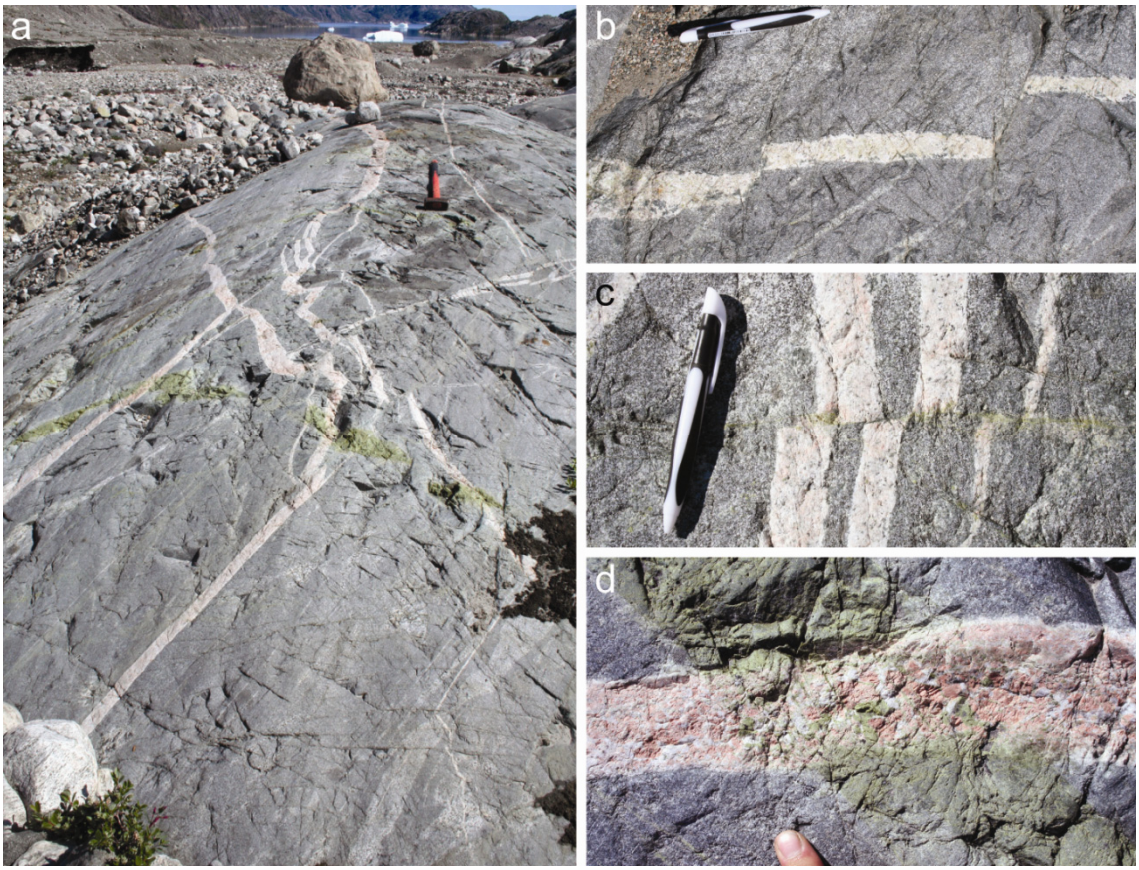

Figure 40. *Brittle strike-slip faulting. (a) Dioritic outcrop in Figure 41a, with an epidotized conjugate fault set, displacing felsic veins (hammer is ~0.9 m long). (b) Sinistrally offset felsic vein (pen is 14 cm long). (c) Dextrally offset feklsic veins (pen is 14 cm long). (d) Epidote vein partly intruding a felsic pegmatite vein (finger nail for scale).*

The inferred stress fields and kinematic shear models in Figure 41(b-c, p. 45) are not consistent with other observations, however, in that (1) the NE-SW foliation-parallel and dextral shear zone is inconsistent with the way that the foliation at both Stærkodder Vig and Halvdans Fjord bends into apparent sinistral shear zones, and (2) the NNE-SSW directed compressional stress field inferred from the conjugate fault set is opposite to what a in the Vend Om Intrusion indicates (Figure 8b). Thus, more complex models may be considered, including the possibility of WSW-ENE striking and apparently dextral strike-slip faults being the mentioned reversed fault links between neighbouring thrusts.

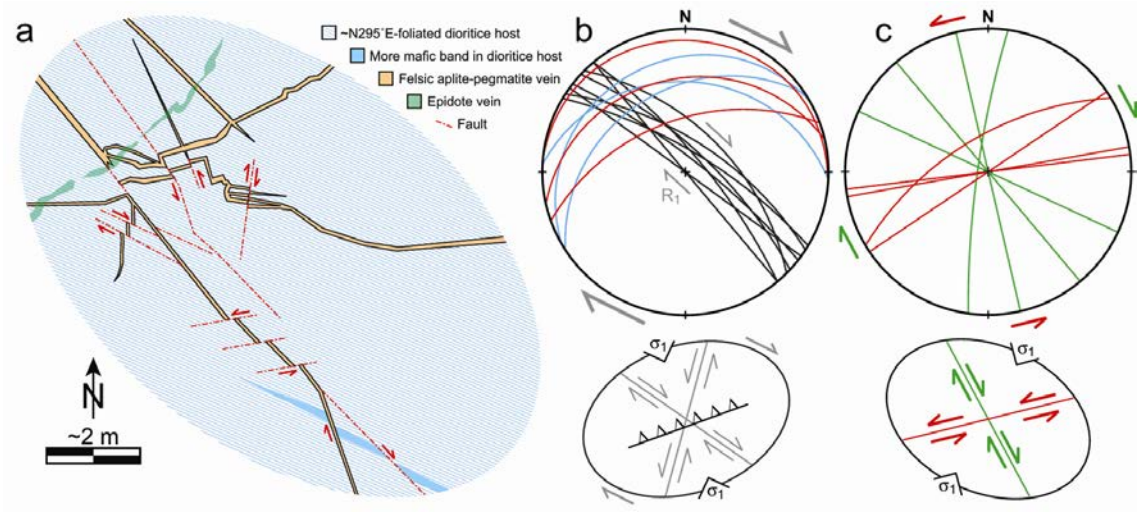

Figure 41. *Compilation of brittle structures observed in outcrop depicted in Figure 40. (a) Sketched outcrop of conjugate faulted felsic veins and foliation bands. Structural analysis of (b) pseudotachylite faults (black) and thrusts (blue), as well as three tectonic low-angle faults (red), and (c) a conjugate set of sinistral (red) and dextral (green) strike-slip faults, in the Stærkodder Vig area. Gently NNW-dipping thrusts in (b) indicate top-to-SSE directed compression (σ_1 in lower strain ellipse), possibly generated within a WNW-ESE trending dextral shear zone (grey displacement arrows). The conjugate fault set in (c) is consistent with NNE-SSW directed compression.*

The Ruinnæsset intrusion

The Ruinnæsset intrusion is the largest and best investigated of the SAP intrusions (Blichert-Toft et al 1995). It has a rhomb-shaped outline measuring c. 3×3 km, as it outcrops along the shore lines of the junction between Nordre Skjoldungen Sund and Mørkesund (Fig. 42). The intrusion is dominated by coarse grained rocks ranging widely in composition from gabbro and diorite to monzonite and syenite, with much less abundant ultramafic rocks and granite. The main lithology is constituted by coarse grained monzonite to syenite that commonly shows rhytmical layering as defined by *c.* 5-20 cm thick modally distinct layers rich in hornblende, pyroxene and Fe-Ti oxides. The new mapping seems to suggest that there is a systematic distribution of rock types within the intrusion, with the western part mainly being comprised of syenites and monzonites, whereas the eastern part also comprises more mafic lithologies, such as pyroxenites, gabbros and diorites, as well as significantly more meta-dykes and sheets. The contact to the surrounding gneisses is sometimes demonstrably intrusive, other places it is tectonic. Based on the new field work minor adjustments of the location of intrusion contacts were made at four shore outcrops, as well as along Vigge Gletcher (labelled red X's in Figure 42).

The intrusion is cut by multiple generations of late sheets and dykes of granitic or syenitic composition. Some of these intrusions have irregular outlines and appear to intrude at a late magmatic phase into a semi-ductile (mush-like) host. Similarly, mafic bands and veins rich in magnetite and apatite (so-called nelsonites) are observed to intrude the bulk lithologies in irregular fashions, suggesting intrusion under semi-crystallised conditions. The presence of nelsonite was also noted by previous workers who considered a process of liquid immiscibility at a late stage of the magmatic evolution (Blichert-Toft et al 1995).

A reconnaissance investigation was undertaken by dinghy along most of the shoreline outcrops, from which a detailed photographic coverage suggests that the density (frequency) of tabular intrusions increases towards the SE – possibly as a result of entering a large SE-dipping inclined sheet swarm that was observed along cliff surfaces across the entire northern part of the Skjoldungen Island. More felsic sheets, dykes and veins may be subdivided into quartz-bearing pinkish and quartz-poor purple pegmatites-aplites, which tend to cut the mafic sheets and dykes. Most tabular intrusions were investigated within a weekly layered (monzo-)syenite that include a possible margin-parallel band of brecciated (ultra)mafic blocks some hundreds of meters inside the north-eastern margin of the Ruinnæsset intrusion (Figure 43).

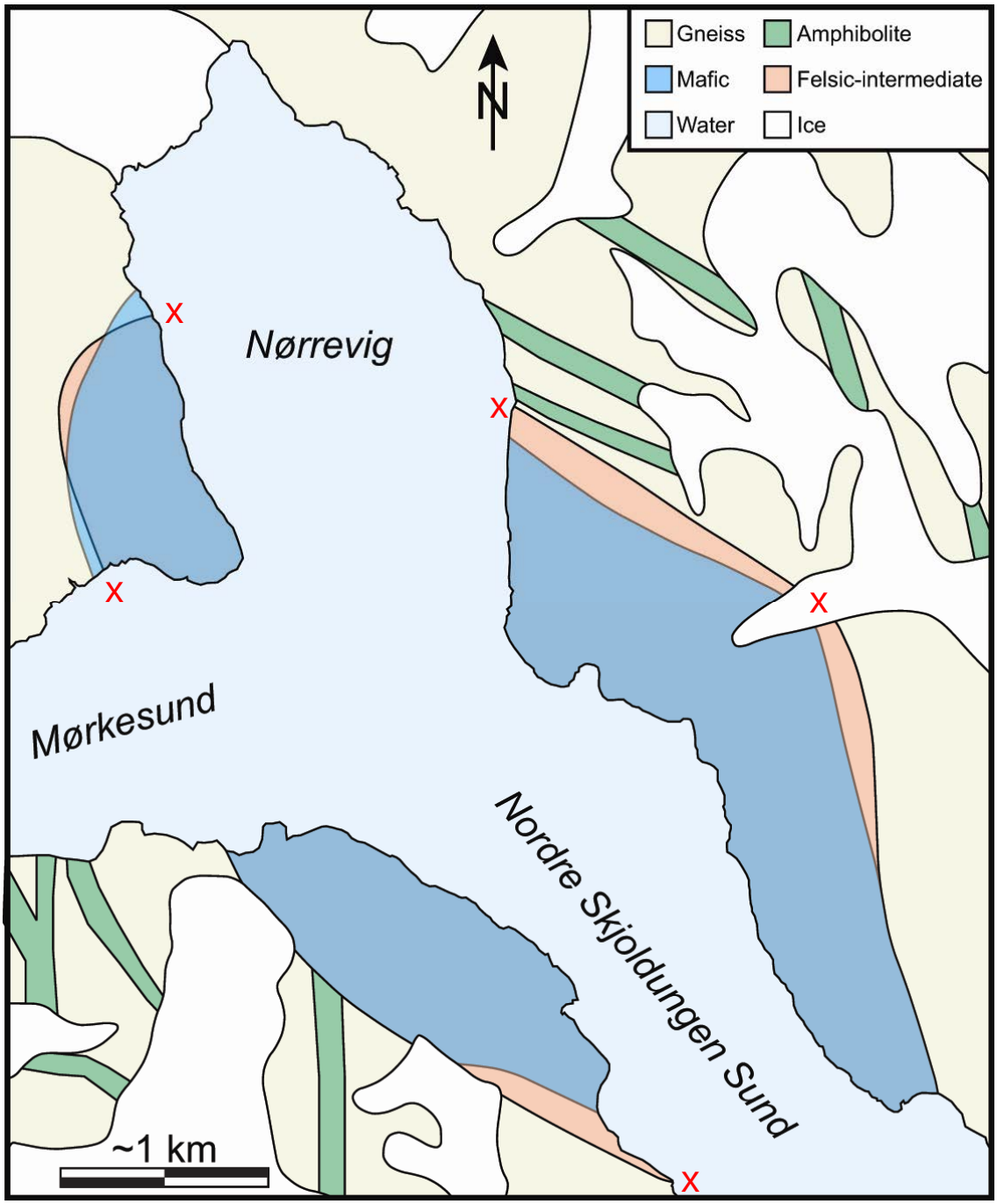

Figure 42. *The geological map of Escher (1990) indicates the Ruinnæsset intrusion to consist of gabbro and diorite. However, the intrusion includes a broader continuous compositional span with gabbro, monzogabbro, monzodiorite, monzonite and syenite, and with volumetrically much smaller fractions of granite and ultramafic rocks. The new field work indicates that the felsic–intermediate rock types preferentially occur at the margins, and the more mafic rocks towards the centre.*

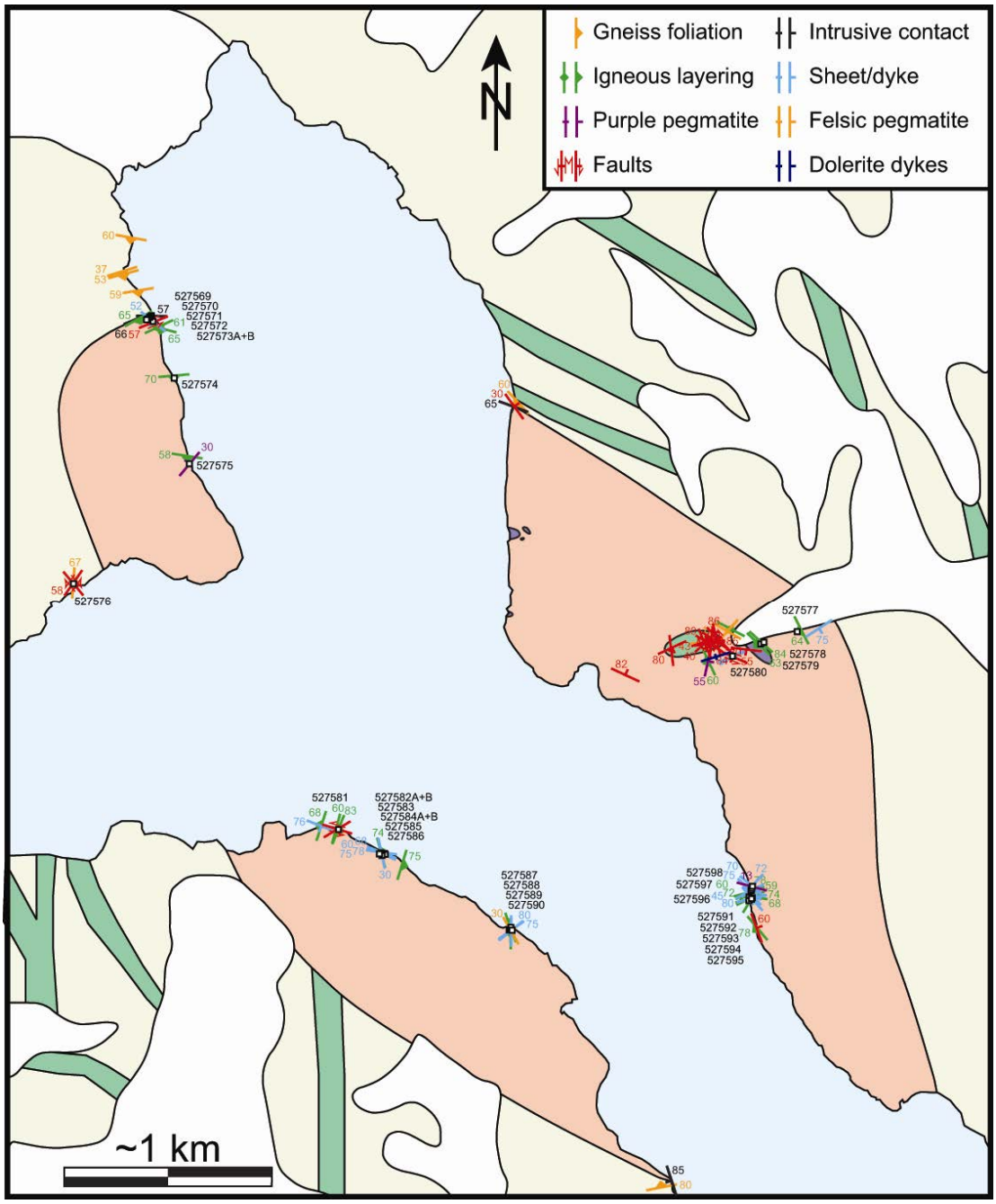

Figure 43. *Preliminary conception of the Ruinnæsset intrusion, upon which are added observed bodies of ultramafic rocks (purple), a large monzonitic inclusion (green), as well as all structural measurements and sample localities collected by the authors in 2011.*

Contact relationships to the basement

Most of the contact relationships of the Ruinnæsset intrusion were difficult to identify because of the resemblance between the agmatitic host gneiss and locally sheared felsic rocks of the Ruinnæsset intrusion. However, in the northern part of the intrusion the contact to the basement is well exposed and magmatic, as previously pointed out by Thomsen (1998). At this locality the contact consists a *c.* 3 m wide zone dominated by pegmatitic rocks, occasionally with miarolithic cavities, and at places containing up to 30 cm long den-

tritic amphiboles that grow perpendicular to the contact (Figure 45). This contact zone is locally cut by a *c.* 2 m wide pyroxenitic intrusion with an upper and lower chilled margin, which appears to have been cut/abraded by the interior part of the intrusion (Figure 46).

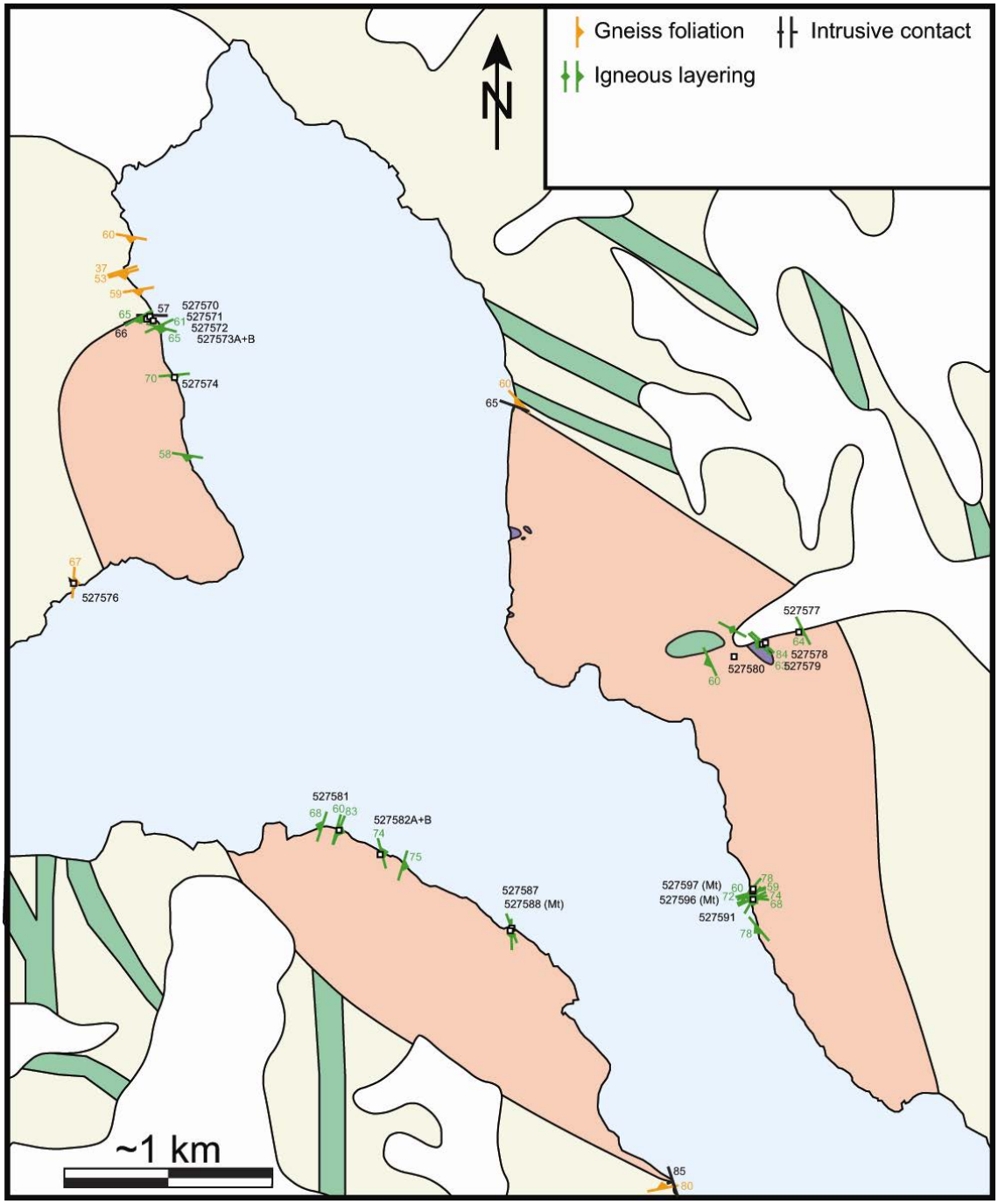

Figure 44. *Structural measurements on rocks of the Ruinnæsset intrusion and the adjacent basement gneisses. Note a general parallelism between host gneiss foliations and igneous layering along the north-eastern contact, whereas the igneous layering tends to be more oblique along the south-western margin.*

Figure 45. *The north-western contact of the Ruinnæsset intrusion, where a >3 m wide zone with spectacular dentritic amphiboles grow perpendicular to the contact plane. (a) The contact (approximately along the green line) dips into the intrusion (left) by nearly 60°S. (b) Close-up of dentritic amphiboles at red arrow in (a) are locally up to 30 cm long.*

The north-eastern contact of the Ruinnæsset intrusion appears to be partially sheared and parallel to a steeply foliated host gneiss, whereas a wide and highly xenolithic felsic intrusion (not shown) along its south-eastern margin was mistaken as its agmatitic host gneiss. The latter misinterpretation meant that we never visited the south-eastern contact of the Ruinnæsset intrusion and we therefore maintain its previously mapped location (cf., Figure 42). The contact along Vigge Gletcher was also never reached in the field but is, nevertheless, moved slightly eastward, because syenitic outcrops were tracked beyond the old location of this contact. Towards the south-west, the host gneiss appears to have been veined

and brecciated by a characteristically alkali feldspar-phyric chilled melt (not shown). More mapping may well lead to further modifications to the outline of this large intrusion.

Figure 46. *A c. 2 m wide pyroxenitic band across an otherwise amphibole dendritic contact zone, shown from two perspectives (a & b). An upper and lower chilled margin to this band suggest that it is a later intrusion, which appears to have been cut/abraded by the syenitic interior (to the left in these photos).*

Internal architecture

The interior of the Ruinnæsset intrusion is characterized by predominantly monzonitic rocks, which may be weakly foliated and layered. This layering/foliation is predominantly steep to vertical. Measurements in Figure 44 indicate that igneous layering is sub-parallel to the host gneiss foliations and along the northern-eastern intrusive contacts of the Ruinnæsset intrusion, whereas steeply dipping measured layers/foliations tend to strike more obliquely to the current outline of the intrusion's SW-margin. More magnetite- and apatite rich (Blichert-Toft 1995) dark nelsonitic bands accentuate the layering in some outcrops (Figure 47). This layering is in some places through-like, cross bedded and more irregularly distorted (Figure 47b), and it appears that the dark bands may locally have been re-mobilized into cross cutting veins (Figure 54b).

More melanocratic (mela-gabbroic to pyroxenitic) parts of the Ruinnæsset intrusion (Figure 48) are found within a zone, that is located some hundreds of meters inside and may extend along the eastern margin of the intrusions (Figure 44). These (ultra)mafic parts appear to be large xenoliths because these appear to be highly metamorphosed and are cut by regular felsic (syenitic?) veins (Figure 48b).

Figure 47. *Mafic magnetite- and apatite bearing fine grained nelsonitic layers within monzonitic rocks of the Ruinnæsset intrusion. (a) Nearly vertical layering cut by a felsic pegmatite vein. (b) Contorted layering.*

Minor intrusions

The north-western part of the Ruinnæsset intrusion is relatively barren of later dykes, sheets and veins, whereas the intrusive density of such minor tabular intrusions increases drastically towards its south-eastern part. Some of the mafic sheets appear to belong to a roughly SW–NE striking and moderately SE–dipping swarm, which is observed on steep cliffs around the north-western part of the Skjoldungen Island. Otherwise, the impression is that a large abundance of different types and orientations of tabular intrusions are found throughout the south-eastern part of the Ruinnæsset intrusion. This transition towards a possible southern satellite of the mozoninitic-syenitic Ruinnæsset intrusion, discovered in 2012, is being investigated as an Honours project in 2015, by Philip Geldenhuys.

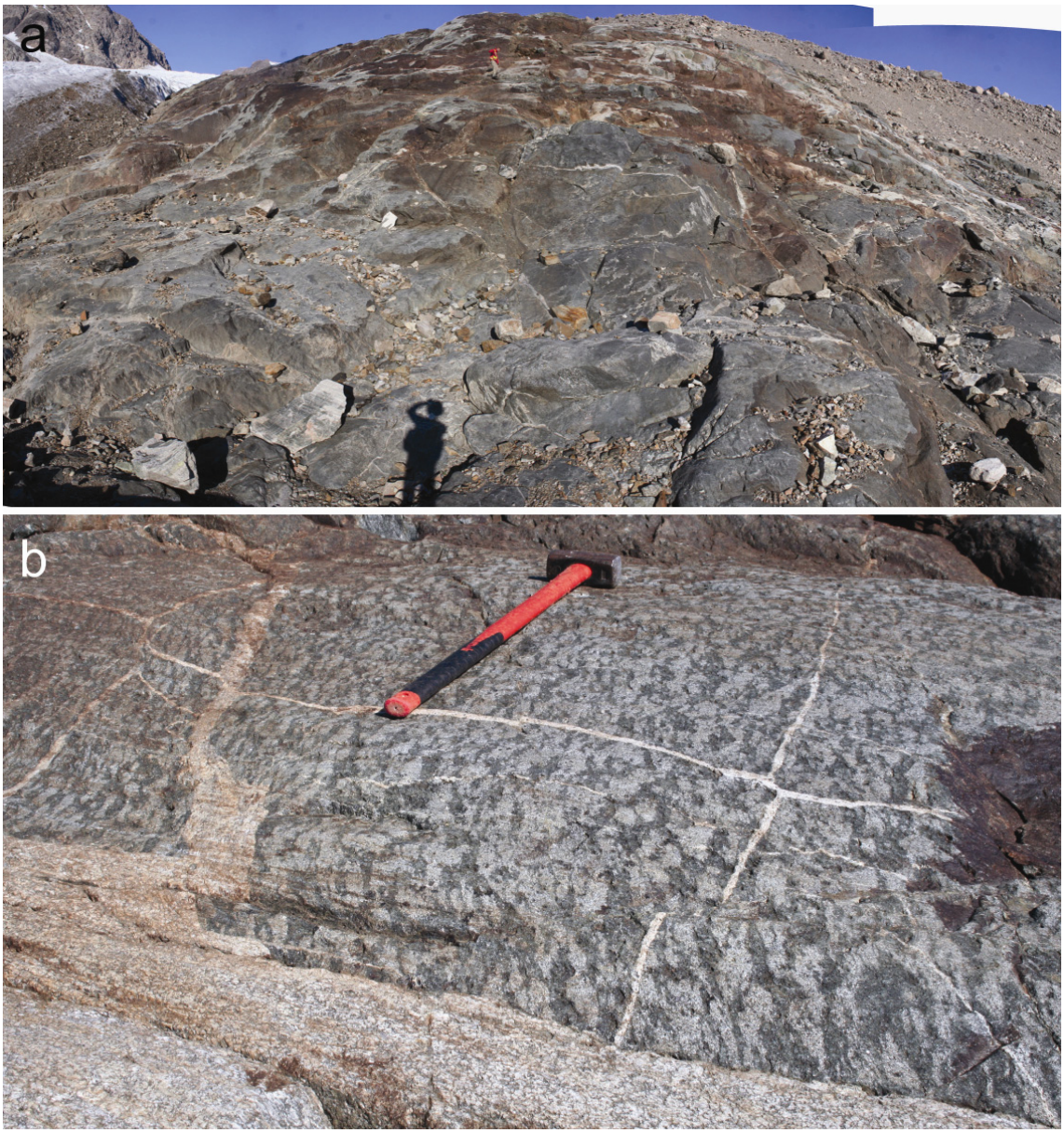

Figure 48. *Large ultramafic part within the Ruinnæsset intrusion, just south of Vigge Gletcher. (a) Overview of most of the outcrop (person as scale). (b) Close-up of foliated, spotted ultramafic rocks that are cross-cut by late regular felsic veins.*

Some initially brecciating and veining intrusions appear to have experienced slight semi-ductile shearing (Figure 48), whereas the angular geometries of most other intrusions suggest that these were injected into a brittle part of the intrusion. In general, felsic pegmatites appear to be the last intrusive phase (e.g. Figure 51), but these are also cut by Proterozoic dolerite dykes of yet unknown ages (Figure 52). Some quartz-poor purple pegmatites appear to be restricted within the Ruinnæsset intrusion, and are believed to represent fluid-rich late-stage segregations from the crystallized (monzo)syenitic intrusion. These purple pegmatites are generally cut by Proterozoic dolerite dykes and felsic pegmatites, but generally cut other intrusions There may be a tendency, but no systematic, sequence of more melanocratic (mafic) sheets being cut by more leucocratic (felsic) sheets (e.g., Figure 52), which could reflect injections from a single differentiating magma chamber. Most of these

sheets are displaced by faults (e.g., Figure 53), which in some cases appear to have been intruded by the felsic pegmatites and associated aplites (Figure 54b).

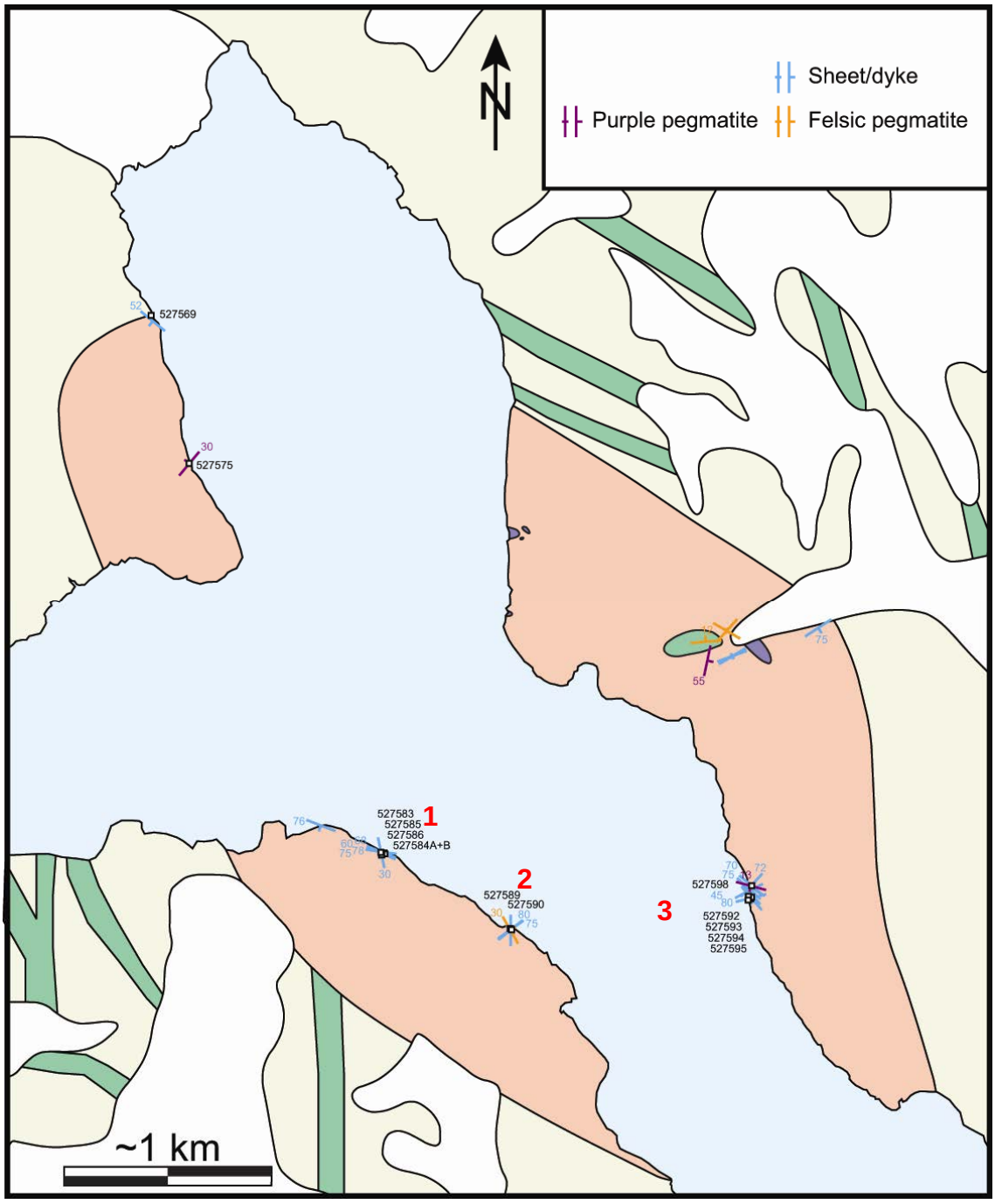

Figure 49. *Measured minor intrusions within the Ruinnæsset intrusion, as well as main sample locations 1-3, sketched and described in more detail in Figures 54 and 55a, as well as in the text.*

From more detailed mapping at sampling localities 1-3 (Figure 49), cross cutting relationships provide some first impression of the general sequence of intrusions (where "←" = "intruded by":

1. Figure 54a: (1) more or less layered (monzo)syenites ← (2) NW-SE trending mafic sheets ← (3) purple pegmatites ← (4) Felsic sill/Dolerite dyke (no direct cross cutting relationship between the latter two, but the dolerite dyke is presumably younger).
2. Figure 54b: (1) (monzo)syenites with distinct magnetite-rich layering appear to have segregated into cross cutting veins ← (2) three different (ultra)mafic sheets, where a NW-SE striking sheet is cut by a SW-NE trending sheet ← (3) a possible conjugate fault set that may be consistent with roughly N-S extension ← (4) Felsic aplite vein that partly follows a fault and is cut by an associated(?) felsic pegmatite sill.
3. Figure 55a: (1) (monzo)syenites, with many, variably distorted magnetite-rich layers (Figure 47) ← (2) two generations of feldspar-phyric (agglomerophyric by Blicher-Toft et al. 1995) intrusions (Figure 55c) ← (3) mafic sheets, including a greenish (epidotized?) sheet (Figure 55b), which at this locality may be roughly coeval with magnetite rich 'segregation' veins ← (4) a third type of feldspar-phyric intrusion with unusually long phenocrysts (Figure 55e) ← (5) purple pegmatites (Figure 55b) ← (6) felsic pegmatites (Figure 55d).

Figure 50. *Dark, very irregular and roughly N-S trending intrusions appear to have been partly brecciating and veining a brittle Ruinnæsset syenite, which subsequently experienced some semi-ductile shearing.*

Figure 51. *Many cross cutting sheets and veins in the Ruinnæsset rocks are all cut by a pale felsic pegmatite. Outcrop in the foreground is c. 4 m high. South-eastern side of Nordre Skjoldungen Sund.*

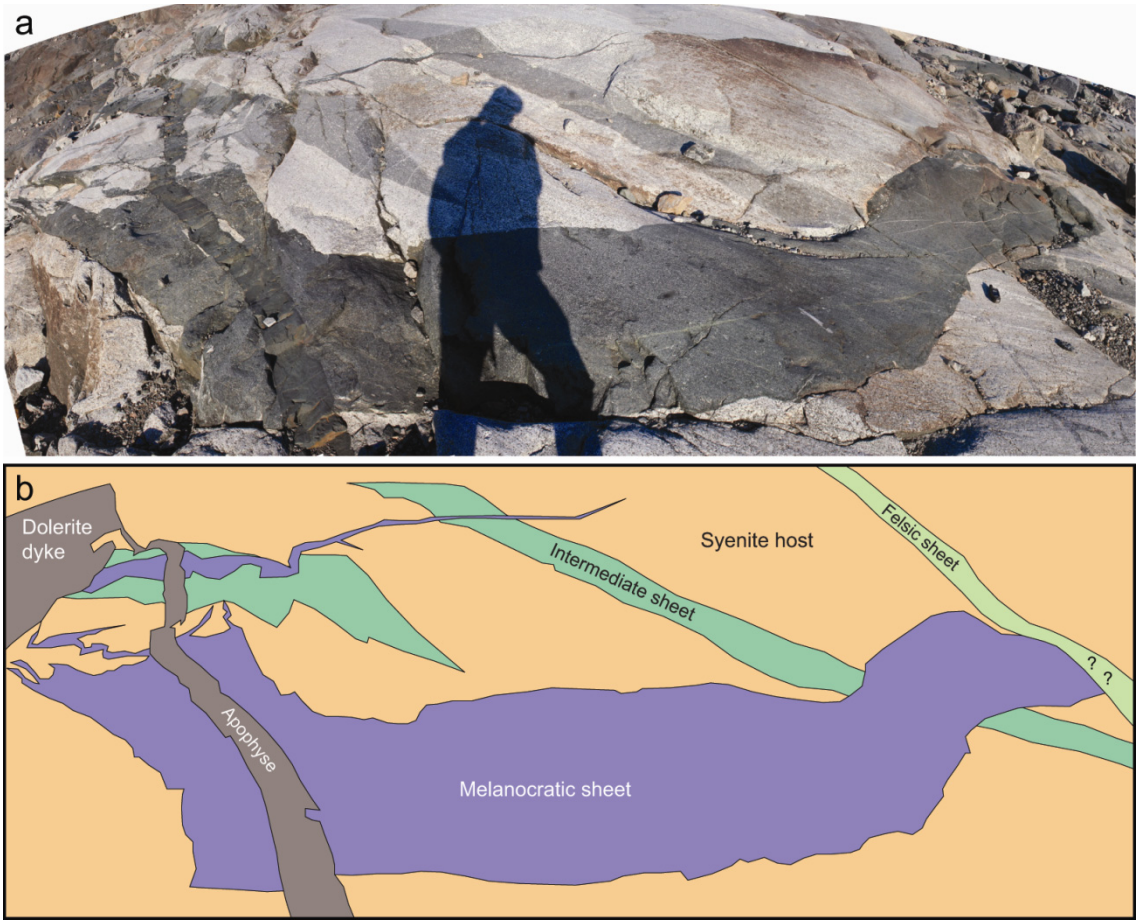

Figure 52. *A c. 30 cm wide apophyse to a Proterozoic dyke cuts melanocratic to leucocratic sheets near Vigges Gletcher. GPS receiver for scale to the right of the photo.*

Figure 53. *Apparent sinistral displacement of many cross cutting sheets and veins, along a low-angle fault. Outcrop on south-eastern side of Nordre Skjoldungen Sund is c. 4 m high.*

In summary, these preliminary observations record the following episodes of intrusive activity following the emplacement and crystallization of the Ruinnæsset intrusion: (I) Several injections of NNW-SSE trending feldspar-phyric dykes have phenocrysts that resemble the cumulate part of the intrusion; (II) differently orientated sub-parallel swarms of mafic sheets were probably injected from different magma chamber sources, roughly at the same time that magnetite-rich layers may have been locally remobilized into cross cutting veins; (III) Local 'purple' pegmatites were emplace prior to regional felsic pegmatites and aplites.

Berger et al. (2014) investigated the exhumation history of the Ruinnæsset Intrusion and the surrounding basement by combining zircon geochronological data from SAP rocks with the specific observation of pressure indicators for shallow emplacement depths in form of the sampled miarolithic cavities in rocks of the Ruinnæsset Intrusion. This study showed that the investigated area represents a deeply eroded section of an orogen (e.g., granulite facies conditions), which later was intruded by plutons during exhumation. The data suggested granulite facies conditions at c. 2750 Ma followed by shallow-level emplacement at c. 2700 Ma for this part of the Skjoldungen Alkaline Province. Using these P-t data exhumation rates of c. 0.45 km/Ma were estimated, which is in the range of erosion-related rates in the late stages of modern orogens (Berger et al., 2014).

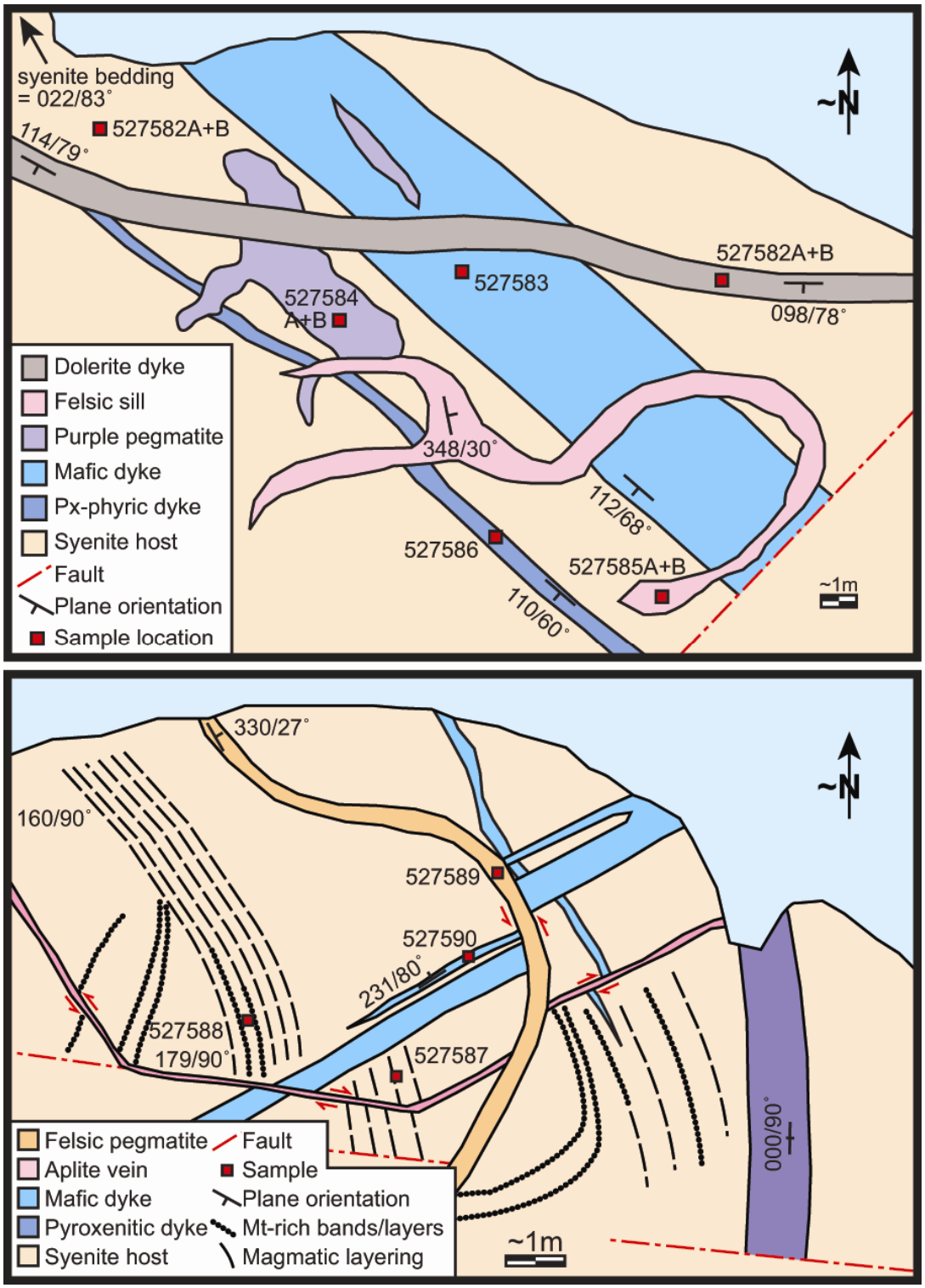

Figure 54. *Sketched maps of sample localities within the Ruinnæsset intrusion along the south-western shoreline of Nordre Skjoldungen Sund (Figure 49). (a) Locality 11TFK087: More northerly sample location 1, where an E-W trending dolerite dyke and a fine-grained felsic sill cut an irregular purple pegmatite and two parallel mafic dykes (one of which is pyroxene-phyric). (b) Locality 11TFK089: A felsic pegmatite sheet cuts an aplite that partially follows a conjugate fault set. These felsic intrusions cut a sub-orthogonal set of mafic dykes (one of which is pyroxenitic). The host syenite exhibits an irregular vertical layering, emphasized by magnetite rich bands, which appear to have been re-mobilized and emplaced across the bedding.*

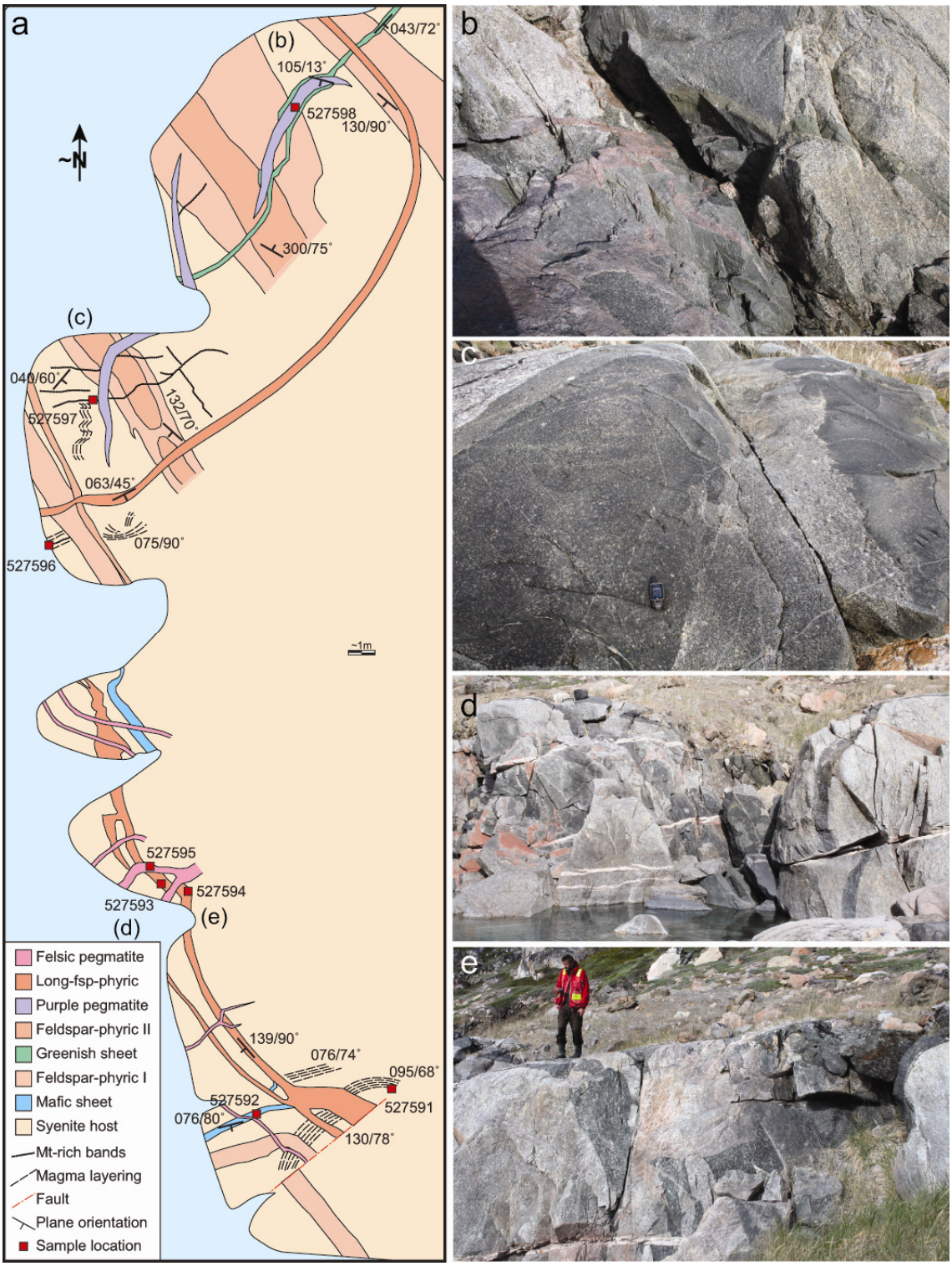

Figure 55. *Sample locality 3 within the Ruinnæsset intrusion and along the NE-shore of Nordre Skjoldungen Sund (Figure 49). (a) Sketched map. (b) A 0.1 m thick, greenish and fine grained sheet cuts a feldspar-phyric dyke and both are cut by a purple pegmatite. (c) Two generations of, or a compositionally zoned, feldspar-phyric dykes (gps-receiver as scale). (d) Felsic pegmatite sills cut all other sheet intrusions (outcrop c. 4 m high). (e) long-feldspar-phyric dyke (below person) together with a more ordinary feldspar-phyric dyke. Both cut by a felsic pegmatite.*

Hermods Vig

The last field camp was pitched on a gabbroic peninsular just north of Hermods Vig (Figure 56), from where two effective days of field work was done, firstly, on coastal outcrops of the gabbroic intrusion around camp and, secondly, on the southern parts around Njords Gletscher (Figure 57). The mapped extent of the gabbroic intrusion around camp appears to be correct, whereas indications of a much larger mafic intrusion around Njords Gletscher is reduced to a <1 km long and few hundreds of meters wide intrusion on the southern SW-side of the valley (Figure 56). Compared to original field maps in 1:50 000 the Escher compilation exaggerates the amount of intrusive material and the present observations are in better agreement with original field maps.

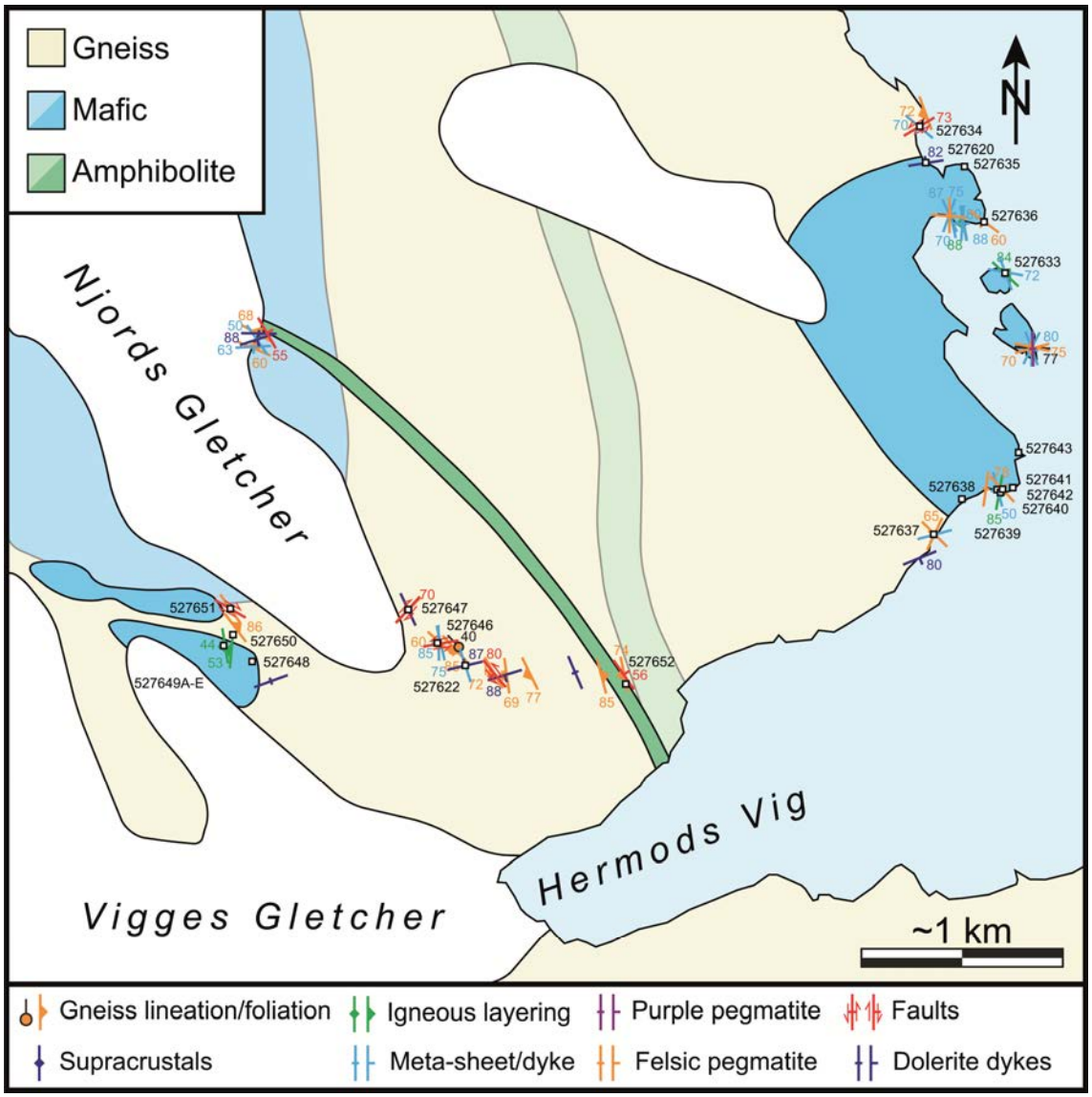

Figure 56. *Preliminary conception of the Hermods Vig Area, where the main changes to Escher (1990; paler blue and green) include a considerable reduction of a mafic intrusion (blue) around Njords Gletscher and possible relocation of a supracrustal band (green). All superimposed structural measurements around Hermods Vig are also shown on subsequent maps.*

Gneiss basement

Gneiss-amphibolite foliations are steeply WSW-dipping and may change up through the Njords Gletscher Valley, from being more N-S trending towards the south and more NW-SE trending towards the north; a curvature that is mimicked by a *c.* 50 m thick supracrustal band (Figure 57). The agmatitic gneiss in this area is relatively felsic but contains strands of elongated amphibolites boudins, which commonly are parasitically S-, Z- and M-folded (one fold axis measured to be 40°→317°). A *c.* 2 m wide, 50 m long, foliation parallel and highly metamorphosed pyroxenitic band (composed of green clinopyroxene, brown orthopyroxene, phlogopite and some interstitial plagioclase) was sampled (527647).

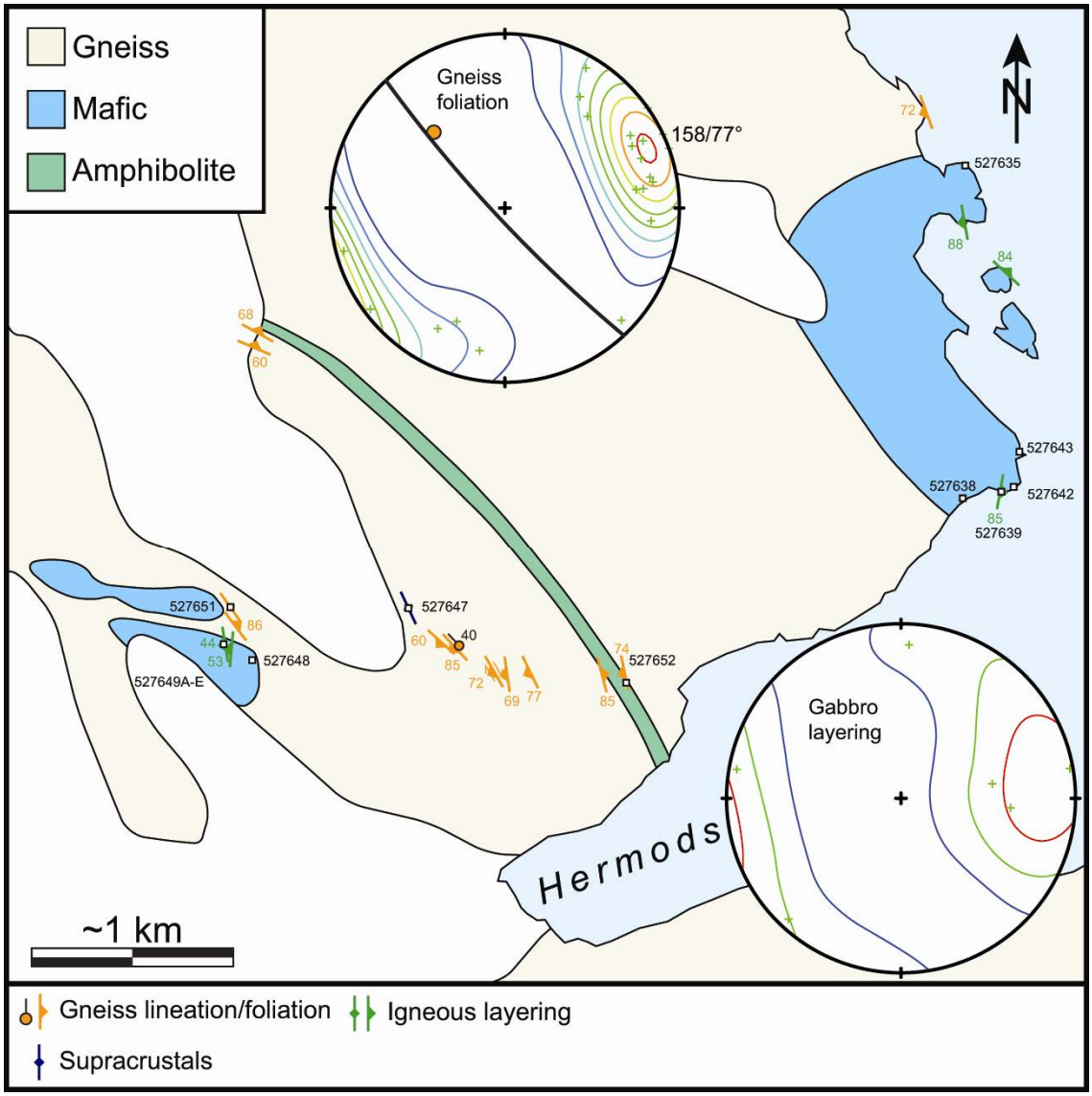

Figure 57. *Gneiss-amphibolite foliations/lineations and gabbroic layering around Hermods Vig, superimposed on a revised geological map of the area. Contoured poles to planes for each of these structures are shown in stereographical plots, constructed as in Figure 8.*

Gabbroic intrusions

Original features of the gabbroic intrusion north of the mouth of Hermods Vig is heavily obscured by secondary mafic-felsic dykes, sheets and veins (see below). Faint layering (Figure 58a) at three localities are all steeply and roughly N-S to E-W trending, and do not conform to the semi-circular outline of the intrusion (Figure 57). It is commonly a normal gabbro, with sporadic mela-gabbroic, and perhaps even ultramafic, parts (Figure 58b). The lower parts of the gabbroic outcrops on the SW-side of Njords Gletscher are, on the other hand, much more distinctly layered (Figure 59).

Figure 58. *Shoreline outcrops along the outer northern part of Hermods Vig. (a) Nearly vertical and N-S trending, faint gabbroic layering in coastal outcrops along the southern part of the Hermods Vig Intrusion (Figure 57), cut by an angular felsic (syenitic) intrusion. (b) More ultramafic part of the complex, cut by regular felsic sheets. Both exposures are c. 2 m high.*

Figure 59. *(on next page): The gabbroic intrusion on the SW-side of the Njords Gletscher Valley. (a) Outline of mafic outcrops as viewed from the east. Arrow indicates section in (b), where at least two rusty and moderately W-dipping zones are exposed. (c) The uppermost rusty zone, located by white arrow in (b). (d) Relatively fresh exposure of magnetite rich bands within the upper rusty zone in (c), inter-bedded amongst gabbroic layers (hammer head is 5 cm wide). (e) Five samples (527549A-E) collected from various layers in (d).*

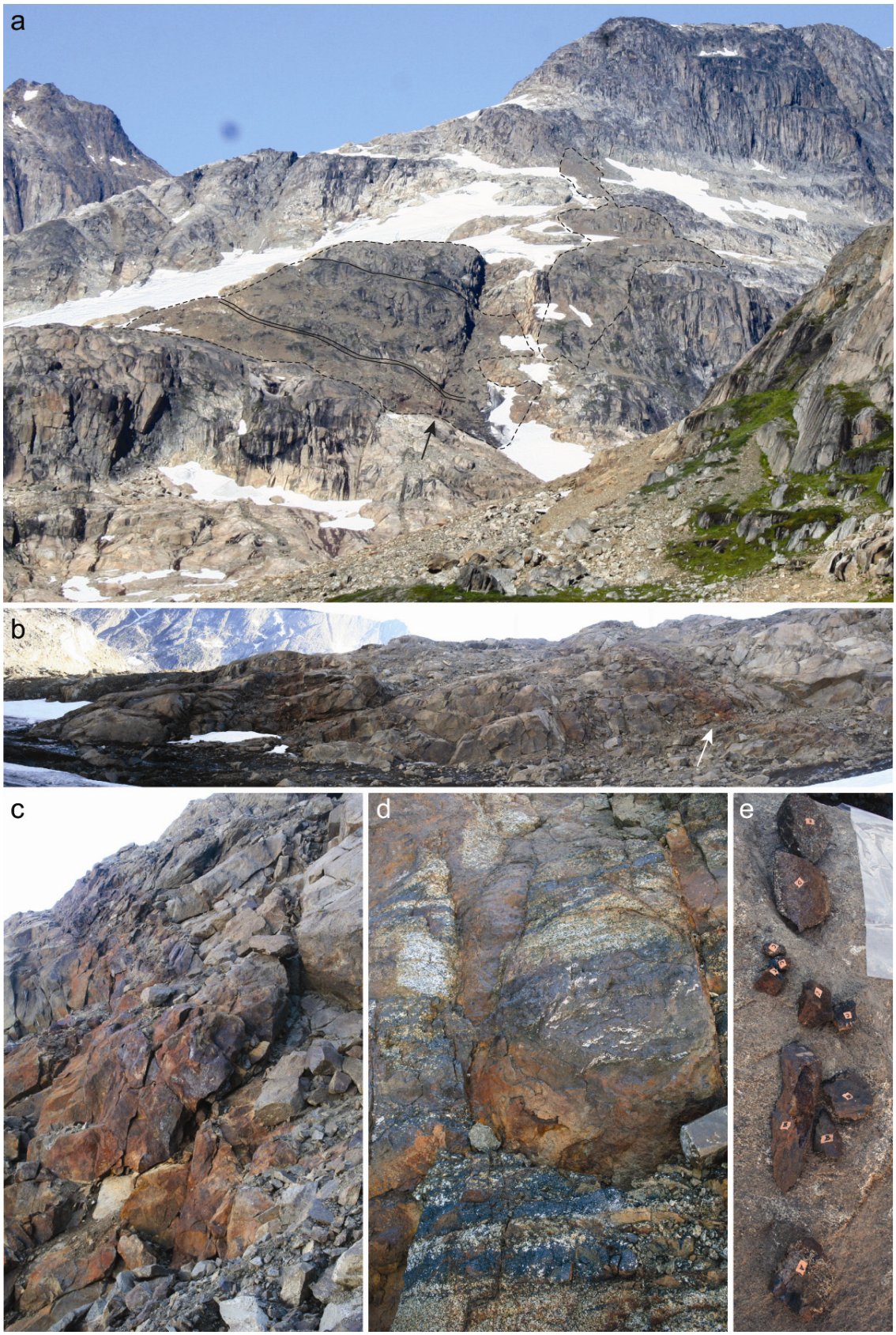
a
b
c
d
e

Secondary intrusions

Whereas very few secondary intrusions appear to cross cut the gabbroic intrusion near Njords Gletcher, the intrusion north of Hermods Vig is extensively intruded by several different types and generations of secondary planar intrusions (Figure 61). The intensity of such intrusions may increase through this intrusion towards the Nordre Skjoldungen Sund. Only one locality was systematically mapped, but not sampled until 2012 (Figure 62). There appears to be many felsic planar intrusions, which generally appear to be younger but not systematically so when photos are studied in more detail. Thus, more melanocratic (e.g., black) veins are observed cutting other, including more felsic-looking, sheets (e.g., Figure 61a).

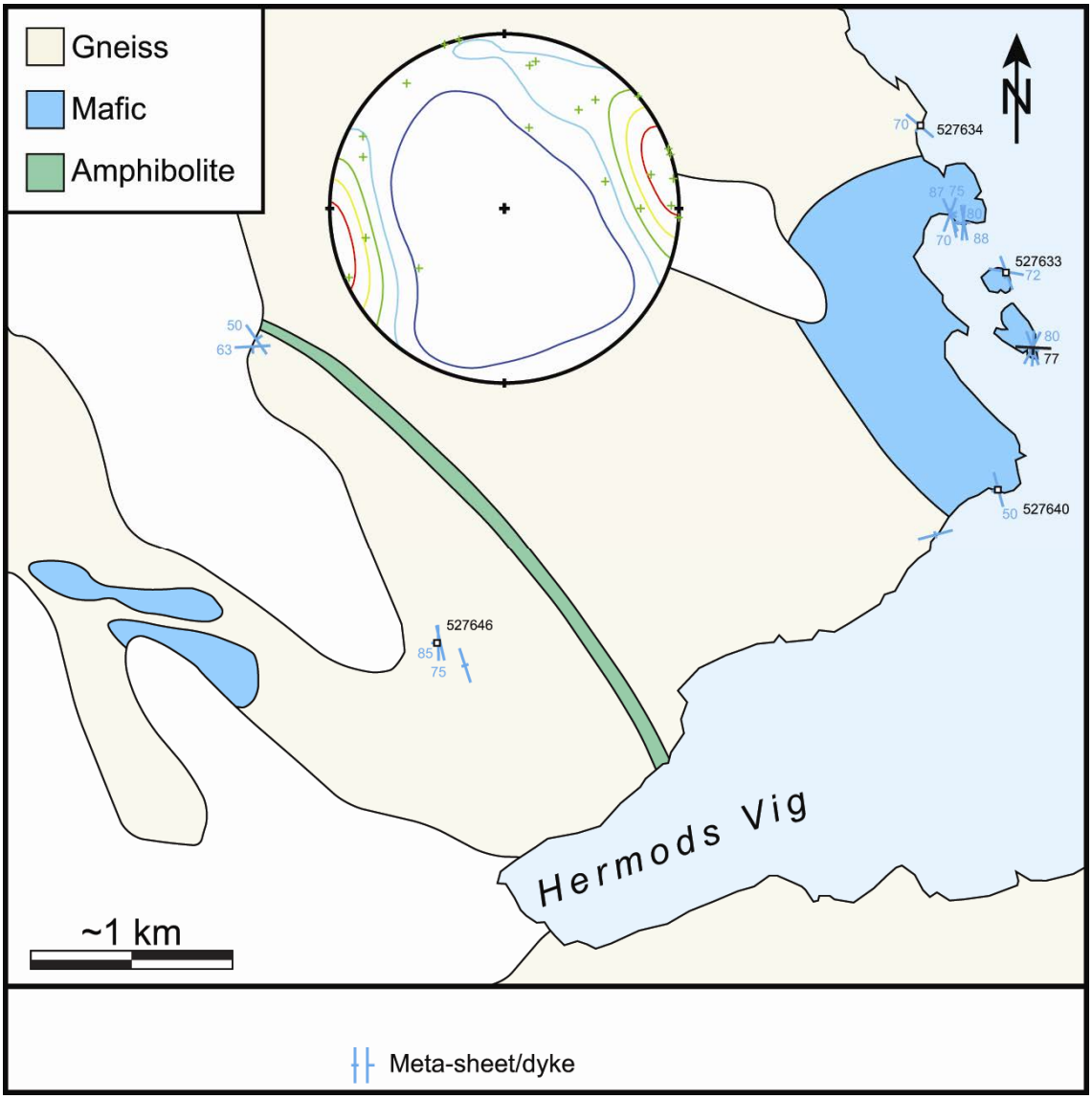

Figure 60. *Secondary sheets and dykes around Hermods Vig superimposed on a revised geological map of the area. Black structure of a black vein. Stereographical plot as in Figure 8.*

Figure 61. *Many different types of cross-cutting planar intrusions in the Hermods Vig Intrusion. (a) An example including a pair of black veins (hammer shaft is 0.6 m long). (b) An example with at least three generations of thicker and different trending dykes.*

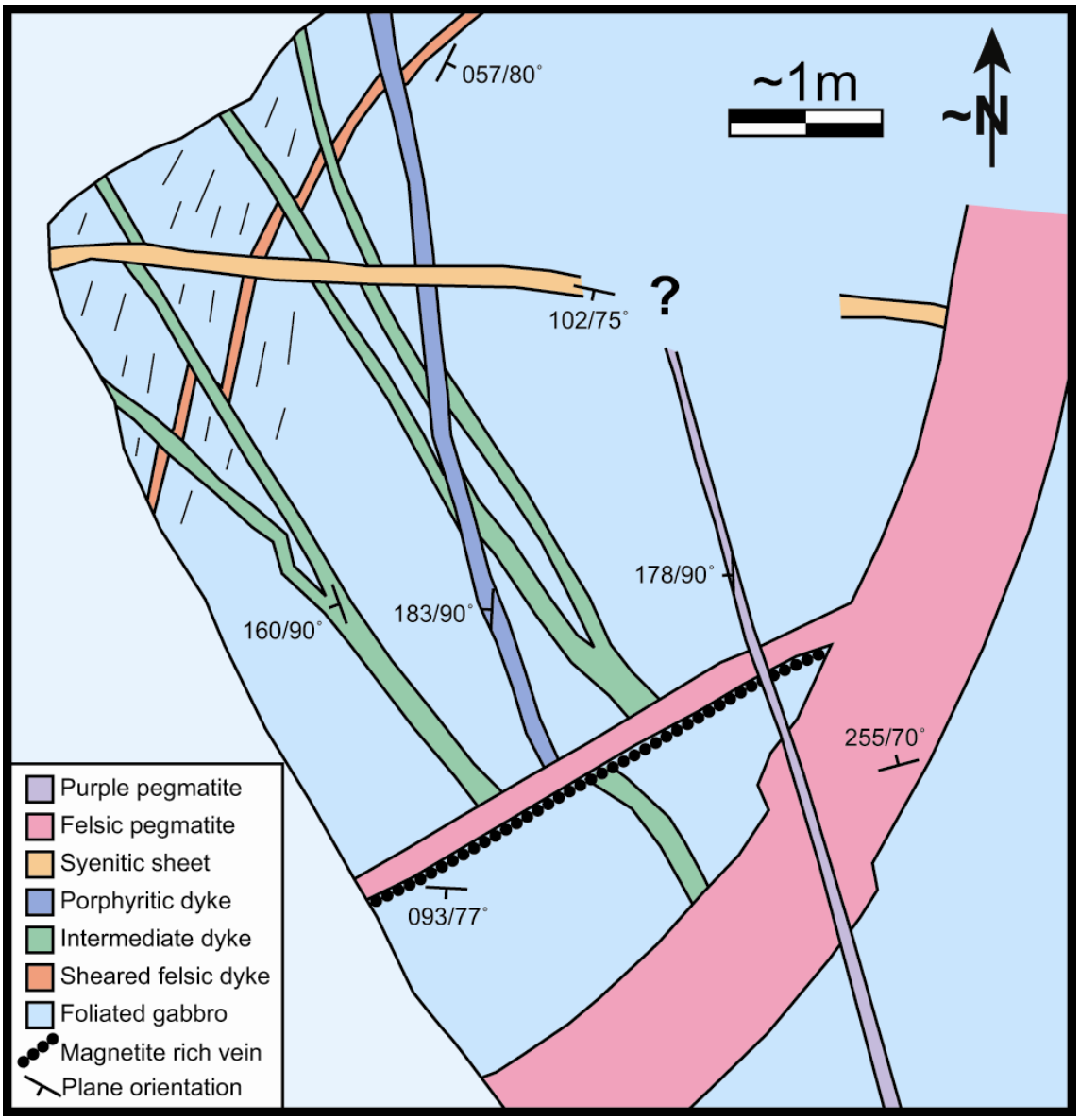

Figure 62. *Cross cutting sheets and dykes within a foliated gabbro, on the southernmost island north of Hermods Vig.*

Brittle faults

A number of minor faults appear to laterally displace sheets below (S of) the Njords's Glacier but, judging from the measured data in Figure 63, not in any systematic conjugate fashion. This may be because displacements predominantly were in vertical (dip-slip) rather than horizontal (strike-slip) directions.

Four out of eight measured felsic pegmatite-aplite dykes are N-S trending and may define an orthogonal pattern together with two E-W trending dykes.

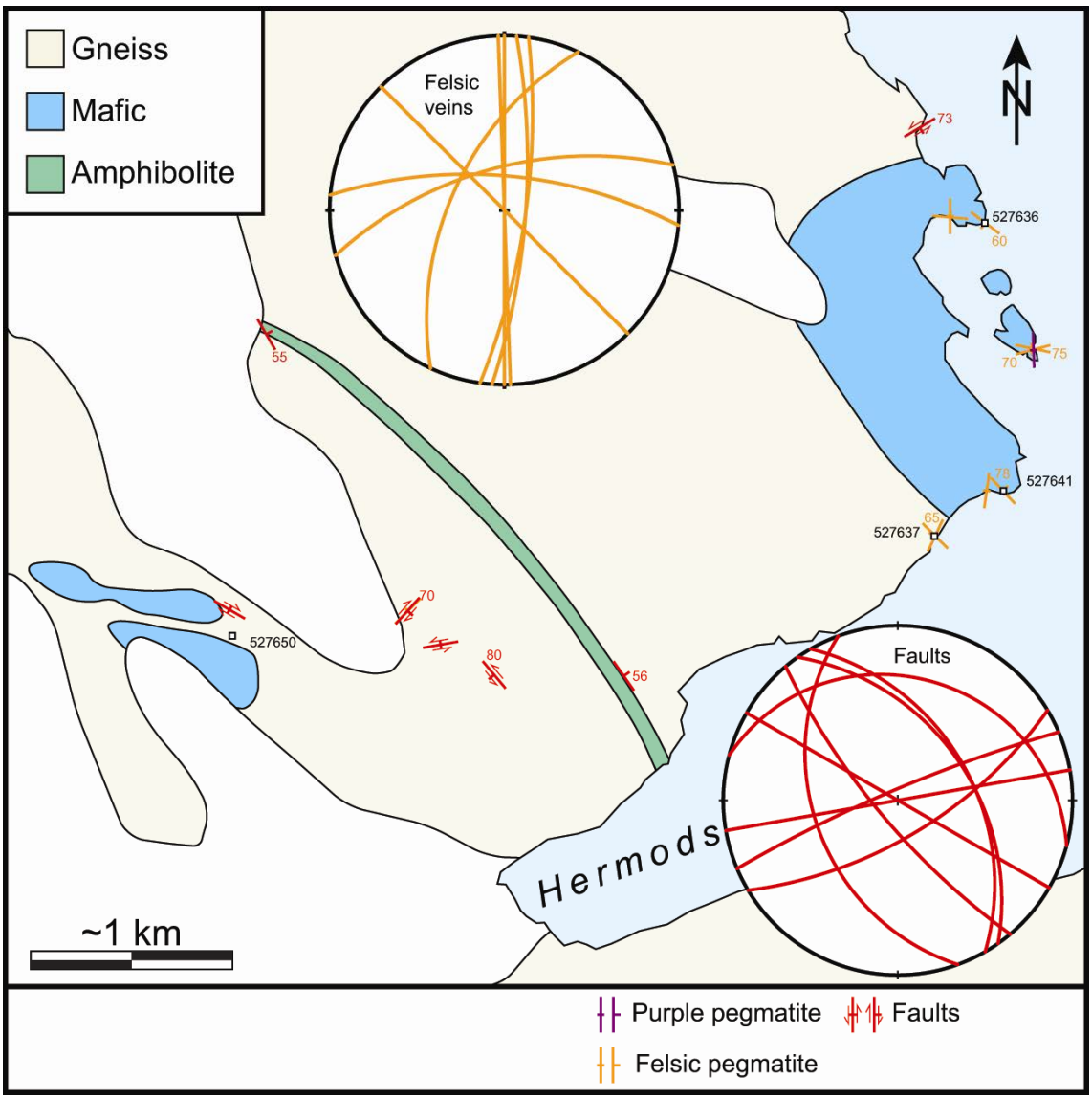

Figure 63. *Faults and felsic aplite-pegmatite dykes around Hermods Vig, superimposed on a revised geological map of the area. Three felsic dykes are sampled, whereas 527650 is a sample of a thick (quartz) syenitic intrusion that appears to separate the two gabbro bodies near Njords Glacier. Planes on stereographical plots as in Figure 8.*

Dolerite dykes

Most dolerite dyke measurements in the Hermods Vig area are (WS)W-(EN)E trending, and with one measurement orientated orthogonally to these (Figure 64). However, many of these measurements could have been made along the same two WSW-ENE trending dykes (each of which is sampled).

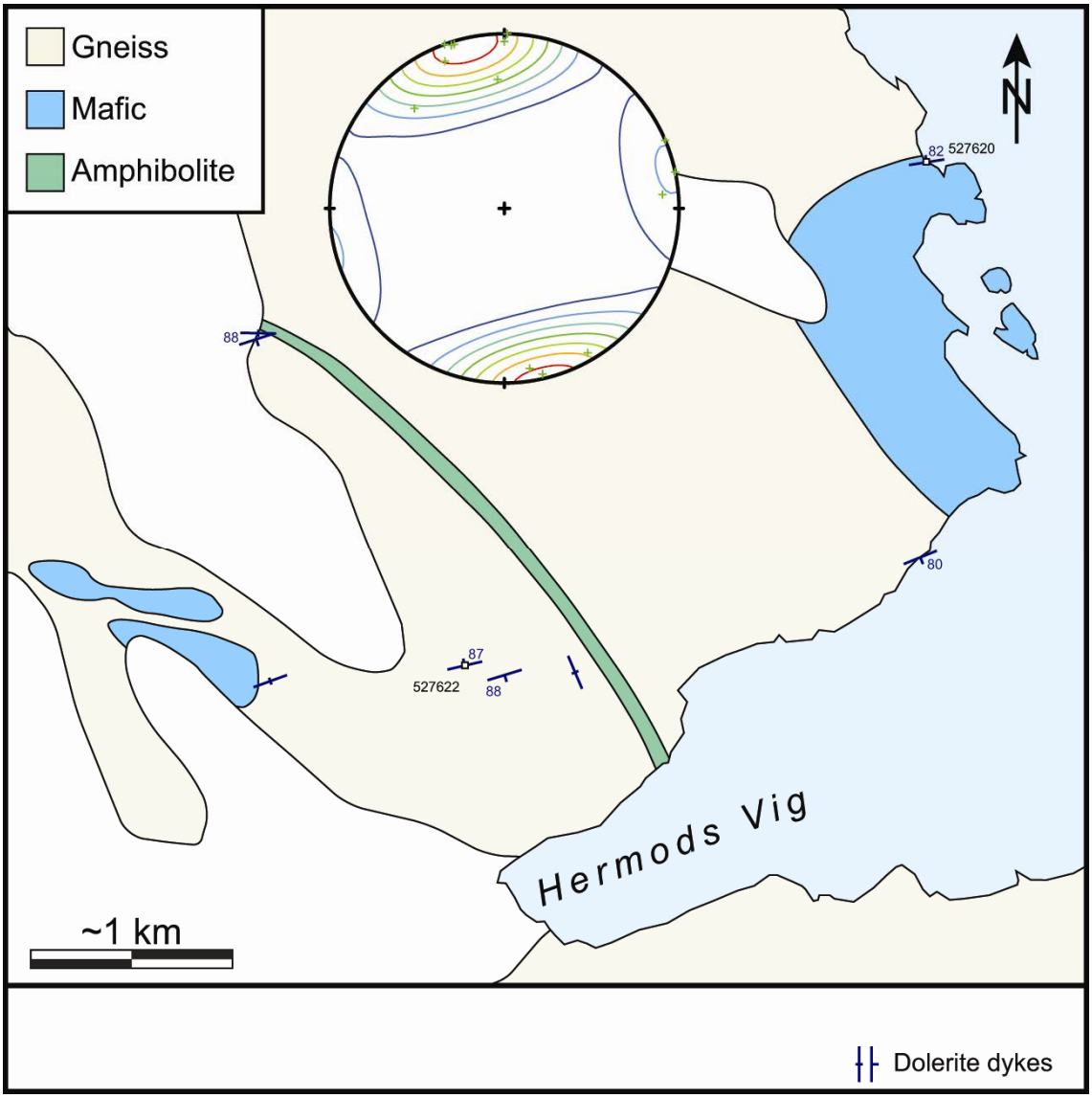

Figure 64. *Dolerite dykes around Hermods Vig, superimposed on a revised geological map of the area. Two WSW-ENE trending dykes are sampled. Stereographical plot as in Figure 8.*

Reco trips and drop-offs

Apart from the data collection associated with the standard field camp and dinghy operations, two days of dedicated helicopter reco flying, one day of helicopter drop off and half a day of dinghy work around M/S 'Fox' were carried out in the central and northwestern part of the Skjoldungen area (Figure 65). These areas included: (1) The intrusions in the Thrymheim 'nunatak' area, (2) the intrusive centre in the Sfinksen area on the inland part of Skjoldungen island, (3) mafic-ultramafic intrusions in Balders Fjord, including two different occurrences, and (4) a mafic-ultramafic dyke-like intrusion in Tværdalen.

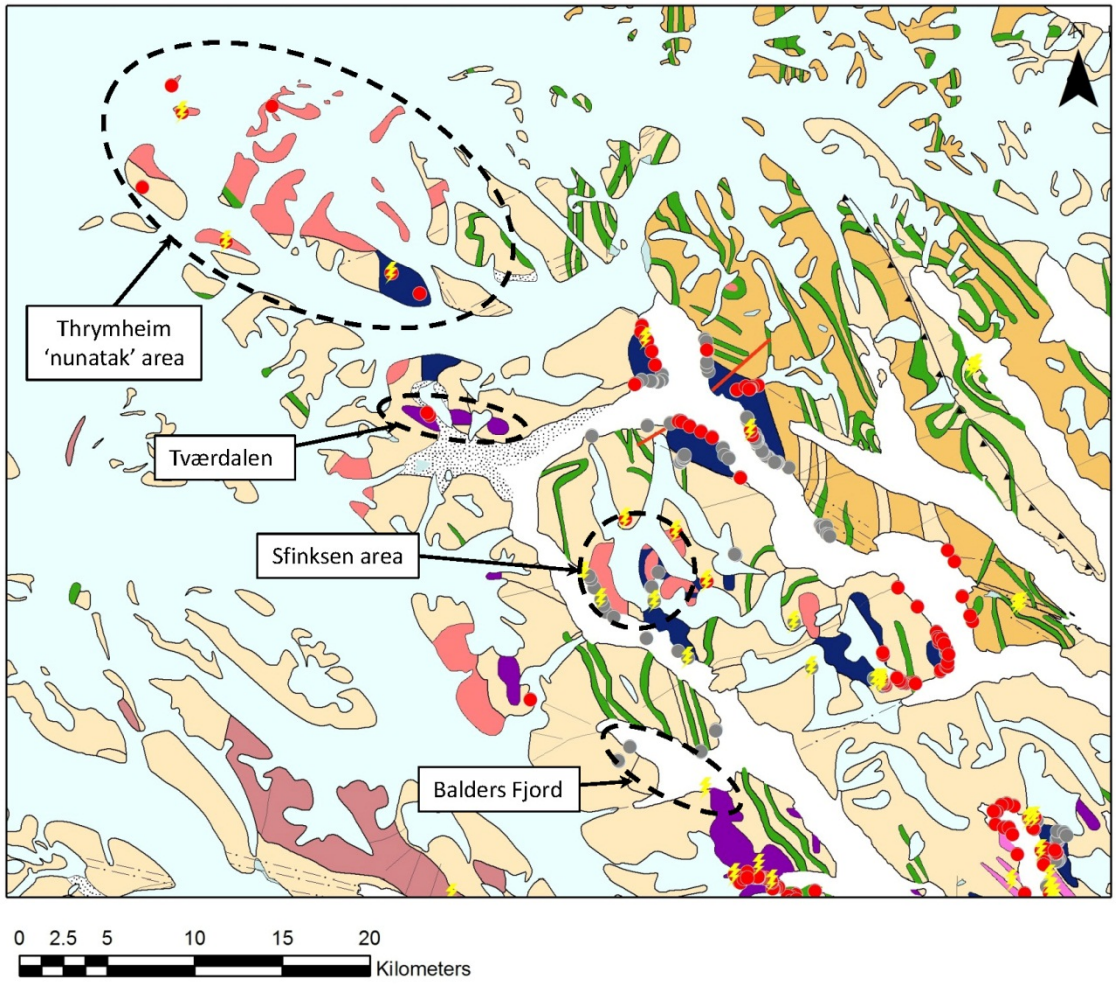

Figure 65. *Geological map showing the localities (red circles) and targeted areas for helicopter reco flying and drop offs (black stippled outlines) during the 2011 field season. Sample sites for the 2012 field work are shown for reference.*

The Thrymheim ‘nunatak’ area

The Thrymheim ‘nunatak’ area was visited by the authors during a joint helicopter reco on the 5th of August together with Alfons Berger and Thomas Ulrich. The nunatak area is dominated by extensive sheet-like intrusions of mainly granite and monzonite that are emplaced into the basement of agmatitic gneiss (Figure 66). The field relationship is intricate and sometimes difficult to establish. This is partly due to the irregular contacts between the SAP intrusions and the basement rocks, and partly because of some apparent similarities between the two lithologies; both rock types typically display a weak to moderate foliation as defined by the alignment of feldspars, and both often contain mafic blocks, either as xenoliths or mafic enclaves. A distinguishing feature in the field, however, seems to be rock colour, as the agmatitic gneisses typically possess a rusty brown colour which is characteristic of retrograded granulite facies rocks (due to a rusty weathering of orthopyroxene), whereas the SAP intrusives that did not experience granulite facies conditions are often more pinkish (Figure 66). Age dating has been undertaken to further verify field distinctions made between SAP intrusions and host basement rocks, and these data will be presented in a separate GEUS report.

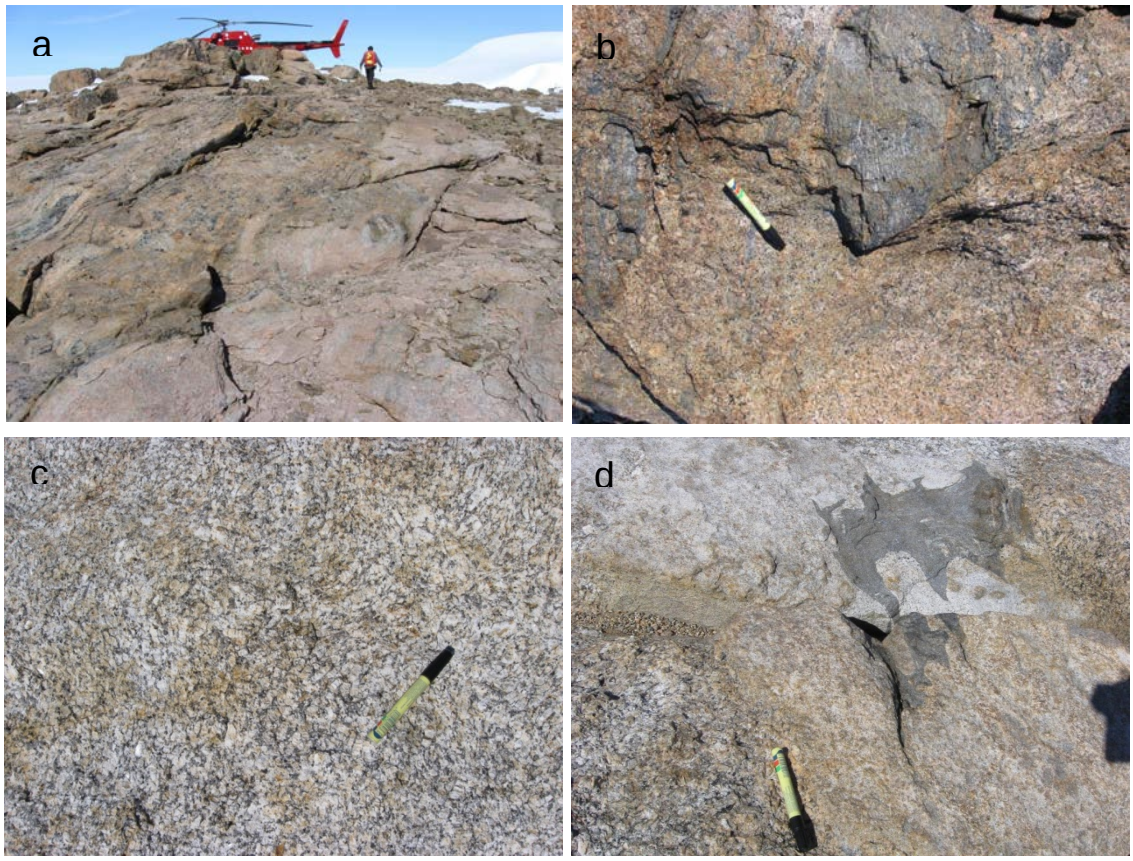

Figure 66. *Examples of the relationship between felsic SAP rocks (quartz syenites, granites ± mafic enclaves and inclusions) and the older agmatitic gneiss basement in the Thrymheim ‘nunatak’ area. (a) Pinkish SAP granite sheet intruding into the agmatitic gneiss basement; note the brownish colour characteristic of retrograded granulite facies rocks. (b) SAP granite with xenoliths of amphibolite. (c) Syntectonically deformed SAP syenite; note the curved foliation as defined by cm-sized feldspar crystals. (d) The same syenite as in (c) intruded by a granitic sheet containing a relatively mafic, deformed enclave.*

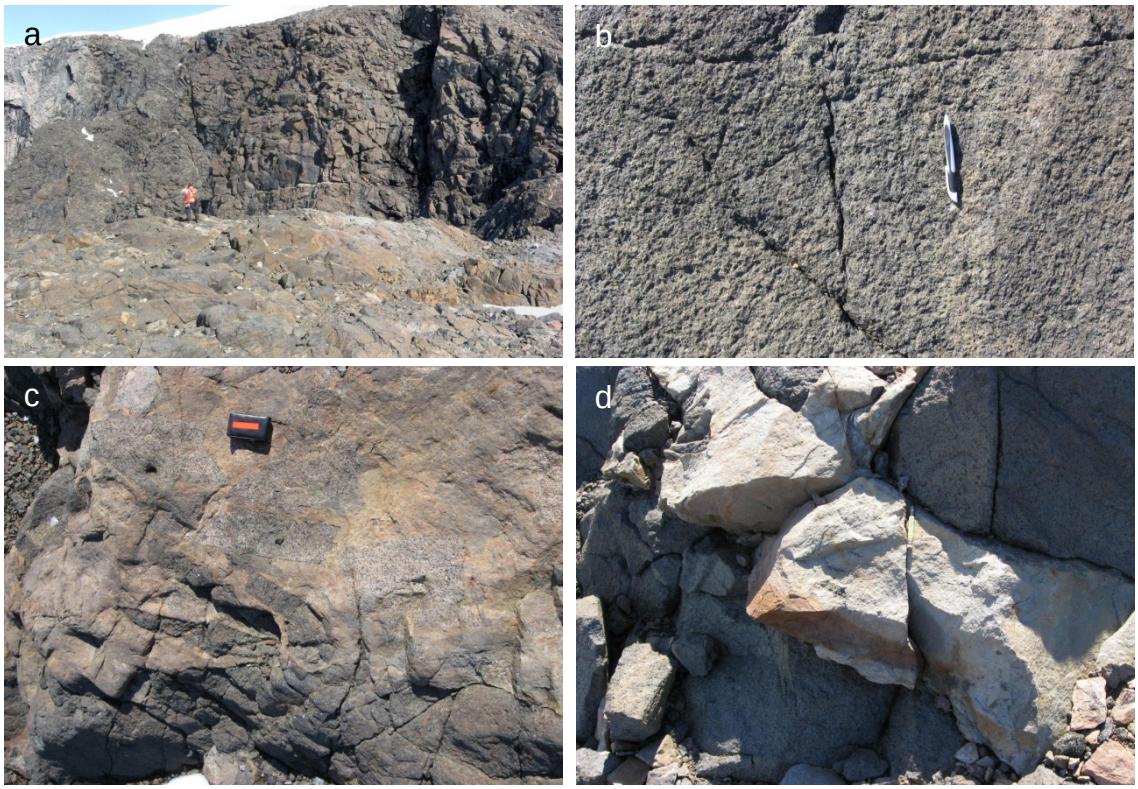

Figure 67. *Station 11TFK0145. The Thrymheim Ultramafic Complex of the Thrymheim 'nunatak' area. (a) Intrusive contact between mafic-ultramafic rocks and agmatitic basement (left), person for scale. (b) Homogenous, coarse grained ultramafic rock (likely cumulate rock), pen for scale. (c) Sharp-edged blocks of coarse grained leucogabbro intruded and brecciated by relatively more felsic melt (gps-receiver is 6 cm long). (d) Fine grained felsic sheet intruding ultramafic rock (felsic sheet is c. 15 cm thick).*

A reco stop was made at the Thrymheim Ultramafic Complex situated in the innermost part of the 'nunatak' area (Figure 65). Although the complex is not shown on the 1 : 500 000 scale map it was identified during 'ground-truthing' by Nielsen and Rosing (1990). Our impression from the short stop we had (*c.* 45 minutes) was that the complex is dominated by mafic-ultramafic rocks with some later intrusive sheets of relatively felsic compositions that locally intrude and brecciate the mafic-ultramafic rocks (Figure 67). The mafic rocks are mainly coarse grained gabbro (no orthopyroxene observed), whereas the ultramafic rocks are dominated by homogeneous, coarse grained pyroxenite (no olivine and little interstitial plagioclase observed) with an equigranular texture, resembling a cumulate rock. The contact to the agmatitic basement is sharp and appears to be of intrusive nature, and accordingly it is believed that the intrusion is part of the SAP.

The Sfinksen intrusion

The north-westernmost part of Skjoldungen island was visited by the authors during a joint helicopter reco together with Troels Nielsen, Bo Møller Stensgaard and Karen Hanghøj on the 6th of August. The area is dominated by the Sfinksen intrusion (*c.* 63°22'59.9"N, 41°40'0.0"W) which intrudes the agmatitic basement and outcrops at the peaks surrounding a glacial valley in a semi-alpine terrain. According to Escher (1990), the Sfinksen intru-

sion is constituted by the Sfinksen Diorite, which includes an early, smaller intrusion of diorite, gabbro and norite, and further to the north a larger circular intrusion, *c.* 3 km in diameter, of the Sfinksen Granite (Figure 65).

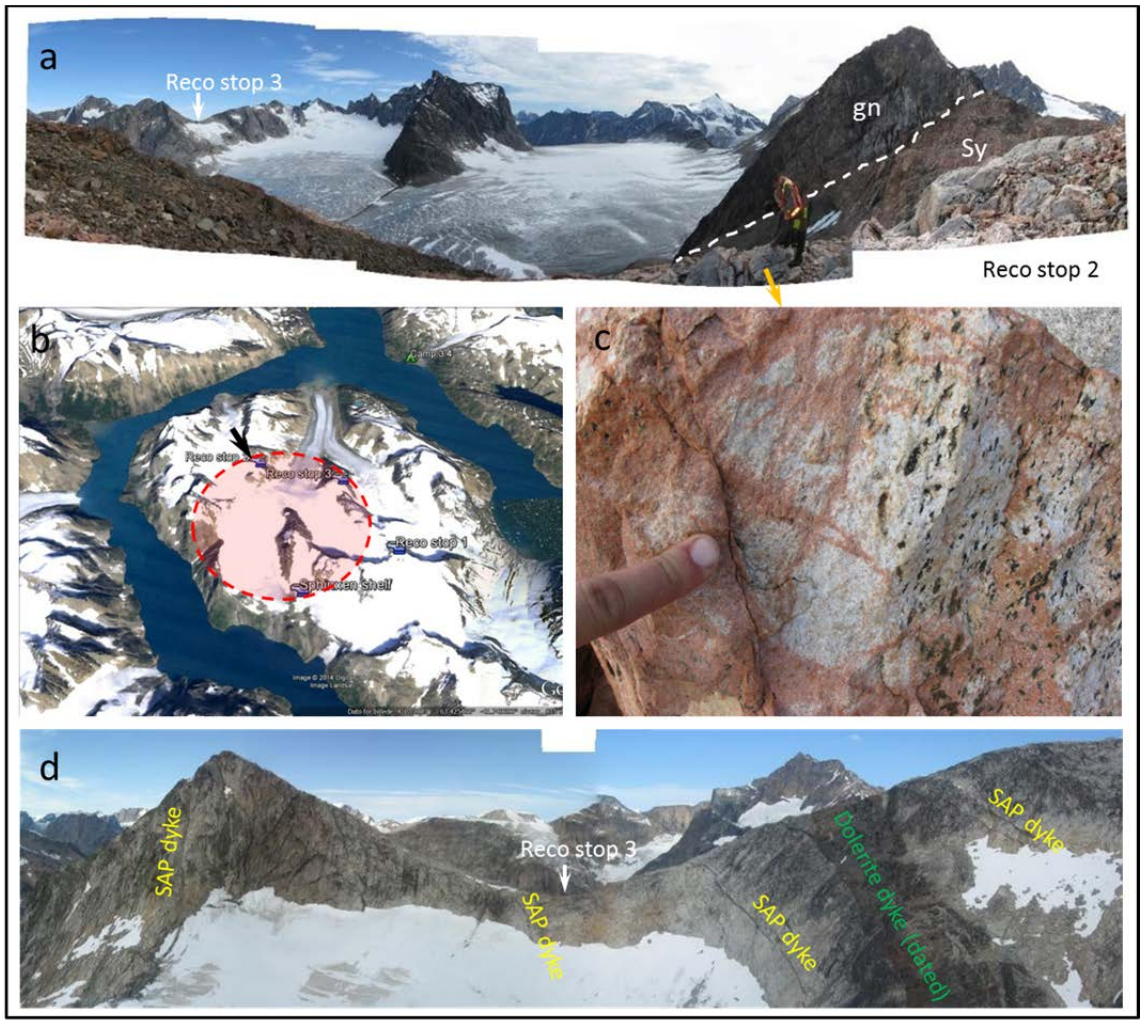

Figure 68. *The Sfinksen intrusion is situated in the north-western part of Skjoldungen island in a semi-alpine terrain. (a) View from Reco Stop 2 towards southeast and the north-western sharp contact to the surrounding gneiss basement (white stippled line). (b) Google Earth map view showing the approximate outline of Sfinksen Granite (see Figure 65 for details) and the locations of reco stops made on August the 5th. Black arrow indicates direction of view in (d). (c) Hydrothermally altered syenite close to the north-western contact (Reco Stop 2). (d) Reco Stop 3 (white arrow): the Sfinksen intrusion is cross-cut by multiple later dykes, including so-called 'deformed SAP dykes' up to 1-2 m thick and of intermediate to mafic in composition.*

The Sfinksen Granite includes a range of granitoid rocks of quartz syenitic to granitic composition that are medium to coarse grained and usually display a weak foliation as defined by alignment of feldspars. The age of the Sfinksen intrusion was believed to be *c.* 2700 Ma, comparable in age to the neighboring Ruinnæsset intrusion (Blichert-Toft et al. 1995). However, new zircon U/Pb age dates on the Granite indicate it to be slightly older, 2.73-2.74 Ga, whereas late stage pegmatites intruding the Sfinksen Diorite are dated to 2.70 Ga (Kokfelt, unpublished data, to be presented in a separate GEUS report).

The Sfinksen area is cut by a series of later sub-parallel grey so-called “deformed SAP dykes”, up to *c.* 2m thick (Figure 68). As in the Halvdan Fjord and Stærkodder Vig areas these dykes have characteristically smeared contacts to the surrounding SAP rocks, indicating that they were only partially consolidated when the dykes intruded.

The three reco stops in the area were all at, or close to, the contact of the circular Sfinksen Granite, which basically reflects that ice covers the central part of the intrusion. The northern contact (visited at Reco Stop 2) is characterized by distinct and widespread red staining of the Sfinksen Granite along joint planes, cracks and surfaces (Figure 68a,c). The extent of the red staining increases towards the contact to the basement agmatitic gneiss where the entire rock is red coloured. The pervasive red staining is likely to reflect circulation of fluids in the contact zone at a late- to post-magmatic stage.

The existing GGU samples from the Sfinksen intrusion encompass a suite of mafic to evolved mildly alkaline rocks constituting an evolutionary trend presumed to be controlled by fractional crystallisation (Blichert-Toft et al. 1995). A number of these samples were collected from the ‘Sfinksen Shelf’ locality as lose blocks of distinctly local origin (cf. Troels Nielsen) (Figure 68b); these rocks include several syenitic compositions which stands in contrast to the granitic compositions sampled in 2011 at reco stops 1-3. The older GGU samples will be included in in the future studies to obtain a more complete picture of the compositional variability of the Sfinksen area.

Meta-dykes in the Sfinksen area

Mafic to intermediate dykes, usually up to 1 meter wide, occur throughout the larger Skjoldungen area, all the way from Halvdans Fjord to the Thrymheim (nunatak) area, and were sampled at various places for geochemical and structural investigations. The dykes generally strike NW-SE and have characteristic blurred contacts to the host rock, giving rise to the field term ‘deformed dykes’ or ‘meta-dykes’. The field relations indicate that these dykes intruded syntectonically, and as such they are considered part of the SAP magmatism. In order to characterize the parental melts of the SAP magmatism these dykes are considered as potentially good candidates – particularly the ones that are least evolved, because they would be relatively unaffected by magma chamber process, such as crystal fractionation and crustal contamination. Figure 68d shows the typical outcrop morphology of the SAP dykes, dissecting the host rocks as a sub-parallel swarm and with semi-regular spacing with blurred irregular contacts.

Balders Fjord

During camp move by dinghy, from Stærkodder Fjord to Ruinnæsset, we overnighted on base ship 'Fox'. This left us with an afternoon to discover two interesting SAP-related intrusions on the outer S-side of Balders Fjord, where Escher (1990) indicates the continuation of a larger ultramafic body, extending from Stærkodder Fjord (Figure 26 and Figure 69a). The authors could only verify a mafic-ultramafic dyke and a minor gabbroic intrusion, but these could not be followed up onto the hill top further to the south. This central part of the peninsula (the area marked with '?') was not visited by the authors in 2011, but was overflown in 2012, and the impression there was that a mafic intrusion exists with numerous irregularly cross-cutting felsic pegmatites, consistent with earlier observations by Troels Nielsen. Thomsen (1998) also adds another layered mafic-ultramafic body to the inner part of Balders Fjord (Figure 69b), observed during our Nunatak-reco (see below). This intrusive body is also on the old field maps, but not as a SAP intrusion but as an unidentified mass of structured mafic unit (referred to as "Kaos-væg"; T. Nielsen, pers. com. 2014).

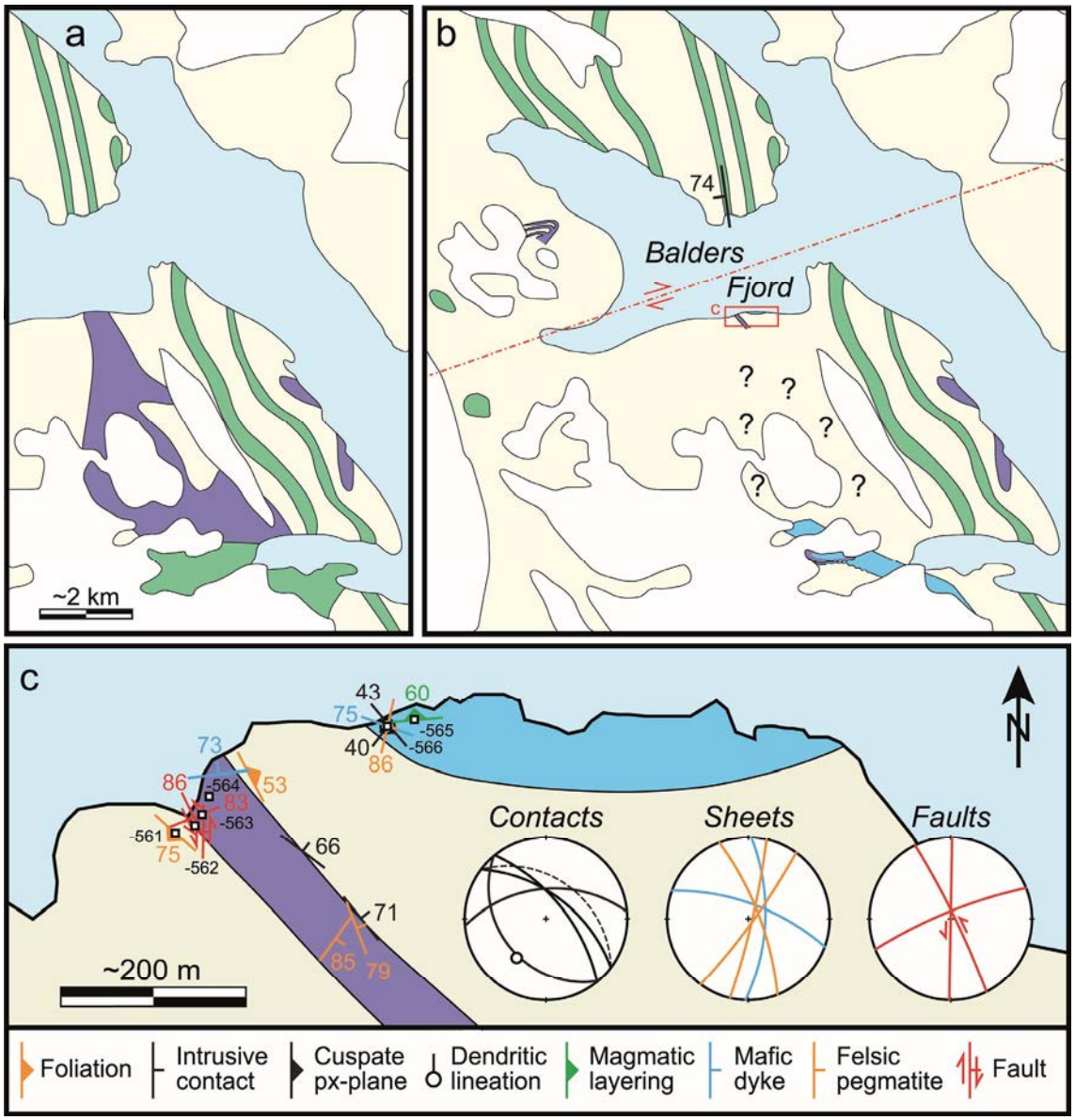

***Figure 69**. (previous page) Geological information on the Balders Fjord area. (a) Escher's (1990) map of basement gneiss, amphibolite and ultramafic rocks; the large mafic-ultramafic intrusion is too large and inconsistent with the original compiled field map of Troels Nielsen (GEUS map archive). (b) The authors could only verify a mafic-ultramafic dyke and a minor gabbroic intrusion, but these could not be followed onto the hill top to the south (the area marked with '?'). Note that the ultramafic body in the inner (western) part of the fjord (Thomsen, 1998) is not on Escher's (1990) map. (c) Enlarged map view of investigated area along S-side of Balders Fjord, showing the mapped extent of the mafic-ultramafic dyke and minor gabbroic intrusion, onto which all of this report's structural measurements and sample localities (527- prefix omitted from each label) are superimposed. Stereographical plots as in Figure 8, show (i) the measured NE-contact of the ultramafic dyke (solid), and a plane perpendicular to the plunge of dendritic pyroxenes (dashed, Figure 74.) along the gabbro intrusion contact, (ii) mafic (blue) and felsic (orange) sheets, and (iii) faults.*

Figure 70. *The mafic-ultramafic dyke at Balders Fjord. (a) View from the SW-margin of the dyke to possible continuation on the on the N-side of the fjord (note opposite steep dips on either side of the fjord). (b) NE-contact of the dyke, where the picture has been mirrored in order to show that it is dipping the same way as the SW-margin in the foreground of (a). From left to right, small hammer shaft point at where the ultramafic part of the dyke in contact with a 1.10 m wide leucogabbroic and a 0.45 m wide gabbroic margin zone that in turn is in contact with the foliated gneiss host to the far right. (c) Detail of a similar gabbroic marginal zone along the dyke's SW-contact, which hosts a rounded ultramafic xenoliths. (d) Detail of the hornblende-porphyroblastic pyroxenite/melgabbro that dominate much of the central parts of the dyke. (e) Brecciation and possible felsic net-veining of an unusually banded unit (upper part of picture) outside a highly irregular NE-margin of the ultramafic part of the dyke (lower part of picture). Red hammer shaft is ~0.9 m long.*

Mafic-ultramafic dyke

The mafic-ultramafic dyke is *c.* 60 m thick and locally orientated *c.* 344/68°, but may exhibit irregular and partly molten contacts as well as be sinistrally segmented up the slope. It is tempting to correlate this mapped dyke on the S-side of Balders Fjord, to a conspicuous dyke-like structure (amphibolite band by Escher 1990) on the fjord's N-side (Figure 70a), resulting in a more northerly orientation of 172/74°. The N-side was never visited.

The mafic-ultramafic dyke appears to have more (leuco)gabbroic margins (Figure 70b-c), which may reflect either a composite intrusion or the contamination by partially melted host rocks. Much of the dyke's central parts appear to be predominantly ultramafic, composed of similar hornblende-porphyroblastic melagabbro or plagioclase-bearing pyroxenite (Figure 70d) as observed along the marginal zone off the Vend Om Intrusion. The dyke is cut by fine grained mafic and felsic aplite-pegmatite sheets – including a brecciated zone of felsic (back)veined angular xenoliths (Figure 70e) – as well as some brittle faults (Figure 69c).

Gabbroic intrusion with a dendritic pyroxene margin

The edge of a gabbroic intrusion is exposed a little more than 100 m east of the mafic-ultramafic dyke, and may combined have led Escher (1990) to correlate these outcrops and mafic-ultramafic outcrops in the Stærkodder Vig area into the large ultramafic body in Figure 69(a). In detail, however, it appears that the mafic-ultramafic dyke and the *c.* 500 m wide edge of a more plutonic gabbro are not part of the same body. The inland extent of the gabbroic intrusion is well constrained by the fact that a *c.* 3 m wide and conspicuous leucocratic contact zone (Figure 71), with spectacular inward protruding dendritic pyroxenes, can be correlated around some typically rounded and low gabbroic outcrops (Figure 72) and back out into the fjord as shown in Figure 69c.

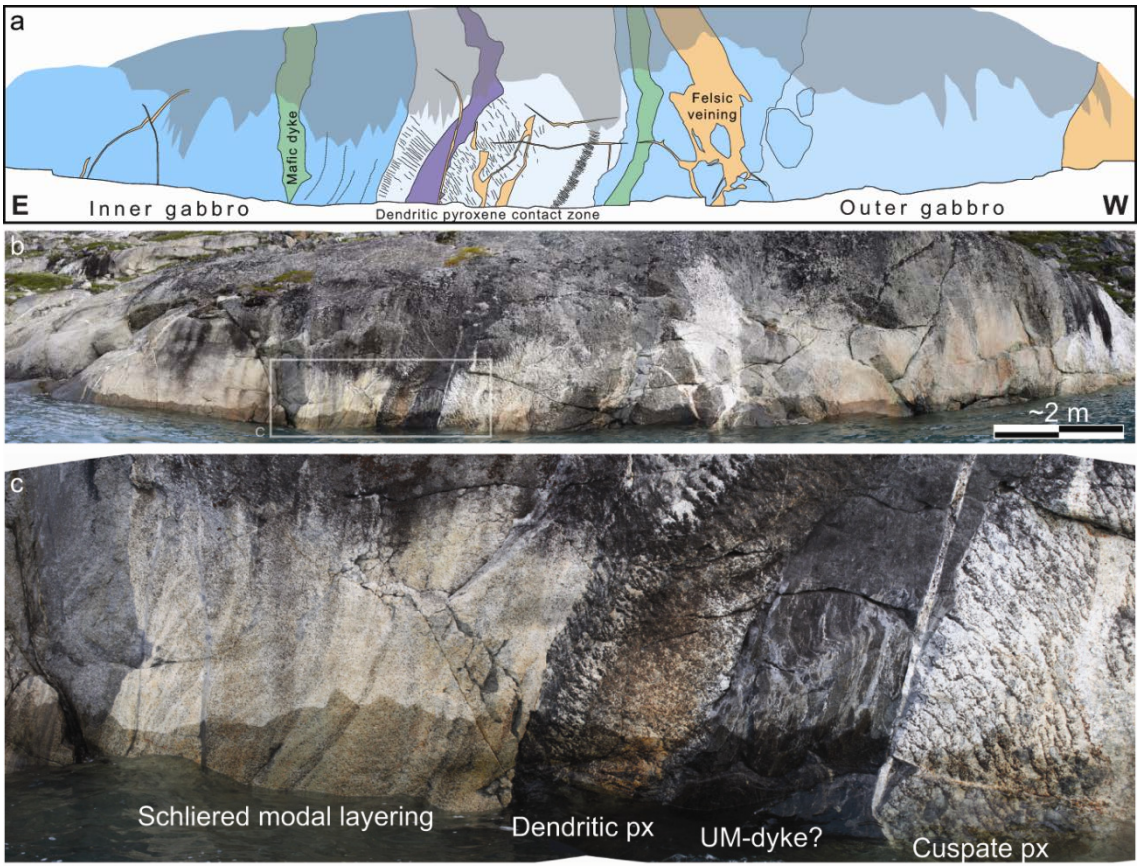

Figure 71. *Spectacular contact zone across the SW-contact of a small gabbroic intrusion. (a-b) Traced panoramic view of outcrops close to the water surface, exhibiting up to three nested intrusions of homogeneous to weakly layered (schliered) medium to coarse grained gabbro (different shades of blue). As enlarged in (c), a c. 3 m wide leucocratic chilled margin with spectacular dendritic and cuspate pyroxenes that grew inwards to the left (east) of this picture, and onto which the schliered gabbro subsequently crystallized as roughly contact-parallel layering.*

Depending on the erosional section through the dendritic pyroxenes, these typically appear either more rarely as branching growth structures that are up to 0.5 m long, or more commonly as cuspate sections through what appears to be flat crystal ‘branches’. On the plane of these flat ‘branches’, the growth direction of denritic ‘branches’ in Figure 73a has a plunging lineation that is orientated perpendicular the intrusion’s contact plane (dashed curve on inserted stereographical plot in Figure 74). A weakly layered and schliered gabbroic interior (Figure 71) is evidently orientated at only a slightly oblique angle to the neighbouring contact (Figure 74).

Figure 72. *Overview of leucocratic contact zone with dendritic pyroxenes. (a) Contact extending inland above low and smooth gabbroic hills in the foreground, before outcropping c. 500 m farther east along the shore. (b) More common cuspate erosive appearance of the dendritic pyroxenes within the leucocratic contact zone. Person provides a scale.*

Figure 73. *Details showing (a) typical dendritic pyroxenes that grew from lower left to upper right, and (b) typical cuspate erosive appearance of such dendritic crystals. Contact is cut by both an older mafic and a younger felsic sheet. GPS receiver is ~12 cm and pen is ~14 cm long.*

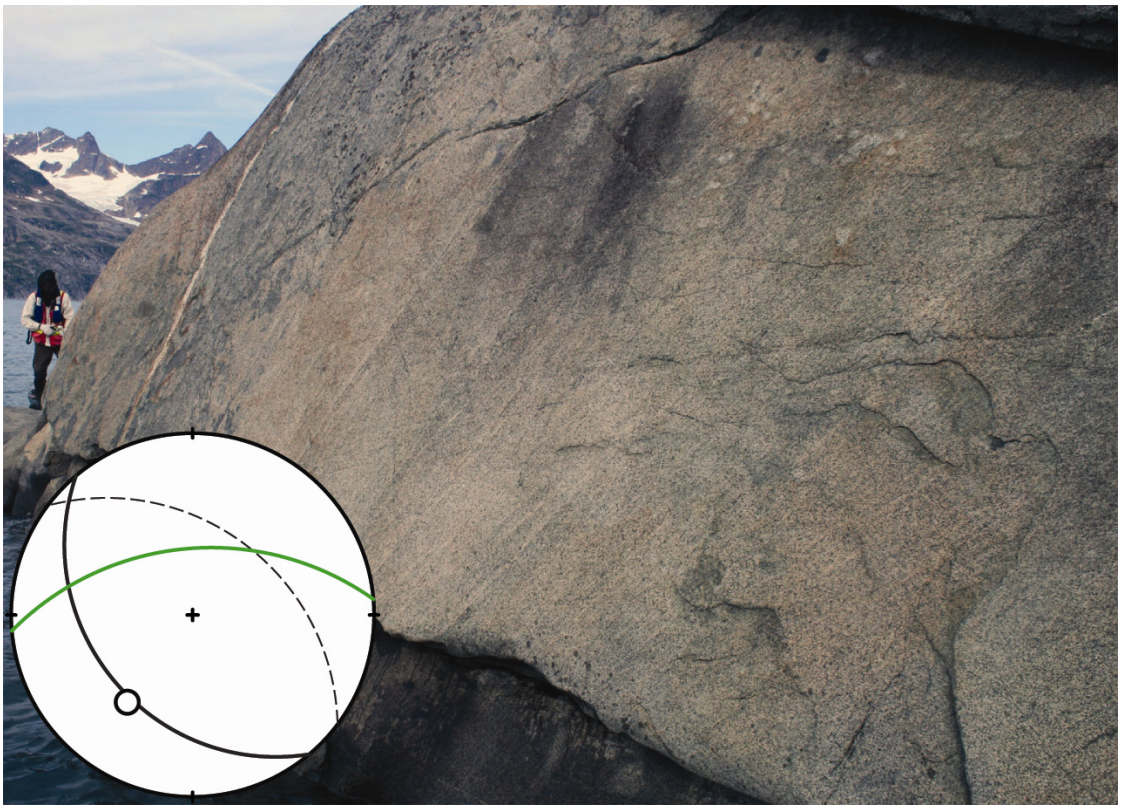

Figure 74. *Faint gabbroic layering inside dendritic pyroxene contact zone. Inserted stereographical diagram compares the orientation of this layering (green curve) with the inward growth direction (lineation = O) of the dendritic pyroxenes in Figure 73a on their cuspate planes (black solid curve) in Figure 73b, and a presumed orthogonal intrusion margin defined by this lineation (dashed curve). From this comparison, it can be seen that this particular internal layering is only slightly oblique to the nearby steep contact of the intrusion.*

The Balders Fjord lopolith

Only a helicopter fly-by allowed us to study and photograph an (ultra)mafic intrusion, well exposed on the upper, inner northern cliffs of the Balders Fjord (Figure 75a-b). As suggested by Thomsen (1998), this intrusion appears in cross section to resemble a typical stack of hypabyssal lopoliths (e.g., Figure 75c). The intrusion was sampled in 2012, both *in situ* on the top of the cliff during a short drop off, and as talus/scree at the foot hills of the cliff side.

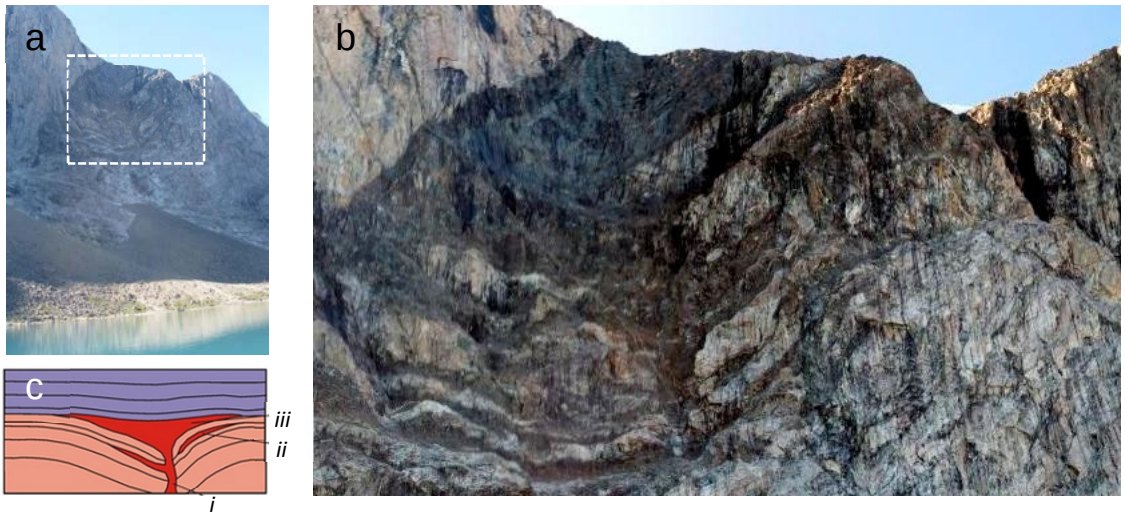

Figure 75. *Mafic-ultramafic lopolith intrusion exposed near the top of a c. 1200 m high north-east facing mountain cliff in Balders Fjord. (a) Photograph taken from the sea side; stippled box shows the enhanced view in (b) which shows a high resolution composed image taken during a helicopter fly-by. (c) Schematic illustration of a text book example of a small concordant lopolith with a characteristic feeder (i), concordant sills (ii) and intrusive lopolith body (iii). Small lopoliths are usually associated with emplacement of magma into upper crust.*

Dronning Maries Tværdal

Dronning Maries Tværdal was visited by the authors, together with Alfons Berger and Tomas Ulrich, during a whole day drop-off on the 2nd of August. This hanging valley was targeted because of Escher's (1990) large ultramafic intrusion, which by Nielsen & Rosing (1990) was named the Marie Dal Ultramafic Centre (Figure 76). Overflying the area, however, it quickly became clear that only a minor, steeply dipping and dyke-like ultramafic intrusion exists. Furthermore, the intrusion was difficult to access and could only be reached at the top of a steep snow/ice-covered scree cone (Figure 77). Consequently, only two samples were collected of a more gabbroic (527651) and a more pyroxenitic (527950) part of the intrusion. Whereas a gabbroic outcrop could be reached below the snow fan (Figure 78a), 527650 was sampled from the scree because the apparently more ultramafic northern part of the intrusion was never directly accessed (Figure 78b). Looking from west, it is not evident that there is a continuation of an ultramafic intrusion across to the eastern side of the valley (Figure 79). Towards the north (Figure 79a), however, it is possible to discern the outline of a less foliated and slightly more brown weathered mafic (gabbroic, diorite in early field maps) intrusion, approximately as outlined by Escher (1990) in Figure 76.

.

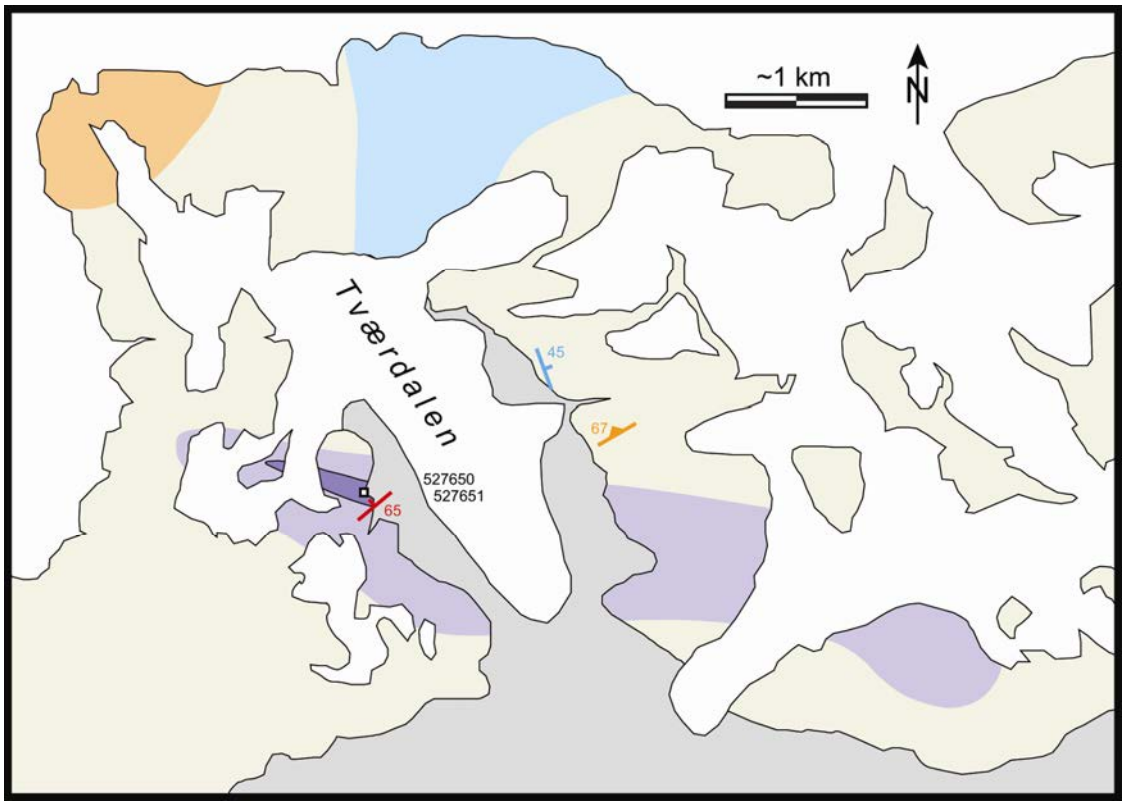

Figure 76. *Geological information on the area around Dronning Maries Tværdal (aka Tværdalen). Only the ultramafic intrusion (pale purple) on Escher's (1990) map – including basement gneiss (pale yellow) as well as felsic (orange) and mafic (blue) intrusions – was investigated and found to be grossly exaggerated in its extent. The author's only verified a dyke-like mafic-ultramafic intrusion as indicated in dark purple, and from which two samples were collected.*

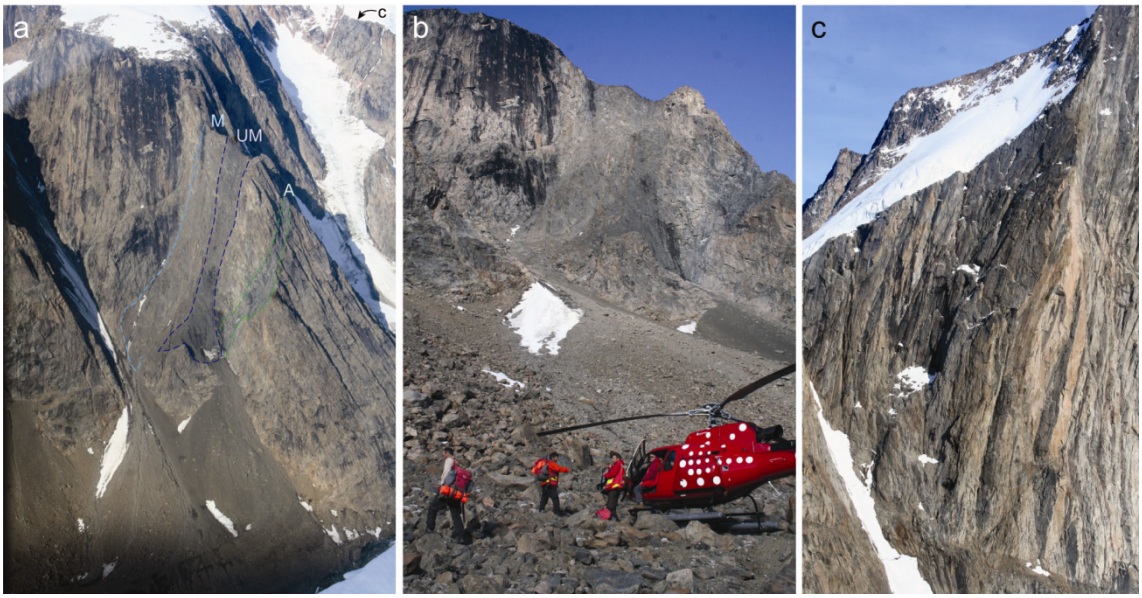

Figure 77. *Extent of the dyke-like mafic-ultramafic intrusion as (a) outlined from an oblique aerial photograph, (b) as viewed from the helicopter landing spot, and (c) viewed behind the mountain ridge in (a).*

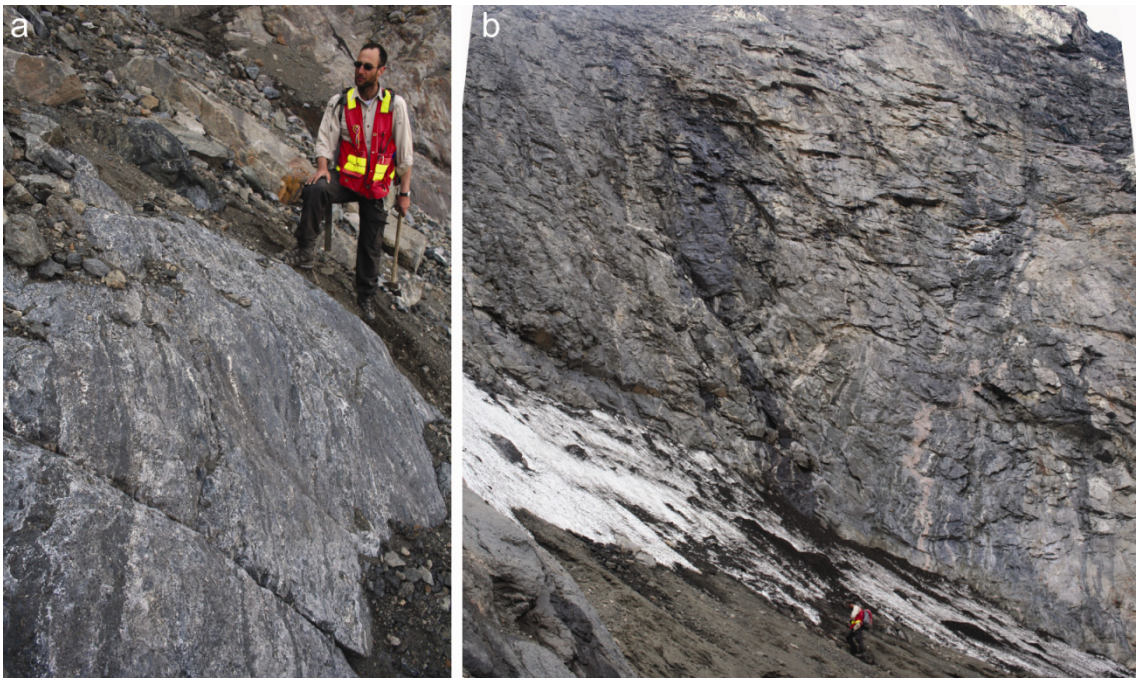

Figure 78. *Outcrops along the accessible base of the intrusion. (a) A heterogeneous mela-gabbroic outcrop below the snow fan was sampled (527651), whereas (b) ultramafic scree boulders sampled outcrops above the snow fan (527650). Thomas Ulrich provides a scale in both photographs.*

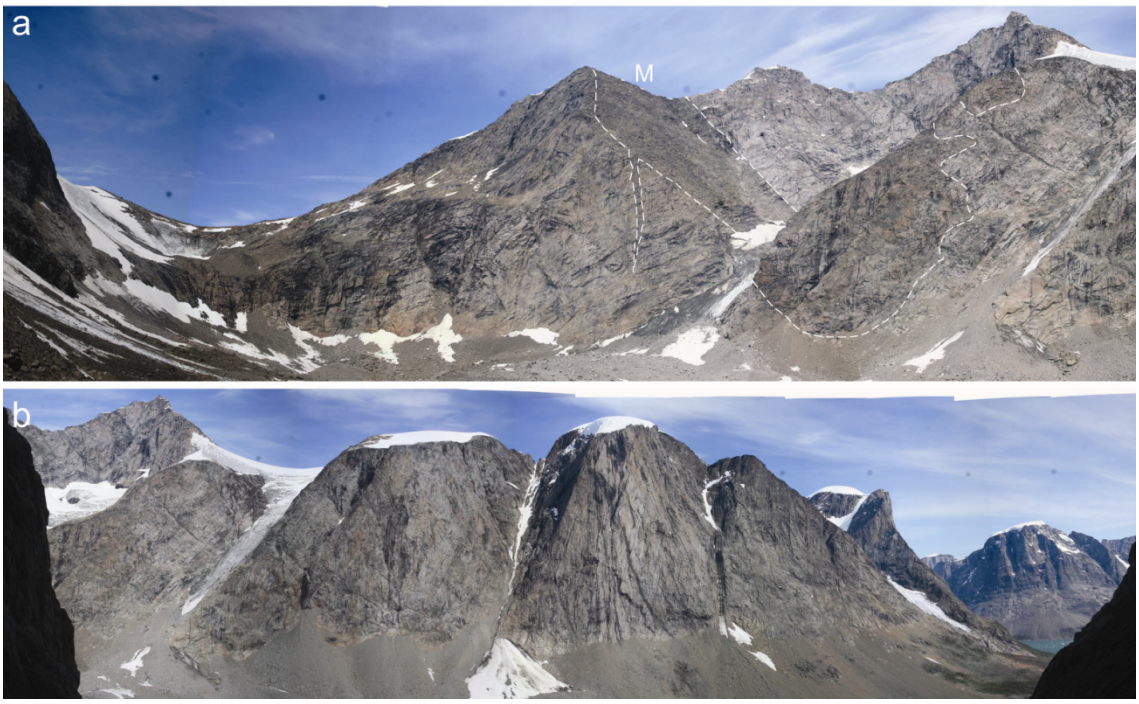

Figure 79. *View from the W-side of Dronning Maries Tværdal. (a) Northern part of the E-side of Tværdalen, where a weakly foliated and slightly brown weathered mafic (gabbroic?) intrusion is outlined by white dashed lines. (b) From the foot of the ultramafic intrusion in Figure 78, the southern part of the E-side of Tværdalen only appears to expose regularly foliated gneiss (240/67°), end thereby not represent a continuation of an ultramafic intrusion.*

Note on the economic potential

The greatest potential for an economic deposit in the SAP seems to be related to the semi-massive oxide layers within some of the gabbroic intrusions at Vend Om and Njords Gletscher. Magnetite seems to be the dominant oxide phase in all of these intrusions, followed by ilmenite, and such occurrences are elsewhere in the world, e.g. in Bushveld, South Africa, being mined for vanadium. Preliminary microprobe analysis across a magnetite/ilmenite layer in Njords Gletscher (in the middle part of the intrusion) indicate *c.* 0.75 wt. % V_2O_5 in magnetite (Árting, 2013). Our current best estimate is that the occurrences are not of economic importance, mainly due to too small tonnages apart from the logistical challenges of mining operations in East Greenland.

Eight whole rock analyses of the most Cu-rich ultramafic samples with disseminated sulphides (likely pentlandite and chalopyrite) only showed insignificant concentrations of Platinum Groups Elements (PGE) or gold (Au).

Magnetite and apatite-rich nelsonitic bands within the Ruinnæsset intrusion are presumably too thin and dispersed to be of sufficient economic importance for mining, but further exploration is needed in order to determine any higher volume occurrences.

References

Árting, T.B., 2013: A detailed study of a Fe-Ti oxide band in the Njords Gletscher intrusion, Skjoldungen Alkaline Province, South-East Greenland. Unpublished Bc.S. Thesis, University of Copenhagen, 69 pp.

Berger, A., Kokfelt, T.F., & Kolb, J., 2014: Exhumation rates in the Archean from pressure–time paths: Example from the Skjoldungen Orogen (SE Greenland). *Precambrian Research* **255**, 774-790.

Blichert-Toft, J., Rosing, M.T., Lesher, C.E. & Chauvel, C., 1995: Geochemical constraints on the origin of the late Archaean Skjoldungen alkaline igneous province, SE Greenland. *Journal of Petrology* **36**, 515-561.

Cawthorn, R.G., Eales, H.V., Walraven, F., Uken, R. & Watkeys, M.K., 2006: The Bushveld Complex. In: Johnson, M.R., Anhaeusser, C.R. & Thomas, R.J., (Eds.). The Geology of South Africa. Geological Society of South Africa. Johannesburg/Council of Geoscience, Pretoria, 261-281.

Escher, J.C. (compiler), 1990: Geological map of Greenland 1:500 000, sheet 14, Skjoldungen. Copenhagen, Geological Survey of Greenland.

Graaf, J., 2012. *Petrogenesis of late-kinematic dykes and sheets within the 2.7 Ga Skjoldungen Alkaline Province, South-East Greenland*. Unpublished Honours Thesis, Stellenbosch University, 51 pp.

Grobbelaar, M., 2012. *Petrographical and geochemical variations across the layered ultramafic-mafic Vend-Om intrusion within the 2.7 Ga Skjoldungen Alkaline Province, southeast Greenland*. Unpublished Honours Thesis, Stellenbosch University, 66 pp.

Kolb, J., Thrane, K., & Bagas, L., 2013: Field relationship of high-grade Neo-to Mesoarchaean rocks of South-East Greenland: Tectonometamorphic and magmatic evolution. *Gondwana Research* **23**, 471-492.

Nex, P.A.M., 2004: Formation of bifurcating chromitite layers of the UG1 in the Bushveld Igneous Complex, an analogy with sand volcanoes. *Journal of the Geological Society, London*, 161, 903–909.

Nielsen, T.F., 2004: The Shape and Volume of the Skaergaard Intrusion, Greenland: Implications for Mass Balance and Bulk Composition. *Journal of Petrology* **45,** 507-530.

Nielsen, T.F. & Rosing, M.T., 1990: The Archaean Skjoldungen alkaline province, South-East Greenland. *Rapport Grønlands Geologiske Undersøgelse* **148,** 93-100.

Nutman, A.P. & Rosing, M.T., 1994: SHRIMP U-Pb zircon geochronology of the late Archaean Ruinnæsset syenite, Skjoldungen alkaline province, southeast Greenland. *Geochimic. et Cosmochimic. Acta* **58,** 3515-3518.

Parsons, I., 1987: Origins of igneous layering. **196**, Springer, 666 pp.

Thomsen, H.S. 1998: Geological and experimental constraints on the formation of the Late Archaean Skjoldungen Alkaline Province, Southeast Greenland and Petrogenetic implications of late stage amphibole growth in arc environments. Unpublished Ph.D. thesis, University of Copenhagen. 134 pp.

Wager, L. R. & G. M. Brown., 1953: Layered intrusions. *Medd. dansk geol. Foren*. **12**, 335-349.

Appendix

Table A1. *List of samples taken during the 2011 field season in the Skjoldungen area*

Sample[§]	Latitude (deg N)	Longitude (deg W)	Station ID	Place name	Description / field name	Chem.	PTS	U-Pb
527501	63.15322	-41.47867	11MBK003	Vend Om Gabbro	Medium-coarse grained melano-gabbro. Green and brown px, interstitial hbl and plag. Locally pegmatic hbl and intrusive felsic veins.	x		
527502	63.15322	-41.47867	11MBK003	Vend Om Gabbro	Porphyritic leucocratic diorite cut by hbl veins. Could maybe be sidewall rock.	x		
527503	63.15322	-41.47867	11MBK003	Vend Om Gabbro	Porphyritic gabbro w/ 5 cm hbl phenocrysts in matrix of px+pl	x		
527504	63.15322	-41.47867	11MBK003	Vend Om Gabbro	Medium-coarse grained gabbro. Cross cuts porphyric mafic gabbro.	x		
527505	63.15322	-41.47867	11MBK003	Vend Om Gabbro	Leucocratic pegmatite cross cuts mafic gabbro	x		x
527506	63.15252	-41.47714	11MBK005	Vend Om Gabbro	Leucocratic pegmatite cross cuts mafic gabbro			x
527507	63.15206	-41.47326	11MBK007	Vend Om Gabbro	Intermediate meta-dyke	x		
527508	63.15268	-41.47110	11MBK011	Vend Om Gabbro	3x1m body of UM w/ more felsic veins. Intrudes into cpx-pl-hbl gabbro at eastern contact to basement	x		
527509	63.15253	-41.47102	11MBK012	Vend Om Gabbro	Gneiss migmatite	x		x
527510	63.15298	-41.47151	11MBK013	Vend Om Gabbro	Hybrid gneiss/gabbro rock, slightly foliated	x		
527511	63.15434	-41.47879	11MBK014	Vend Om Gabbro	Gabbro, dark, aphyric	x		
527512	63.15434	-41.47879	11MBK014	Vend Om Gabbro	Medium-coarse grained muttled gabbro, somewhat fractured /altered	x		
527513	63.15523	-41.47390	11MBK017	Vend Om Gabbro	Medium-coarse grained porphyric melanogabbro. Roof zone of intrusionweathered sample.	x		
527514	63.15472	-41.47537	11MBK018	Vend Om Gabbro	Medium grained leucogabbro (possible melt composition?)	x		
527515	63.15496	-41.47236		Vend Om Gabbro	Layered gabbro	x		
527516	63.15496	-41.47236		Vend Om Gabbro	Layered gabbro	x		
527517	63.15474	-41.47286		Vend Om Gabbro	Medium grained gabbro	x		
527518	63.15356	-41.47471	11MBK023	Vend Om Gabbro	Rusty Mt-rich layer w/ sulphide staining	x		
527519	63.15356	-41.47471	11MBK023	Vend Om Gabbro	Rusty Mt-rich layer w/ sulphide staining	x		
527520	63.15383	-41.47209	11MBK024	Vend Om Gabbro	Layered leucogabbro, equigranular. Mafic layers can be followed over 20-50 m. Layers are steeply dipping towards N.	x		
527521_B	63.15381	-41.47311		Vend Om Gabbro	Rusty Mt-rich layer c. 0.4m thick, base	x		
527521_C	63.15381	-41.47311		Vend Om Gabbro	Rusty Mt-rich layer c. 0.4m thick, center	x		
527521_T	63.15381	-41.47311		Vend Om Gabbro	Rusty Mt-rich layer c. 0.4m thick, top	x		
527522	63.15464	-41.47264		Vend Om Gabbro	Anorthosite as bands in gabbro	x	x	
527522_M	63.15464	-41.47264		Vend Om Gabbro	Gabbro associated w/ anorthosite	x		
527523	63.15427	-41.47392	11MBK025	Vend Om Gabbro	Medium grained layered gabbro	x	x	
527524	63.15392	-41.47483	11MBK026	Vend Om Gabbro	Melanocratic bands in layered gabbro		x	
527525	63.15359	-41.47519	11MBK027	Vend Om Gabbro	Layered gabbro w/ felsic layers. Sample taken 20m stratigraphically below 527424.	x	x	
527526	63.15364	-41.47550	11MBK028	Vend Om Gabbro	Very coarse grained gabbro common as xenolith throughout the layered gabbro sequence	x	x	
527527	63.15355	-41.47593	11MBK029	Vend Om Gabbro	Medium grained layered mela-gabbro w/ thin plag-rich bands	x	(x)	
527528	63.27619	-41.35051	11TFK005	Halvdans Fjord	Gneissose granite	x		x
527529	63.27668	-41.34955	11TFK006	Halvdans Fjord	Large amphibolite w/in migmatitic gneiss (irregularly foliated)	x		
527530	63.27681	-41.34679	11TFK009	Halvdans Fjord	Float sample of brecciated pyroxenite (spectacular)			
527531	63.26859	-41.36959	11TFK020	Halvdans Fjord	Diorite weak foliation (w/ zoned UM xenoliths)	x	x	
527532	63.25817	-41.36553	11TFK021	Halvdans Fjord	Medium - coarse grained, weakly foliated diorite at eastern margin, contact to migmatitic gneiss, cut by pegmatites and a few "metadykes"	x	x	
527533	63.27183	-41.37314		Halvdans Fjord	Diorite weakly foliated, w/ UM xenoliths	x		
527534	63.24486	-41.36483		Halvdans Fjord	Weakly foliated granite	x	x	x
527535	63.23820	-41.35960	11TFK028	Halvdans Fjord	Ca. 7.5 m thick metadyke in granite, w/ backveins from granite	x		
527536	63.22698	-41.32619	11TFK029	Halvdans Fjord	Tracking diorite-gneiss contact	x	x	
527537	63.22926	-41.32946	11TFK030	Halvdans Fjord	Tracking diorite(+UM xenoliths)-gneiss contact	x	x	
527538	63.23763	-41.33151	11TFK033	Halvdans Fjord	Spotted gabbro in contact w/ "granite"	x	x	
527539	63.23906	-41.33021		Halvdans Fjord	S-margin of cgr gabbro-melagabbro-gabbro band	x	x	
527540	63.23928	-41.33126		Halvdans Fjord	Aplitic part of pegmatite	x		x
527541	63.25392	-41.33610	11TFK034	Halvdans Fjord	Foliated hbl-poikilitic spotted gabbro (fine - medium grained gabbro w/ <2 x 6 cm hbl oikocrysts)	x	x	
527542	63.25392	-41.33610	11TFK034	Halvdans Fjord	Leucocratic pegmatite dyke			
527543	63.25240	-41.33683	11TFK035	Halvdans Fjord	Melagabbro w/ brown opx + green cpx + interstitial plg + poikilitic amphibole	x	x	
527544	63.25240	-41.33683	11TFK035	Halvdans Fjord	Medium grained diorite, distinctly foliated, in contact bw/ melagabbro and underlying layered gabbro. Contains gneissic xenoliths.	x	x	
527545	63.25198	-41.33645	11TFK036	Halvdans Fjord	Contact bw/ upper part of lower melagabbro and overlying schliered gabbro	x	x	

Sample§	Latitude (deg N)	Longitude (deg W)	Station ID	Place name	Description	Chem.	PTS	U-Pb
527546	63.25198	-41.33645	11TFK036	Halvdans Fjord	Hbl porphyric melagabbro		x	
527547	63.25929	-41.33795	11TFK002	Stærkodder Vig	Gneissose granite	x		x
527548	63.24316	-41.62475	11TFK039	Stærkodder Vig	Metadyke, <0.3m wide	x		
527549	63.24316	-41.62475	11TFK039	Stærkodder Vig	Gabbro, weakly foliated	x	x	
527550	63.24167	-41.61897	11TFK042	Stærkodder Vig	Very mafic amphibolite, w/ large hbl crystals	x		
527551	63.25398	-41.65996	11TFK052	Stærkodder Vig	Leucocratic pegmatite dyke			x
527552	63.25397	-41.66149	11TFK054	Stærkodder Vig	Pseudotachylite			
527553	63.25437	-41.66701	11TFK057	Stærkodder Vig	Hbl-porphyroblastic metagabbro	x	x	
527554	63.25437	-41.66701	11TFK057	Stærkodder Vig	Leucogabbro cut by spotted gabbro	x	x	
527555	63.25418	-41.66441	11TFK058	Stærkodder Vig	Diorite	x		
527556	63.25413	-41.66134	11TFK059	Stærkodder Vig	Diorite (hbl-spotted)	x		
527557	63.25413	-41.66134	11TFK059	Stærkodder Vig	Medium-coarse grained granodioritic gneiss near contact to diorite/gabbro	x		x
527558	63.25662	-41.67315	11TFK060	Stærkodder Vig	Foliated medium grained amphibolite	x		
527559	63.25567	-41.68811	11TFK061	Stærkodder Vig	Fine grained metadyke, <0.4m wide	x		
527560	63.25567	-41.68811	11TFK061	Stærkodder Vig	Granodioritic gneiss, oriented sample			x
527561_A	63.30040	-41.71559	11MBK034	Stærkodder Vig	Xenoliths of amphibolite and coarse grained UM in gneiss	x		
527561_B	63.30040	-41.71559	11MBK034	Stærkodder Vig	Fsp porphyric moderately foliated granodioritic gneiss w/ mafic and UM xenoliths	x		x
527562	63.30040	-41.71559	11MBK034	Stærkodder Vig	Contact between leucogabbro and host gneiss	x	x	
527563	63.30040	-41.71559	11MBK034	Stærkodder Vig	Contact between plg-bearing pyroxenite and leucogabbro	x	x, x	
527564	63.30040	-41.71559	11MBK034	Stærkodder Vig	Poikilitic cpx orthopyroxenite w/ interstitial plg-pods	x	x	
527565	63.30071	-41.71038	11MBK038	Stærkodder Vig	Mgr-cgr diorite w/ faint layering	x	x	
527566	63.30071	-41.71038	11MBK038	Balders Fjord	Leucocratic gabbro with mafic layers in 'colliflower' structure / dendrritic growth of cpx in plane 140/43 orthogonal to layers 265/60	x	x	
527569	63.53300	-41.75764	11TFK072	Ruinnæsset	Kfsp porphyric syenite with mineral filled miarolithic cavity			x
527570	63.53300	-41.75764	11TFK072	Ruinnæsset	Pyroxenite, hbl-porphyritic	x	x	
527571	63.53300	-41.75764	11TFK072	Ruinnæsset	Felsic vein	x	x	
527572	63.53300	-41.75764	11TFK072	Ruinnæsset	Very coarse grained hbl porphyric syenite			
527573	63.53300	-41.75764	11TFK072	Ruinnæsset	Coarse grained foliated syenite	x	x	
527574	63.53300	-41.75764	11TFK072	Ruinnæsset	Syenite, foliated	x	x	
527575	63.51931	-41.74862	11TFK075	Ruinnæsset	Purple pegmatite	x		
527576	63.50975	-41.77346	11TFK076	Ruinnæsset	Gneiss, foliated	x		
527577	63.50602	-41.63052		Ruinnæsset	Syenite, cgr, foliated	x	x	
527578	63.50540	-41.63868	11TFK081	Ruinnæsset	Pyroxenite, fgr	x	x	
527579	63.50483	-41.64093	11TFK082	Ruinnæsset	Pyroxenite, hbl-poikilitic (large angular xenolith)	x	x	
527580	63.50432	-41.64246	11TFK084	Ruinnæsset	Syenite, cgr	x	x	
527581	63.48918	-41.72146	11TFK086	Ruinnæsset	Syenite, cgr	x	x	
527582	63.48689	-41.71250	11TFK087	Ruinnæsset	Syenite, cgr, foliated	x	x	
527583	63.48689	-41.71250	11TFK087	Ruinnæsset	Metadyke, oldest	x	x	
527584	63.48689	-41.71250	11TFK087	Ruinnæsset	Purple pegmatite	x		
527585	63.48689	-41.71250	11TFK087	Ruinnæsset	Fine-grained syenitic sheet w/ well developed schistosity. Cross cuts purple pegmatite.			x
527586	63.48689	-41.71250	11TFK087	Ruinnæsset	Px-phyric (dolerite/meta?) dyke	x	x	
527587_L	63.48052	-41.68759	11TFK089	Ruinnæsset	Syenite, cgr, layered leucocratic part	x	x	
527587_M	63.48052	-41.68759	11TFK089	Ruinnæsset	Syenite, cgr, layered, mesocratic part	x	x	
527588	63.48052	-41.68759	11TFK089	Ruinnæsset	Mt-rich part of pronounced layer in qtz syenite			
527589	63.48052	-41.68759	11TFK089	Ruinnæsset	Felsic aplite-pegmatite sheet	x		
527590	63.48052	-41.68759	11TFK089	Ruinnæsset	Metadyke, fgr, aphyric(+px+plg?)	x		
527591	63.48267	-41.64318	11TFK091	Ruinnæsset	Sample of magmatic layered nordmarkite, oriented sample		x	
527592	63.48267	-41.64318	11TFK091	Ruinnæsset	Metadyke (very irregular aphyric dark)	x		
527593	63.48267	-41.64318	11TFK091	Ruinnæsset	Feldspar-glomerophyric dyke	x	x	
527594	63.48267	-41.64318	11TFK091	Ruinnæsset	Long-feldspar phyric dyke	x	x	
527595	63.48267	-41.64318	11TFK091	Ruinnæsset	Felsic aplite-pegmatite	x		
527596	63.48333	-41.64337	11TFK092	Ruinnæsset	Mt-rich layer	x	x	
527597	63.48333	-41.64337	11TFK092	Ruinnæsset	Mt-rich layer	x	x	
527598	63.48333	-41.64337	11TFK092	Ruinnæsset	Purple pegmatite (w/ miarolithic cavities)	x		x
527601	65.62351	-37.65675	11TFK014	Tasiilaq	20 cm thick melagabbroic and magnetic (mt-rich) dykelet in cgr Tasiilaq norite host	x	x	
527602	63.15089	-41.47096	11MBK030	Vend Om Gabbro	Large E-W trending dolerite dyke, SE margin sampled for geochemistry	x		
527603	63.15089	-41.47096	11MBK030	Vend Om Gabbro	Large E-W trending dolerite dyke, central part sampled for badd dating			x (bad)
527604	63.15089	-41.47096	11MBK030	Vend Om Gabbro	Large E-W trending dolerite dyke, central part sampled for geochemistry	x		
527605	63.15161	-41.47395	nm	Søndre Skjoldungen Sund	50-60m thick, E-W trending dolerite dyke (Paleoproterozoic?), small sample for geochron			x (bad)
527606	63.15161	-41.47395	nm	Søndre Skjoldungen Sund	50-60m thick, E-W trending dolerite dyke (Paleoproterozoic?), large sample for chemistry	x		

Sample§	Latitude (deg N)	Longitude (deg W)	Station ID	Place name	Description	Chem.	PTS	U-Pb
527607	63.27117	-41.34596	11TFK004	Halvdans Fjord	Dolerite dyke, 7m wide (Paleoproterozoic?), chilled contact sample	x		x (bad)
527608	63.27668	-41.34955	11TFK006	Halvdans Fjord	Meta-dyke	x		
527609	63.27644	-41.34316	11TFK008	Halvdans Fjord	Migmatised amphibolite	x		x
527610	63.27681	-41.34679	11TFK009	Halvdans Fjord	Meta-dyke	x		
527611	63.27681	-41.34679	11TFK009	Halvdans Fjord	Meta-dyke	x		
527612	63.27675	-41.34733	11TFK010	Halvdans Fjord	Meta-dyke	x	x	
527613	63.25718	-41.32083		Halvdans Fjord	Pyroxenite sheet	x	x	
527614	63.25727	-41.32061		Halvdans Fjord	Meta-dyke	x		
527615	63.25765	-41.32077		Halvdans Fjord	Meta-dyke	x	x	
527616	63.25784	-41.32058	11TFK025	Halvdans Fjord	Leucogabbro	x	x,x	
527617	63.25798	-41.32098	11TFK026	Halvdans Fjord	Leucocratic aplite sheet	x		
527618	63.25935	-41.32243	11TFK027	Halvdans Fjord	Dolerite dyke (Paleoproterozoic?)	x		x (bad)
527619	63.23034	-41.33026	11TFK031	Halvdans Fjord	Dolerite dyke, 7m wide (Paleoproterozoic?)	x		x (bad)
527620	63.37094	-41.44084	nm	Hermods Vig	Coarse grained gabbro (dolerite dyke)	x		
527621	63.39842	-41.48449	11TFK114	Ruinnæsset	Dolerite dyke (Paleoproterozoic?)	x		
527622	63.34960	-41.48615	11TFK121	Hermods Vig	Dolerite dyke, 10m wide (Paleoproterozoic?)	x		
527623	63.59285	-42.23498	11TFK137	Thrymheim	Dolerite dyke, 18m wide, plg phyric (Paleoproterozoic?)	x		
527624	63.66146	-42.17541	11TFK141	Thrymheim	2m wide dolerite dyke	x		
527625	63.44074	-41.79188	11TFK145	Sfinksen	8-10m wide dolerite dyke into nordmarkite	x		
527626	63.43314	-41.73435	11TFK146	Sfinksen	Dolerite dyke, ca. 50m wide	x		
527630	63.49879	-42.01066	11TFK093	Tværdalen drop-off	Hbl-poikilitic gabbro very coarse grained with bio	x	x	
527631	63.49879	-42.01066	11TFK093	Tværdalen drop-off	Coarse grained gabbro with pyroxenite vein/inclusion	x	x	
527632	63.49879	-42.01066	11TFK093	Tværdalen drop-off	Coarse grained melagabbro with biotite	x		
527633	63.36533	-41.43278	11TFK096	Hermods Vig	Mafic dyke	x		
527634	63.37203	-41.44192	11TFK099	Hermods Vig	Meta-gabbroic dyke	x	x	
527635	63.37082	-41.43724	11TFK101	Hermods Vig	Coarse grained gabbro (sparsely intruded by metadykes)	x	x	
527636	63.36840	-41.43521	11TFK102	Hermods Vig	Medium grained granitic dyke in coarse grained gabbro	x		
527637	63.35427	-41.44157	11TFK103	Hermods Vig	Coarse grained quartz syenite	x	x	x
527638	63.35487	-41.44081	11TFK104	Hermods Vig	Coarse grained gabbro (large dyke?)	x	x	
527639	63.35653	-41.43462	11TFK105	Hermods Vig	Coarse grained foliated and layered gabbro	x	x,x	
527640	63.35653	-41.43462	11TFK105	Hermods Vig	Fine graine pale grey sheet	x		
527641	63.35653	-41.43462	11TFK105	Hermods Vig	Medium grained syenite (irregular intrusion)	x	x,x	
527642	63.35653	-41.43288	11TFK106	Hermods Vig	Hbl-poikilitic gabbro	x	x	
527643	63.35861	-41.43257	11TFK107	Hermods Vig	Nearly ultramafic xenolith in syenite	x	x	
527644	63.41600	-41.42555	11TFK113	Langenæs	Hydrothermally altered rusty stained zone in gneiss basement	x		
527645	63.34960	-41.48615	11TFK121	Hermods Vig	8m wide fine grained meta-dolerite, cut by later dolerite dyke	x		
527646	63.35056	-41.48857	11TFK123	Hermods Vig	Irregular intermediate fsp-phyric metadyke	x		
527647	63.35210	-41.49145	11TFK124	Njords Gletcher	Phlog-rich ultramafic inclusion	x	x	
527648	63.34948	-41.50634	11TFK127	Njords Gletcher	Coarse grained gabbro	x	x	
527649_B	63.35031	-41.50817	11TFK128	Njords Gletcher	Very Mt-rich layer in gabbro	x		
527649_D	63.35031	-41.50817	11TFK128	Njords Gletcher	Less Mt-rich layer in gabbro	x	x	
527649_E	63.35031	-41.50817	11TFK128	Njords Gletcher	Coarse grained gabbro	x		
527650	63.35041	-41.50797	11TFK129	Njords Gletcher	Fine grained felsic (syenitic?) intrusion in coarse grained to pegmatitic heterogeneous gabbro	x		x
527651	63.35160	-41.50832	11TFK131	Njords Gletcher	Coarse grained gabbro w/ contact	x		x
527652	63.34873	-41.47022	11TFK135	Hermods Vig	Mafic (dioritic?) rock near Hermods Vig	x		
527653	63.35058	-41.91064	11TFK136	Balders Fjord, W	Qtz monzonite	x		
527654	63.59285	-42.23498	11TFK137	Thrymheim	Monzonite, cgr weakly fol	x		x
527655	63.59285	-42.23498	11TFK137	Thrymheim	Medium grained qtz syenite	x		
527656	63.59285	-42.23498	11TFK137	Thrymheim	Qtz syenite, mgr, red-colored	x		
527657	63.62265	-42.32901	11TFK138	Thrymheim	Hornfels, +sulphide min.	x		
527658	63.62265	-42.32901	11TFK138	Thrymheim	Leucocratic pegmatite dyke, red colored	x		
527659	63.66014	-42.27941	11TFK139	Thrymheim	Granite fgr, intrudes agmatitic gneiss	x		x
527660	63.66014	-42.27941	11TFK139	Thrymheim	Mafic enclave in qtz syenite (=ALB 536082)	x		
527661	63.67419	-42.29025	11TFK140	Thrymheim	Qtz syenite	x		
527662	63.67419	-42.29025	11TFK140	Thrymheim	Fine grained qtz syenite	x		
527663	63.67419	-42.29025	11TFK140	Thrymheim	Amphibolite, inclusion in agmatitic gneiss	x		
527664	63.67419	-42.29025	11TFK140	Thrymheim	Mafic enclave in qtz syenite	x		
527665	63.67419	-42.29025	11TFK140	Thrymheim	Qtz syenite	x		
527666	63.66146	-42.17541	11TFK141	Thrymheim	Pyroxenite, hbl-phlog	x		
527667	63.66146	-42.17541	11TFK141	Thrymheim	Qtz syenite	x		
527668	63.66146	-42.17541	11TFK141	Thrymheim	Medium grained qtz syenite intrudes gabbro	x		
527669	63.66146	-42.17541	11TFK141	Thrymheim	Monzonite	x		
527670	63.66146	-42.17541	11TFK141	Thrymheim	Melagabbro, phlog	x		
527671	63.66146	-42.17541	11TFK141	Thrymheim	Pyroxenite, hbl	x		
527672	63.66146	-42.17541	11TFK141	Thrymheim	Qtz syenite vein	x		
527673	63.66146	-42.17541	11TFK141	Thrymheim	Felsic pegmatite in gabbro (showing solid state deformation (for A. Berger)	x		
527674	63.57303	-42.04634	11TFK142	Thrymheim	Monzonite, cgr	x		
527675	63.57303	-42.04634	11TFK142	Thrymheim	Qtz syenite (intrudes 527674)	x		x

Sample§	Latitude (deg N)	Longitude (deg W)	Station ID	Place name	Description	Chem.	PTS	U-Pb
527676	63.40676	-41.70211	11TFK144	Sfinksen	Monzonite Fsp por	x		
527677	63.40676	-41.70211	11TFK144	Sfinksen	Monzonitic metadyke	x		
527678	63.40676	-41.70211	11TFK144	Sfinksen	Qtz syenite, cgr	x		x
527679	63.44074	-41.79188	11TFK145	Sfinksen	Qtz syenite	x		x
527680	63.44074	-41.79188	11TFK145	Sfinksen	Syenite, red colored	x		
527681	63.43314	-41.73435	11TFK146	Sfinksen	Monzonite	x		
527682	63.43314	-41.73435	11TFK146	Sfinksen	Gabbro dyke, cgr	x		
527683	63.43314	-41.73435	11TFK146	Sfinksen	Px-phyric dyke	x		
527684	63.43314	-41.73435	11TFK146	Sfinksen	Monzonite dyke, fsp porphyric	x		
527685	63.43314	-41.73435	11TFK146	Sfinksen	Qtz syenite, cgr	x		x

§ All sample numbers are GGU#. Sample numbers followed by a capital letter (subscript A, B, L, M, G) indicate that the sample was split into two or more fractions, i.e. a heterogeneous sample.

Table A2. List of structural measurements taken in the Skjoldungen area

gpsID	Latitude	Longitude	Altitude	Area	Structure	Thickness (m)	Strike (°RHR)	Dip (°)	DipDir (°)
w012	63.15254	-41.47719	-13	Vend Om Fjord	Felsic pegmatite	0.20	58	85	148
w013	63.15262	-41.47666	12	Vend Om Fjord	Felsic vein	0.05	229	84	319
w013	63.15262	-41.47666	12	Vend Om Fjord	Mafic dyke segment	0.02			
w014	63.15242	-41.47608	3	Vend Om Fjord	Dolerite dyke	1.50	54	90	144
w014	63.15242	-41.47608	3	Vend Om Fjord	Felsic pegmatite	0.15	12	80	102
w014	63.15242	-41.47608	3	Vend Om Fjord	Hornblende veins		275	55	5
w016	63.15220	-41.47295	16	Vend Om Fjord	Metadyke	1.00	155	90	65
w028	63.15254	-41.47069	115	Vend Om Fjord	Foliation (gneiss)		310	80	40
w039	63.15418	-41.47850	30	Vend Om Fjord	Dolerite dyke	2.00	67	80	157
w041	63.15417	-41.47810	34	Vend Om Fjord	Felsic vein		130	90	40
w044	63.15492	-41.47750	59	Vend Om Fjord	Foliation (gneiss)		327	64	57
w045	63.15466	-41.47739	81	Vend Om Fjord	Dolerite dyke	0.20	36	56	126
w061	63.15463	-41.47083	223	Vend Om Fjord	Intrusive contact		135	88	225
w063	63.15465	-41.47067	197	Vend Om Fjord	Magmatic layering		133	90	43
w073	63.15296	-41.47689	23	Vend Om Fjord	Metadyke	0.02	158	90	68
w074	63.15316	-41.47645	36	Vend Om Fjord	Fault		164	80	254
w077	63.15356	-41.47592	47	Vend Om Fjord	Foliation (gneiss)		275	40	5
w077	63.15356	-41.47592	47	Vend Om Fjord	Magmatic layering		222	16	312
w078	63.15363	-41.47573	50	Vend Om Fjord	Magmatic layering		199	28	289
w079	63.15362	-41.47569	67	Vend Om Fjord	Magmatic layering		254	43	344
w080	63.15359	-41.47587	71	Vend Om Fjord	Fault		190	80	280
w080	63.15359	-41.47587	71	Vend Om Fjord	Magmatic layering		130	24	220
w081	63.15362	-41.47530	69	Vend Om Fjord	Foliation (gabbro)		222	43	312
w082	63.15381	-41.47549	77	Vend Om Fjord	Fault		190	80	280
w082	63.15381	-41.47549	77	Vend Om Fjord	Fault +slickensides→24°N		184	76	274
w082	63.15381	-41.47549	77	Vend Om Fjord	Fault +slickensides→30°E		284	76	14
w083	63.15359	-41.47519	46	Vend Om Fjord	Felsic pegmatite	0.20	168	77	258
w084	63.15356	-41.47524	99	Vend Om Fjord	Fault (dextral)		266	48	356
w084	63.15356	-41.47524	99	Vend Om Fjord	Fault (dextral)		274	76	4
w084	63.15356	-41.47524	99	Vend Om Fjord	Fault +slickensides→10°W		117	75	207
w085	63.15374	-41.47486	63	Vend Om Fjord	Magmatic layering		250	37	340
w085	63.15374	-41.47486	63	Vend Om Fjord	Pseudotachylite	0.50			
w086	63.15368	-41.47480	74	Vend Om Fjord	Magmatic layering	1.00	226	33	316
w090	63.15363	-41.47439	87	Vend Om Fjord	Magmatic layering		225	48	315
w091	63.15359	-41.47438	101	Vend Om Fjord	Magmatic layering	0.60	222	54	312
w094	63.15381	-41.47311	109	Vend Om Fjord	Magmatic layering	0.40	252	62	342
w095	63.15377	-41.47290	143	Vend Om Fjord	Magmatic layering		241	53	331
w096	63.15383	-41.47238	134	Vend Om Fjord	Magmatic layering		253	42	343
w097	63.15382	-41.47220	143	Vend Om Fjord	Magmatic layering		194	66	284
w098	63.15387	-41.47190	156	Vend Om Fjord	Magmatic layering		204	78	294
w101	63.15386	-41.47211	162	Vend Om Fjord	Magmatic layering		203	54	293
w103	63.15405	-41.47198	182	Vend Om Fjord	Magmatic layering		179	58	269
w104	63.15430	-41.47197	181	Vend Om Fjord	Magmatic layering		164	47	254
w105	63.15433	-41.47196	178	Vend Om Fjord	Magmatic layering		135	60	225
w107	63.15464	-41.47264	218	Vend Om Fjord	Fault (dextral)		116	90	26
w107	63.15464	-41.47264	218	Vend Om Fjord	Magmatic layering		127	88	217
w110	63.15416	-41.47413	127	Vend Om Fjord	Magmatic layering		146	54	236
w112	63.15429	-41.47420	145	Vend Om Fjord	Magmatic layering		147	66	237
w113	63.15413	-41.47424	113	Vend Om Fjord	Magmatic layering		313	20	43
w114	63.15416	-41.47472	116	Vend Om Fjord	Fault (sinistral)		208	35	298
w115	63.15383	-41.47481	114	Vend Om Fjord	Magmatic layering		267	40	357
w116	63.15380	-41.47503	139	Vend Om Fjord	Fault		180	90	90
w116	63.15380	-41.47503	139	Vend Om Fjord	Magmatic layering		235	28	325
w117	63.15367	-41.47511	77	Vend Om Fjord	Magmatic layering		250	20	340
w125	63.15161	-41.47395	9	Vend Om Fjord	Dolerite dyke	55.00	90	90	0
w127	63.27066	-41.34474	16	Halvdans Fjord	Foliation (gneiss)		341	72	71
w128	63.27112	-41.34590	16	Halvdans Fjord	Dolerite dyke	7.00	236	64	326
w129	63.27119	-41.34627	16	Halvdans Fjord	Foliation (gneiss)		136	83	226
w131	63.27616	-41.35046	12	Halvdans Fjord	Fault (epidote)		233	80	323
w131	63.27616	-41.35046	12	Halvdans Fjord	Foliation (gneiss)		98	86	188
w131	63.27616	-41.35046	12	Halvdans Fjord	Foliation (gneiss)		113	84	203
w131	63.27616	-41.35046	12	Halvdans Fjord	Metadyke		13	62	103
w131	63.27616	-41.35046	12	Halvdans Fjord	Metadyke		20	71	110
w132	63.27674	-41.34955	20	Halvdans Fjord	Felsic pegmatite	0.10	42	63	132
w132	63.27674	-41.34955	20	Halvdans Fjord	Foliation (gneiss)		132	80	222
w132	63.27674	-41.34955	20	Halvdans Fjord	Metadyke	0.25	159	90	69
w133	63.27692	-41.34806	65	Halvdans Fjord	Fault (dextral)		30	90	120
w133	63.27692	-41.34806	65	Halvdans Fjord	Foliation (gneiss)		121	70	211
w134	63.27648	-41.34320	162	Halvdans Fjord	Dolerite dyke		59	65	149
w134	63.27648	-41.34320	162	Halvdans Fjord	Felsic pegmatite		85	60	175
w134	63.27648	-41.34320	162	Halvdans Fjord	Foliation (gneiss)		37	72	127
w134	63.27648	-41.34320	162	Halvdans Fjord	Metadyke	0.15	11	90	101
w135	63.27692	-41.34667	92	Halvdans Fjord	Metadyke	1.00	178	80	268
w135	63.27692	-41.34667	92	Halvdans Fjord	Metadyke	1.30	344	72	74

gpsID	Latitude	Longitude	Altitude	Area	Structure	Thickness (m)	Strike (°RHR)	Dip (°)	DipDir (°)
w136	63.27687	-41.34715	88	Halvdans Fjord	Fault (epidote)		225	80	315
w137	63.27676	-41.34736	85	Halvdans Fjord	Fault (sinistral, epidote)		187	85	277
w137	63.27676	-41.34736	85	Halvdans Fjord	Metadyke	0.35	28	75	118
w138	63.28279	-41.36631	3	Halvdans Fjord	Foliation (gneiss S2)		185	90?	95
w138	63.28279	-41.36631	3	Halvdans Fjord	Foliation (gneiss)		65		155
w138	63.28279	-41.36631	3	Halvdans Fjord	Foliation (gneiss)		122	66	212
w138	63.28279	-41.36631	3	Halvdans Fjord	Fracture		35	78	125
w139	63.28418	-41.37439	-2	Halvdans Fjord	Fault (sinistral)	0.02	60	90?	150
w139	63.28418	-41.37439	-2	Halvdans Fjord	Fault (sinistral)		226	70	316
w139	63.28418	-41.37439	-2	Halvdans Fjord	Fault slickenside DDD		110	30?	200
w139	63.28418	-41.37439	-2	Halvdans Fjord	Foliation (gneiss)		107	85	197
w139	63.28418	-41.37439	-2	Halvdans Fjord	Metadyke	0.04	317	78	47
w140	63.28373	-41.38043	18	Halvdans Fjord	Foliation (gneiss)		93	76	183
w141	63.28055	-41.38610	2	Halvdans Fjord	Dolerite dyke		222	72	312
w141	63.28055	-41.38610	2	Halvdans Fjord	Foliation (gneiss)		132	80	222
w142	63.28050	-41.38884	6	Halvdans Fjord	Fault (sinistral)	0.05	165	90?	75
w142	63.28050	-41.38884	6	Halvdans Fjord	Foliation (gneiss S2)		184	90?	94
w142	63.28050	-41.38884	6	Halvdans Fjord	Foliation (gneiss)		110	80	200
w142	63.28050	-41.38884	6	Halvdans Fjord	Metadyke	0.20	83	70	173
w143	63.28130	-41.39125	-14	Halvdans Fjord	Dolerite dyke	0.60	59	51	149
w146	63.27410	-41.38818	4	Halvdans Fjord	Foliation (gneiss)		102	60	192
w148	63.27183	-41.37314	1	Halvdans Fjord	Foliation (diorite)		83	72	173
w148	63.27183	-41.37314	1	Halvdans Fjord	Metadyke	0.20			
w149	63.26849	-41.36961	0	Halvdans Fjord	Foliation (diorite)		102	72	192
w150	63.25820	-41.36573	5	Halvdans Fjord	Foliation (diorite)		200	70	290
w151	63.25989	-41.33459	27	Halvdans Fjord	Felsic pegmatite		310	40	40
w151	63.25989	-41.33459	27	Halvdans Fjord	Foliation (gabbro)		338	70	68
w154	63.26000	-41.33327	51	Halvdans Fjord	Metadyke		130	90?	40
w155	63.26014	-41.33303	54	Halvdans Fjord	Metadyke	0.90	147	90	57
w156	63.26014	-41.33261	54	Halvdans Fjord	Felsic pegmatite	0.10			
w156	63.26014	-41.33261	54	Halvdans Fjord	Felsic pegmatite	0.40	200	70	290
w156	63.26014	-41.33261	54	Halvdans Fjord	Metadyke	0.15			
w157	63.25980	-41.33198	56	Halvdans Fjord	Metadyke	0.77	167	75	257
w159	63.25718	-41.32083	149	Halvdans Fjord	Metadyke	0.10	113	90	23
w159	63.25718	-41.32083	149	Halvdans Fjord	Metadyke	1.20	3	80	93
w160	63.25713	-41.32069	145	Halvdans Fjord	Metadyke	0.50	235	76	325
w161	63.25727	-41.32061	149	Halvdans Fjord	Metadyke	0.50	150	84	240
w163	63.25765	-41.32077	162	Halvdans Fjord	Metadyke	7.00			
w164	63.25765	-41.32071	160	Halvdans Fjord	Foliation (gabbro)		325	70	55
w165	63.25781	-41.32058	180	Halvdans Fjord	Foliation (gabbro)		311	65	41
w166	63.25792	-41.32115	185	Halvdans Fjord	Metadyke	0.30	312	75	42
w167	63.25935	-41.32225	219	Halvdans Fjord	Fault (slickensides)		132	90	42
w168	63.25924	-41.32244	218	Halvdans Fjord	Dolerite dyke	17.50	167	74	257
w169	63.25931	-41.32290	214	Halvdans Fjord	Foliation (gabbro)		318	64	48
w170	63.25917	-41.32354	201	Halvdans Fjord	Foliation (gabbro)		307	67	37
w171	63.25652	-41.36545	6	Halvdans Fjord	Foliation (gneiss)		210	83	300
w173	63.25021	-41.36624	3	Halvdans Fjord	Foliation (gneiss)		243	70	333
w178	63.23816	-41.35940	0	Halvdans Fjord	Metadyke	7.50	137	80	227
w179	63.23843	-41.36004	4	Halvdans Fjord	Metadyke	7.50	137	80	227
w180	63.23868	-41.36044	11	Halvdans Fjord	Metadyke	0.10	335	80	65
w180	63.23868	-41.36044	11	Halvdans Fjord	Metadyke	7.50	137	80	227
w181	63.23595	-41.34406	-4	Halvdans Fjord	Foliation (gneiss)		305	80	35
w182	63.22684	-41.32618	-1	Halvdans Fjord	Foliation (gneiss)		110	60	200
w197	63.23035	-41.33020	3	Halvdans Fjord	Dolerite dyke	7.00	247	85	337
w198	63.23185	-41.33213	7	Halvdans Fjord	Foliation (granite)		35	50	125
w198	63.23185	-41.33213	7	Halvdans Fjord	Foliation (metadyke)		178	90?	88
w198	63.23185	-41.33213	7	Halvdans Fjord	Metadyke		139	84	229
w199	63.23764	-41.33151	4	Halvdans Fjord	Intrusive contact		138	37	228
w203	63.24910	-41.33460	0	Halvdans Fjord	Magmatic layering		285	55	15
w204	63.25380	-41.33609	22	Halvdans Fjord	Felsic pegmatite	0.70	132	49	222
w204	63.25380	-41.33609	22	Halvdans Fjord	Foliation (gabbro)		354	74	84
w205	63.25393	-41.33574	-2	Halvdans Fjord	Dolerite dyke	0.07	210	76	300
w206	63.25243	-41.33699	24	Halvdans Fjord	Magmatic layering		344	72	74
w207	63.25164	-41.33717	6	Halvdans Fjord	Magmatic layering		330	63	60
w208	63.25203	-41.33681	9	Halvdans Fjord	Magmatic layering		1	78	91
w209	63.25935	-41.33868	1	Halvdans Fjord	Felsic pegmatite		97	90	187
w209	63.25935	-41.33868	1	Halvdans Fjord	Foliation (gneiss)		337	84	67
w209	63.25935	-41.33868	1	Halvdans Fjord	Metadyke	0.05	352	80	82
w211	63.24421	-41.61491	93	Stærkodder Fjord	Foliation (gneiss)		5	88	95
w214	63.24411	-41.61992	155	Stærkodder Fjord	Foliation (amphibolite gneiss)		355	82	85
w215	63.24310	-41.62480	203	Stærkodder Fjord	Foliation (v weak)		285	65	15
w215	63.24310	-41.62480	203	Stærkodder Fjord	Metadyke	0.10	304	80	34
w215	63.24310	-41.62480	203	Stærkodder Fjord	Metadyke	0.10	315	65	45

gpsID	Latitude	Longitude	Altitude	Area	Structure	Thickness (m)	Strike (°RHR)	Dip (°)	DipDir (°)
w215	63.24310	-41.62480	203	Stærkodder Fjord	Metadyke	0.30	287	85	17
w216	63.24322	-41.62384	191	Stærkodder Fjord	Foliation (v heterogenous, gneiss)		295	78	25
w218	63.24094	-41.62624	153	Stærkodder Fjord	Foliation (v heterogenous, amphibolite gneiss)		290	72	20
w218	63.24094	-41.62624	153	Stærkodder Fjord	V heterogenous foliation		326	76	56
w219	63.24187	-41.61907	164	Stærkodder Fjord	Foliation		333	84	63
w220	63.24267	-41.61554	145	Stærkodder Fjord	Foliation		324	85	54
w221	63.24827	-41.63905	29	Stærkodder Fjord	Fault (brittle)		301	80	31
w221	63.24827	-41.63905	29	Stærkodder Fjord	Foliation		319	80	49
w221	63.24827	-41.63905	29	Stærkodder Fjord	Metadyke	3.00			
w222	63.24814	-41.64220	33	Stærkodder Fjord	Fault (cataclast, dextral, R2?)	1.00	167	90	77
w222	63.24814	-41.64220	33	Stærkodder Fjord	Foliation		295	52	25
w223	63.24796	-41.64378	20	Stærkodder Fjord	Foliation		282	47	12
w223	63.24796	-41.64378	20	Stærkodder Fjord	Thrust (top-to-SSE, dragfolds?)		250	20	340
w224	63.24810	-41.64460	112	Stærkodder Fjord	Foliation		272	85	2
w224	63.24810	-41.64460	112	Stærkodder Fjord	Fault dextral, R2? pseudotachylite)		153	56	243
w224	63.24810	-41.64460	112	Stærkodder Fjord	Thrust (top-to-SSE, pseudotachylite)		237	42	327
w224	63.24810	-41.64460	112	Stærkodder Fjord	Thrust (top-to-SSE, pseudotachylite)		240	23	330
w225	63.24745	-41.64476	138	Stærkodder Fjord	Foliation		297	85	27
w225	63.24745	-41.64476	138	Stærkodder Fjord	Semi-ductile top-to-S thrust with drag folded foliation		275	9	5
w226	63.24779	-41.64651	96	Stærkodder Fjord	Thrust (cataclastic)	2.50	258	80	348
w226	63.24779	-41.64651	96	Stærkodder Fjord	Foliation		308	76	38
w227	63.24831	-41.64480	92	Stærkodder Fjord	Foliation		307	74	37
w228	63.24985	-41.64643	111	Stærkodder Fjord	Foliation		299	78	29
w229	63.25055	-41.64621	62	Stærkodder Fjord	Thrust (top-to-SSE, pseudotachylite)		273	37	3
w230	63.25092	-41.64597	62	Stærkodder Fjord	Foliation		278	78	8
w231	63.25149	-41.64693	16	Stærkodder Fjord	Foiation-parallel		290	56	20
w231	63.25149	-41.64693	16	Stærkodder Fjord	Foliation		290	56	20
w232	63.25196	-41.64711	38	Stærkodder Fjord	Thrust (top-to-SSE, pseudotachylite)	0.20	185	35	275
w233	63.25298	-41.65197	46	Stærkodder Fjord	Foliation		293	74	23
w234	63.25283	-41.65222	14	Stærkodder Fjord	Fault zone	1.50	0	76	90
w234	63.25283	-41.65222	14	Stærkodder Fjord	Foliation		298	73	28
w235	63.25302	-41.65333	9	Stærkodder Fjord	Brittle geometry	0.05	307	70	37
w235	63.25302	-41.65333	9	Stærkodder Fjord	Metadyke (brittle geometry)	0.30	9	82	99
w235	63.25302	-41.65333	9	Stærkodder Fjord	Foliation		300	80	30
w236	63.25316	-41.65419	33	Stærkodder Fjord	Gneiss?		297		27
w236	63.25316	-41.65419	33	Stærkodder Fjord	Shear zone (sinistral)		263		353
w236	63.25316	-41.65419	33	Stærkodder Fjord	Sinistrally displaced metadykes		224		314
w237	63.25321	-41.65417	26	Stærkodder Fjord	Foliation		330	70	60
w238	63.25346	-41.65614	30	Stærkodder Fjord	Foliation		323	81	53
w240	63.25389	-41.65988	53	Stærkodder Fjord	Fault A (dextral, displaced veins)		188	84	278
w240	63.25389	-41.65988	53	Stærkodder Fjord	Fault B (sinistral, displaced veins)		80		170
w240	63.25389	-41.65988	53	Stærkodder Fjord	Fault C (dextral, displaced veins)		115		205
w240	63.25389	-41.65988	53	Stærkodder Fjord	Fault D (dextral, displaced veins)		140		230
w240	63.25389	-41.65988	53	Stærkodder Fjord	Foliation E		300	75	30
w242	63.25403	-41.66061	28	Stærkodder Fjord	Foliation		313	68	43
w242	63.25403	-41.66061	28	Stærkodder Fjord	Foliation		323	74	53
w242	63.25403	-41.66061	28	Stærkodder Fjord	Lineation on above foliation plane		17	64	107
w243	63.25417	-41.66135	33	Stærkodder Fjord	Foliation (diorite><granodiorite)		334	78	64
w244	63.25397	-41.66161	58	Stærkodder Fjord	Fault (pseudotachylite)	0.10	313	77	43
w245	63.25402	-41.66452	68	Stærkodder Fjord	Foliation (local)		327	82	57
w246	63.25396	-41.66471	61	Stærkodder Fjord	Contact (leuco-diorite><metagabbro)		143		233
w248	63.25406	-41.66509	64	Stærkodder Fjord	Irregular/schliered cm-wide dark bands		313	72	43
w249	63.25396	-41.66511	65	Stærkodder Fjord	Magmatic layering (dark band)	3.00			
w250	63.25410	-41.66552	73	Stærkodder Fjord	Magmatic layering (diorite)		312	67	42
w252	63.25403	-41.66564	64	Stærkodder Fjord	Fault (sinistral, reidel, drag folds)		56	90	146
w253	63.25406	-41.66606	93	Stærkodder Fjord	Foliation (gneiss)		307	78	37
w253	63.25406	-41.66606	93	Stærkodder Fjord	Shears (sinistral, 0.4 m displacement)		82	47	172
w255	63.25410	-41.66629	73	Stærkodder Fjord	Lineation (on above foliation plane = 26→60°)				
w255	63.25410	-41.66629	73	Stærkodder Fjord	Foliation (weak)		301	64	31
w256	63.25389	-41.66677	94	Stærkodder Fjord	Foliation (poss rotated)		286	70	16
w256	63.25389	-41.66677	94	Stærkodder Fjord	Pseudotachylite fault	0.10	308	82	38
w258	63.25446	-41.66712	114	Stærkodder Fjord	Thrust (extensive?)		257	35	347
w258	63.25446	-41.66712	114	Stærkodder Fjord	Protomylonite (finely foliated)		307	74	37
w259	63.25483	-41.66789	112	Stærkodder Fjord	Epidote vein/fault (with weird clasts)	0.05	69	70	159
w262	63.24853	-41.63885	4	Stærkodder Fjord	Foliation/layering (weak)		313	70	43
w265	63.25571	-41.68801	306	Stærkodder Fjord	Foliation		283	70	13
w265	63.25571	-41.68801	306	Stærkodder Fjord	Foliation		292	66	22
w266	63.25529	-41.68816	292	Stærkodder Fjord	Pseudotachylite	0.10	315	66	45
w266	63.25529	-41.68816	292	Stærkodder Fjord	Metadyke (fgr)	0.37	317	62	47
w267	63.25198	-41.68345	314	Stærkodder Fjord	Pseudotachylite (zone of at least 3 bands/veins)	1.00	140	90	230

gpsID	Latitude	Longitude	Altitude	Area	Structure	Thickness (m)	Strike (°RHR)	Dip (°)	DipDir (°)
w268	63.25177	-41.68335	313	Stærkodder Fjord	Pseudotachylite				
w269	63.25193	-41.68344	317	Stærkodder Fjord	Pseudotachylite (correlates with w267?)		320	80	50
w270	63.25182	-41.68315	320	Stærkodder Fjord	Pseudotachylite (correlates with w267?)				
w271	63.25188	-41.68324	319	Stærkodder Fjord	Pseudotachylite (irregular)		126	90	36
w274	63.25196	-41.68288	313	Stærkodder Fjord	Pseudotachylite		303	72	33
w275	63.25205	-41.68247	316	Stærkodder Fjord	Pseudotachylite vein		127	70	217
w276	63.25209	-41.68260	314	Stærkodder Fjord	Pseudotachylite				
w277	63.25166	-41.68269	327	Stærkodder Fjord	Pseudotachylite				
w278	63.25160	-41.68200	335	Stærkodder Fjord	Pseudotachylite				
w279	63.25153	-41.68180	345	Stærkodder Fjord	Pseudotachylite		301	78	31
w280	63.25168	-41.68202	252	Stærkodder Fjord	Fault (transverse? sinistral 3-4 mdisplacement?)		239	70	329
w281	63.25241	-41.68116	269	Stærkodder Fjord	Fault zone (orange weathered)		303	76	33
w282	63.25255	-41.68091	248	Stærkodder Fjord	Fault zone (orange weathered)		308	84	38
w282	63.25255	-41.68091	248	Stærkodder Fjord	Fault zone (orange weathered)		330	63	60
w283	63.25361	-41.67636	190	Stærkodder Fjord	Felsic pegmatite veins (±metagabbro xenoliths ±metadykes)				
w285	63.25395	-41.67386	170	Stærkodder Fjord	Foliation		323	85	53
w285	63.25395	-41.67386	170	Stærkodder Fjord	Fault zone (irregular, orange weathered)		330	45	60
w286	63.30030	-41.71542	21	Balders Fjord	Metadyke		2	73	92
w287	63.30024	-41.71556	5	Balders Fjord	Foliation (gneiss)		132	75	222
w288	63.30015	-41.71577	7	Balders Fjord	Fault (sinistral)		1	90	91
w288	63.30015	-41.71577	7	Balders Fjord	Fault		248	83	338
w288	63.30015	-41.71577	7	Balders Fjord	Fault (sinistral)		334	86	64
w291	63.30050	-41.71419	4	Balders Fjord	Foliation (weak)		332	53	62
w295	63.30003	-41.71380	16	Balders Fjord	Contact (UM dyke><gneiss)		307	66	37
w297	63.29893	-41.71187	68	Balders Fjord	Contact (UM dyke><gneiss)		321	71	51
w298	63.29874	-41.71153	69	Balders Fjord	Felsic vein	0.30	339	79	69
w299	63.29876	-41.71200	67	Balders Fjord	Felsic pegmatite vein/FZ?		36	85	126
w300	63.29853	-41.71234	77	Balders Fjord	Dyke view		172	74	262
w302	63.30094	-41.71108	3	Balders Fjord	Contact (complex, melagabbro><leucogabbro)	35.00			
w304	63.30065	-41.71056	-2	Balders Fjord	Layering (faint)		265	60	355
w306	63.30075	-41.71094	3	Balders Fjord	Lineation (dendrites)		217	40	307
w306	63.30075	-41.71094	3	Balders Fjord	Plane (dendrites)		140	43	230
w306	63.30075	-41.71094	3	Balders Fjord	Felsic pegmatite vein		13	86	103
w306	63.30075	-41.71094	3	Balders Fjord	Metadyke		290	75	20
w316	63.45922	-41.65723	9	Ruinnæsset	Foliation (gneiss)		259	80	349
w316	63.45922	-41.65723	9	Ruinnæsset	Contact (Ruinnæsset><gneiss)		162	85	252
w317	63.52580	-41.68878	1	Ruinnæsset	Foliation (gneiss)		137	60	227
w317	63.52580	-41.68878	1	Ruinnæsset	Contact (Ruinnæsset><gneiss)		110	65	200
w317	63.52580	-41.68878	1	Ruinnæsset	Fracture/fault (redish)		324	30	54
w320	63.53784	-41.75823	3	Ruinnæsset	Foliation (gneiss)		100	60	190
w321	63.53689	-41.76268	3	Ruinnæsset	Foliation (gneiss)		73	37	163
w321	63.53689	-41.76268	3	Ruinnæsset	Foliation (gneiss)		75	53	165
w322	63.53606	-41.76290	-52	Ruinnæsset	Fault zone (dextral, top to N?)		116	76	206
w322	63.53606	-41.76290	-52	Ruinnæsset	Foliation (gneiss)		81	59	171
w323	63.53299	-41.75784	-3	Ruinnæsset	Foliation (syenite)	1.50	91	57	181
w326	63.53316	-41.75862	25	Ruinnæsset	Band (foliation-parallel)		129	52	219
w326	63.53316	-41.75862	25	Ruinnæsset	Fault (sinistral)		248	57	338
w327	63.53316	-41.75887	31	Ruinnæsset	Foliation (in syenite?)		61	65	151
w327	63.53316	-41.75887	31	Ruinnæsset	Myarolithic cavities				
w327	63.53316	-41.75887	31	Ruinnæsset	Contact (sheared)		67	66	157
w328	63.53217	-41.75638	0	Ruinnæsset	Layering? (syenite)		65	61	155
w329	63.53190	-41.75578	1	Ruinnæsset	Layering? (syenite)		105	65	195
w330	63.52800	-41.75324	2	Ruinnæsset	Foliation/layering (syenite)		85	70	175
w331	63.52377	-41.75016	1	Ruinnæsset	Fault Zone				
w332	63.52034	-41.74731	1	Ruinnæsset	Foliation/layering (syenite)		99	58	189
w332	63.52034	-41.74731	1	Ruinnæsset	Pegmatite (purple)	0.30	220	30	310
w333	63.51054	-41.76982	0	Ruinnæsset	Fault zone (if reidel then sinistral)		140	90	230
w333	63.51054	-41.76982	0	Ruinnæsset	Foliation		4	67	94
w333	63.51054	-41.76982	0	Ruinnæsset	Reidel shears (if so then sinistral)		35	58	125
w336	63.50218	-41.66583	26	Ruinnæsset	Fault zone		295	82	25
w338	63.50371	-41.65805	120	Ruinnæsset	Xenoliths (syenite)				
w339	63.50422	-41.65767	126	Ruinnæsset	Veins (aphyric, irregular)				
w339	63.50422	-41.65767	126	Ruinnæsset	Contact (northern Ruinnæsset, irregular)		120		210
w340	63.50430	-41.65715	127	Ruinnæsset	Fault?		173	90	83
w341	63.50420	-41.65728	133	Ruinnæsset	Fault?		65	80	155
w343	63.50497	-41.65061	200	Ruinnæsset	Faults (many, dextral)		337	80	67
w344	63.50499	-41.64979	211	Ruinnæsset	Felsic pegmatite (little quartz)	0.30	265	12	355
w344	63.50499	-41.64979	211	Ruinnæsset	Fault (N-block-down)		48	40	138

gpsID	Latitude	Longitude	Altitude	Area	Structure	Thickness (m)	Strike (°RHR)	Dip (°)	DipDir (°)
w344	63.50499	-41.64979	211	Ruinnæsset	Fault (N-block-down, 0.3 m displacement)		73	43	163
w345	63.50512	-41.65038	205	Ruinnæsset	Faults (many, dextral)		100	85	190
w347	63.50469	-41.64971	202	Ruinnæsset	Faults (both N- & S-block down displacement)		135	90	225
w347	63.50469	-41.64971	202	Ruinnæsset	Larger fault (sinistral, classical reidels)		167	84	257
w347	63.50469	-41.64971	202	Ruinnæsset	Felsic pegmatite (shallow inclined)				
w349	63.50541	-41.64789	242	Ruinnæsset	Faults				
w350	63.50597	-41.64591	264	Ruinnæsset	Tension gashes (carbonaceous)		42	90	132
w350	63.50597	-41.64591	264	Ruinnæsset	Pull-apart along quartz vein (dilation # to this = 90/90)		0	90	90
w350	63.50597	-41.64591	264	Ruinnæsset	Quartz vein (cuts tension gashes)	0.02	120	90	30
w351	63.50583	-41.64586	264	Ruinnæsset	Veins (segregated Mt?)	0.02	118	90	28
w353	63.50617	-41.63224	418	Ruinnæsset	Foliation/layering		153	64	243
w355	63.50620	-41.62797	476	Ruinnæsset	Foliation/layering		138	85	228
w355	63.50620	-41.62797	476	Ruinnæsset	Sheet (fsp-phyric)	0.50	57	75	147
w355	63.50620	-41.62797	476	Ruinnæsset	Sheet (medium grained)				
w357	63.50497	-41.63986	333	Ruinnæsset	Foliation within UM-xenolith		132	84	222
w358	63.50473	-41.64190	294	Ruinnæsset	Foliation within UM-xenolith		134	63	224
w360	63.50444	-41.64239	289	Ruinnæsset	Shear zone?		97	55	187
w361	63.50414	-41.64413	273	Ruinnæsset	Sheet (older)	0.30	59	90	149
w361	63.50414	-41.64413	273	Ruinnæsset	Faults (two parallel, sinistral)		114	80	204
w361	63.50414	-41.64413	273	Ruinnæsset	Sheets (younger, cross cutting)	0.10	70	90	160
w362	63.50416	-41.64488	259	Ruinnæsset	Sheets (irregular)				
w364	63.50382	-41.64667	232	Ruinnæsset	Dyke (irregular, sheared, fsp-agglomophyric)				
w365	63.50372	-41.64805	222	Ruinnæsset	Dolerite dyke (apophyse cuts sheets)	13.00	75	73	165
w365	63.50372	-41.64805	222	Ruinnæsset	Sheet (older, fsp-phyric)				
w365	63.50372	-41.64805	222	Ruinnæsset	Sheet (younger, aphyric, medium grained)				
w366	63.50358	-41.64838	217	Ruinnæsset	Layering (syenite)		155	60	245
w366	63.50358	-41.64838	217	Ruinnæsset	Purple pegmatite	0.02	12	55	102
w367	63.50392	-41.65109	180	Ruinnæsset	Dolerite dyke				
w368	63.50292	-41.65405	146	Ruinnæsset	Dolerite dyke				
w369	63.50210	-41.65704	74	Ruinnæsset	Dolerite dyke				
6780	63.48949	-41.72500	2	Ruinnæsset	Foliation/layering (3-4 thin Mt-bands)		195	85	285
6780	63.48949	-41.72500	2	Ruinnæsset	Mafic sheet (porphyritic)	0.10	111	76	201
w371	63.48956	-41.72494	1	Ruinnæsset	Layering (syenite)		39	73	129
w371	63.48956	-41.72494	1	Ruinnæsset	Felsic pegmatites (many)		45	8	135
w372	63.48916	-41.72129	-1	Ruinnæsset	Foliation (syenite)		15	60	105
w372	63.48916	-41.72129	-1	Ruinnæsset	Reidel fractures		59	90	149
w372	63.48916	-41.72129	-1	Ruinnæsset	Fault (reidels=sinistral)		107	90	17
w373	63.48946	-41.72140	-8	Ruinnæsset	Layering (syenite)		22	83	112
w374	63.48721	-41.71254	-9	Ruinnæsset	Foliation (syenite)		345	74	75
w374	63.48721	-41.71254	-9	Ruinnæsset	Metadyke (oldest)	0.65	110	60	200
w374	63.48721	-41.71254	-9	Ruinnæsset	Metadyke (px-phyric)	1.20	98	78	188
w374	63.48721	-41.71254	-9	Ruinnæsset	Metadyke (px-phyric)	1.20	114	79	204
w374	63.48721	-41.71254	-9	Ruinnæsset	Metadyke (oldest)	2.00	112	68	202
w374	63.48721	-41.71254	-9	Ruinnæsset	Metasheet (fgr)		348	30	78
w375	63.48607	-41.70838	-3	Ruinnæsset	Layering (syenite)		17	75	107
w376	63.48038	-41.68765	-2	Ruinnæsset	Layering (syenite, curved)		160	90	70
w376	63.48038	-41.68765	-2	Ruinnæsset	Dyke (cuts 231/80-metadyke)		55	75	145
w376	63.48038	-41.68765	-2	Ruinnæsset	Felsic aplite-pegmatite		330	27	60
w376	63.48038	-41.68765	-2	Ruinnæsset	Metadyke (fine grained, aphyric)		231	80	321
w376	63.48038	-41.68765	-2	Ruinnæsset	Dyke (pyroxenitic)		180	90	90
w377	63.48039	-41.68781	-1	Ruinnæsset	Layering (syenite, curved)		179	90	89
w378	63.48031	-41.64157	-1	Ruinnæsset	Contact/shear?		340	60	70
w378	63.48031	-41.64157	-1	Ruinnæsset	Foliation (less sheared syenite)		140	78	230
w379	63.48270	-41.64314	9	Ruinnæsset	Layering (syenite, curved)		64	59	154
w379	63.48270	-41.64314	9	Ruinnæsset	Layering (syenite, curved)		95	68	185
w379	63.48270	-41.64314	9	Ruinnæsset	Layering (syenite)		31	78	121
w379	63.48270	-41.64314	9	Ruinnæsset	Layering (syenite)		76	74	166
w379	63.48270	-41.64314	9	Ruinnæsset	Metadyke (mafic)	0.40	76	80	166
w381	63.48270	-41.64296	14	Ruinnæsset	Dyke (fsp-glomerophyric)		139	90	49
w383	63.48283	-41.64392	3	Ruinnæsset	Magmatic layering (Mt-rich)		66	72	156
w383	63.48283	-41.64392	3	Ruinnæsset	Magmatic layering (Mt-rich)		75	90	165
w383	63.48283	-41.64392	3	Ruinnæsset	Sheet (youngest, long fsp-phyric)	0.50	63	45	153
w384	63.48344	-41.64363	8	Ruinnæsset	Wein (Mt-rich)		40	60	130
w384	63.48344	-41.64363	8	Ruinnæsset	Sheet (thicker, fsp-phyric)		132	70	222
w385	63.48348	-41.64316	2	Ruinnæsset	Sheet (older, greenish)	0.10	43	72	133
w385	63.48348	-41.64316	2	Ruinnæsset	Purple pegmatite (myarolithic cavities)	0.20	105	13	195
w385	63.48348	-41.64316	2	Ruinnæsset	Sheet (younger, greenish cut by long fsp-phyric dyke)	2.50	130	90	40
w386	63.48378	-41.64280	11	Ruinnæsset	Sheet (fsp-phyric)	1.80	300	75	30
w345	63.50512	-41.65038	205	Ruinnæsset	Faults (many, dextral, 0.2 m displacement)		121	90	31

gpsID	Latitude	Longitude	Altitude	Area	Structure	Thickness (m)	Strike (°RHR)	Dip (°)	DipDir (°)
w346	63.50501	-41.64975	205	Ruinnæsset	Fault (dextral, epidote, 0.05 m displacement)		123	80	213
w346	63.50501	-41.64975	205	Ruinnæsset	Faults (dextral? Orthogonal, 1.2 m displacement)		185	86	275
w396	63.50136	-42.01041	584	Hermods Vig	Fractures (two larger)		230	65	320
w397	63.50041	-42.01361	686	Hermods Vig	Fracture (brown-weathered)	0.10	260	60	350
w403	63.36818	-41.43940	-43	Hermods Vig	Felsic pegmatite dyke	0.40	0	90	90
w403	63.36818	-41.43940	-43	Hermods Vig	Felsic pegmatite vein	0.10	275	74	5
w403	63.36818	-41.43940	-43	Hermods Vig	Felsic/intermediate dyke (fine-medium grained)		336	87	66
w403	63.36818	-41.43940	-43	Hermods Vig	Mafic dyke (irregular, pale grey)		20	75	110
w404	63.36820	-41.43850	0	Hermods Vig	Dyke (dark grey)	1.50	348	70	78
e5876	63.36811	-41.43783	-1	Hermods Vig	Foliation (gabbro)	0.05	170	88	260
e5878	63.36815	-41.43775	2	Hermods Vig	Felsic sheet (fine grained)	0.40	4	80	94
e5878	63.36815	-41.43775	2	Hermods Vig	Mafic dyke (oldest, foliation-parallel)	0.25	170	88	260
e5878	63.36815	-41.43775	2	Hermods Vig	Felsic pegmatite vein (youngest)	0.05			
w406	63.36599	-41.43292	1	Hermods Vig	Mt-rich segregations				
w407	63.36606	-41.43307	2	Hermods Vig	Magmatic layering (gabbro)		313	84	43
w407	63.36606	-41.43307	2	Hermods Vig	Dyke (older, paler, fgr)		100	72	190
w407	63.36606	-41.43307	2	Hermods Vig	Dyke (younger, dark, fgr, fsp-phyric)	0.70	160	90	70
w408	63.37317	-41.44082	-36	Hermods Vig	Foliation (gneiss)		160	72	250
w409	63.37360	-41.44105	-6	Hermods Vig	Porphyritic dyke (fjord-parallel)	2.00			
w410	63.37305	-41.44079	-1	Hermods Vig	Shear zone (brittle)	4.00			
w411	63.37249	-41.44144	1	Hermods Vig	Metagabbroic dyke (cut by fgr metadykes & faults)	1.50	130	70	220
w411	63.37249	-41.44144	1	Hermods Vig	Fault zone (sinistral)		59	73	149
w412	63.37094	-41.44084	3	Hermods Vig	Dolerite dyke	9.00	261	82	351
w414	63.36820	-41.43465	4	Hermods Vig	Granitic dyke (medium grained)	1.00	127	60	217
w415	63.35377	-41.44189	5	Hermods Vig	Dolerite dyke	2.00	68	80	158
w416	63.35481	-41.44096	4	Hermods Vig	Felsic vein		135	90	45
w416	63.35481	-41.44096	4	Hermods Vig	Gabbro dyke (oldest, sheared)	1.00	75	90	165
w416	63.35481	-41.44096	4	Hermods Vig	Pegmatite (youngest)		205	65	295
w417	63.35642	-41.43541	4	Hermods Vig	Pegmatite (purple)				
w417	63.35642	-41.43541	4	Hermods Vig	Felsic pegmatites (younger, thinner)		8	80	98
w418	63.35618	-41.43389	5	Hermods Vig	Contact (mgr syenite><gabbro?)		317	78	47
w418	63.35618	-41.43389	5	Hermods Vig	Magmatic layering (gabbro)		10	85	100
w418	63.35618	-41.43389	5	Hermods Vig	Sheet (fgr, pale grey)		165	50	255
w421	63.36266	-41.43077	5	Hermods Vig	Dyke (cgr, porphyritic)	0.20	183	90	93
w421	63.36266	-41.43077	5	Hermods Vig	Foliation (gabbro?)		160	90	70
w421	63.36266	-41.43077	5	Hermods Vig	Sheet swarm? (intermediate, fgr, bifurcating)		160	90	70
w421	63.36266	-41.43077	5	Hermods Vig	Felsic pegmatite (large, irregular)	0.80	255	70	345
w421	63.36266	-41.43077	5	Hermods Vig	Mt-band		93	77	183
w421	63.36266	-41.43077	5	Hermods Vig	Vein (oldest, foliated/sheared, fine grained)		27	80	117
w421	63.36266	-41.43077	5	Hermods Vig	Dyke (syenite)	0.10	102	75	192
w421	63.36266	-41.43077	5	Hermods Vig	Pegmatite vein (youngest)	0.05	178	90	88
w422	63.37893	-41.40108	7	Hermods Vig	Foliation (amphibolite)		172	65	262
w424	63.38225	-41.40359	-3	Hermods Vig	Foliation (amph gneiss)		120	82	210
w424	63.38225	-41.40359	-3	Hermods Vig	Thrust/fracture?		285	30	15
w425	63.38485	-41.40442	-3	Hermods Vig	Dolerite dyke (RV offsets)	1.00			
w426	63.39101	-41.41178	-2	Hermods Vig	Foliation (gneiss)		280	72	10
w427	63.39869	-41.39923	1	Hermods Vig	Dolerite dyke	2.50	175	80	265
w428	63.40678	-41.41511	4	Hermods Vig	Dolerite dyke				
w429	63.40954	-41.41667	3	Hermods Vig	Dolerite dyke				
w430	63.41003	-41.41784	2	Hermods Vig	Metadyke? (deformed amphibolite)	3.50	180	67	270
w431	63.41128	-41.42189	-7	Hermods Vig	Dolerite dyke	1.00	240	85	330
w432	63.41588	-41.42644	-4	Hermods Vig	Fault zone (+sulphide & heamatite)		247	85	337
w433	63.41592	-41.42567	-5	Hermods Vig	Zone (bio-rich)				
w433	63.41592	-41.42567	-5	Hermods Vig	Foliation (gneiss)		185	73	275
w434	63.41978	-41.42811	-2	Hermods Vig	Dyke (sheared)	4.50	107	40	197
w434	63.41978	-41.42811	-2	Hermods Vig	Dyke (pale grey, dolerite?)	0.75	48	66	138
w435	63.39841	-41.48480	7	Hermods Vig	Dolerite dyke	12.50	90	85	180
w435	63.39841	-41.48480	7	Hermods Vig	Dolerite dyke	12.50	90	85	180
w435	63.39841	-41.48480	7	Hermods Vig	Dolerite dyke (locally 160/50 in shear zone)	4.50	168	90	78
w435	63.39841	-41.48480	7	Hermods Vig	Foliation (gneiss)		224	82	314
w435	63.39841	-41.48480	7	Hermods Vig	Shear zone (with dyke)		160	50	250
w436	63.38859	-41.46523	-5	Hermods Vig	Foliation (gneiss)		154	70	244
w437	63.38827	-41.46370	-3	Hermods Vig	Foliation (gneiss)		124	66	214
w440	63.34919	-41.47148	63	Hermods Vig	Foliation (gneiss)		168	74	258
w440	63.34919	-41.47148	63	Hermods Vig	Fracture/fault		325	56	55
w442	63.34908	-41.47255	75	Hermods Vig	Foliation (gneiss)		345	85	75
w443	63.34903	-41.47538	101	Hermods Vig	Dolerite dyke		157	90	67
w444	63.34903	-41.47991	126	Hermods Vig	Foliation (gneiss)		154	77	244

gpsID	Latitude	Longitude	Altitude	Area	Structure	Thickness (m)	Strike (°RHR)	Dip (°)	DipDir (°)
w445	63.34901	-41.48174	140	Hermods Vig	Metadyke (oldest, irregular)		140	90	50
w445	63.34901	-41.48174	140	Hermods Vig	Metadyke (youngest)		52	80	142
w446	63.34893	-41.48214	150	Hermods Vig	Dolerite dyke (regular with long apophyse)	1.70	73	88	163
w446	63.34893	-41.48214	150	Hermods Vig	Foliation (gneiss)		172	69	262
w447	63.34918	-41.48337	160	Hermods Vig	Faults (domino)		140	80	230
w447	63.34918	-41.48337	160	Hermods Vig	Foliation (gneiss)		150	72	240
w448	63.34942	-41.48601	185	Hermods Vig	Dolerite dyke (+rusty marginal zones)	10.00	257	87	347
w448	63.34942	-41.48601	185	Hermods Vig	Metadyke (irregular)	9.00	162	90	72
w449	63.35009	-41.48697	194	Hermods Vig	Fold axial plane (amph gneiss)		137	85	227
w449	63.35009	-41.48697	194	Hermods Vig	Fold axis (317→40°, amph gneiss)				
w450	63.35045	-41.48828	222	Hermods Vig	Foliation (gneiss)		132	60	222
w450	63.35045	-41.48828	222	Hermods Vig	Metadyke	0.10	167	75	257
w450	63.35045	-41.48828	222	Hermods Vig	Fault (sinistral, cuts metadyke)		80	90	170
w451	63.35049	-41.48856	219	Hermods Vig	Metadyke (intermediate, fsp-phyric, cut by pegmatites)	1.40	179	85	269
w452	63.35191	-41.49167	247	Hermods Vig	Enclave (ultramafic)		155		245
w454	63.34880	-41.50620	265	Hermods Vig	Contact (?><leucogabbro)		10		100
w455	63.34882	-41.50485	433	Hermods Vig	Foliation (gneiss)		170	75	260
w455	63.34882	-41.50485	433	Hermods Vig	Dolerite dyke (plg-phyric)		70	90	160
w457	63.35034	-41.50802	449	Hermods Vig	Magmatic layering (Mt)	0.20	171	44	261
w457	63.35034	-41.50802	449	Hermods Vig	Magmatic layering (gabbro+Mt)		185	53	275
w458	63.35056	-41.50855	470	Hermods Vig	Cointact (felsic><gabbro, undulating, no chill)		95	62	185
w459	63.35094	-41.50845	464	Hermods Vig	Foliation (gneiss)		323	86	53
e7612	63.35122	-41.50832	469	Hermods Vig	Banding (gneiss)		145	90	55
e7613	63.35122	-41.50828	470	Hermods Vig	Fault (dextral, reidel)		120	90	30
w460	63.35212	-41.50916	438	Hermods Vig	Z-folds				
w461	63.36348	-41.50648	414	Hermods Vig	Dykelet	0.30	87	63	177
w461	63.36348	-41.50648	414	Hermods Vig	Foliation (gneiss)		293	60	23
w462	63.36393	-41.50538	419	Hermods Vig	Intermediate metasheet (irreg)	8.00	325	50	55
w462	63.36393	-41.50538	419	Hermods Vig	Splayed offset along dolerite dyke	1.20	72	88	162
w463	63.36390	-41.50540	433	Hermods Vig	Foliation		299	68	29
w463	63.36390	-41.50540	433	Hermods Vig	Dolerite dyke (major)		91	90	
w464	63.36438	-41.50583	431	Hermods Vig	Fault Zone (brittle, cut by dolerite dykes)	6.00	330	55	60
w471	63.59275	-42.23500	1230	Hermods Vig	Dolerite dyke (plg-phyric)	18.00	5	90	95
w473	63.66026	-42.27887	1773	Hermods Vig	Foliation		144	83	234
w474	63.67429	-42.29034	1826	Hermods Vig	Flow direction? (in qtz syenite)		153		243
w474	63.67429	-42.29034	1826	Hermods Vig	Foliation (in amphibolite xenolith)		345	70	75
w474	63.67429	-42.29034	1826	Hermods Vig	Aplite vein	0.20	189	72	279
w475	63.66120	-42.17504	1529	Hermods Vig	Dolerite dyke	2.00	147	79	237
w475	63.66120	-42.17504	1529	Hermods Vig	Felsic sheet (hornfels)		140	40	230